P150652_FinalReport

by Krishna Katwa

FILE	5367_KRISHNA_KATWA_P150652_FINALREPORT_128469_1334880146.DOCX (26.27M)		
TIME SUBMITTED	29-APR-2019 05:24PM (UTC+0100)	WORD COUNT	15325
SUBMISSION ID	105726818	CHARACTER COUNT	78129

University of Wales Trinity Saint David

School of Engineering

Major Project (M6X00417) – Weight Saving of a Sports2000 MCR Upright



Prifysgol Cymru
Y Drindod Dewi Sant
University of Wales
Trinity Saint David

Krishna Katwa

P150652

30/04/2019

BEng (Hons) Motorsport Engineering

Abstract

Sports2000 is an extremely competitive championship, the university has competed in the championship since 2014. The competitive nature of the championship is due to the tightly controlled regulations which prevent engine development. This leads to other areas of the car being explored for development opportunities. In such a competitive championship with similar cars, any potential upgrade can lead to a big improvement in on track performance.

The goal of this project was to reduce the mass of the current front suspension upright whilst ensuring that the new design will perform in the same way as the current upright when out on track and under load. This was done through the use of topology optimisation and finite element analysis. The upright was chosen as any reduction in un-sprung mass can have big benefits to the performance of the car.

Overall, the uprights mass was reduced by 0.95kg (26%), exceeding the projects initial aim to save 0.5kg whilst exhibiting similar deformation and stresses well below the elastic modulus of the chosen material when compared to the original upright.

Declaration of Authenticity

This thesis is the result of the author's original research. It has been composed by the author and has not been previously submitted for examination which has led to the award of a degree.

Signed: Krishna Katwa *Date: 30/04/2019*

Acknowledgements

I would like to thank Kelvin Lake for the support throughout the project and helping with the learning of the Design Studio software package, and Tim Tudor for taking time to help when asked despite not being my main supervisor.

I would also like to thank Paul Davies for assistance in designing the twist rig that enabled testing of the suspension upright. And Rhodri Davies for 3D printing the new upright design.

Team MCR were also helpful in lending me the upright to test and I would like to thank them for providing the initial CAD model of the upright.

Contents

Abstract i

Declaration of Authenticity i

Acknowledgements i

1 Introduction 1

1.1 Reasons 1

1.2 Aims 2

1.3 Timing 3

1.4 Resources Needed 5

1.5 Partners 5

2 Literature Review & Background Research 6

2.1 Material Properties 7

2.1.1 Strength of materials 7

2.2 Suitable Materials 9

2.2.1 Aluminium (Currently Used) 9

2.2.2 Composite 9

2.2.3 Steel 11

2.2.4 Material Choice 11

2.3 Finite Element Analysis & Design Topology Optimisation 12

2.3.1 FEA 12

2.3.2 Design Topology Optimisation 15

2.4 Upright Design 18

2.4.1 Weight Saving 19

2.4.2 Geometrical Considerations 20

2.5 Literature Review Conclusion 22

3 Methodology 23

3.1 Attachment Points 23

3.2 Initial CAD Model 24

3.3 Package Space 25

3.4 Non-Designable Region 26
3.5 Optimisation Setup 27
3.5.1 Mesh 27
3.5.2 Package Space Simplification 28
3.5.3 Constraint Setup 29
3.5.4 Static Load Setup 30
3.5.5 Load Case Setup 31
3.5.6 Optimisation Parameters 32
3.6 FEA Model Setup 33
3.6.1 Material Selection 34
3.6.2 Rigid Body Elements Selection (RBE) 35
3.6.3 Static Load Setup 36
3.6.4 Constraint Setup 36
3.6.5 Loadcase Setup 37
4 Results 38
4.1 Practical Testing Results 38
4.2 Optimisation Results 40
4.2.1 Mesh Study 41
4.3 Optimised Upright Design 42
4.3.1 3D Printing 46
4.3.2 MCR Upright 47
4.3.3 Design Considerations 48
4.4 FEA Results 49
4.4.1 Workshop Vs FEA Results (Current Upright) 49
4.4.2 Current Design Vs Proposed Design FEA Results 52
5 Conclusion 70
6 Recommended Further Work 72
7 References 73
8 Appendices 78

8.1 Appendix 1…Supervision Meeting Notes 78
8.2 Appendix 2… Optimisation Mesh Study Time Taken 90
8.3 Appendix 3…Upright Testing Pictures 91
8.4 Appendix 4…FEA Screenshots 96
8.5 Appendix 5… Horizontal Track Load Calculation 154

Table of Figures

Figure 1-1, Current University Car Upright, (Katwa, 2018) 1
Figure 1-2, Updated MCR Upright, (Hughes, 2019) 1
Figure 1-3, University Sports2000 MCR, (UWTSD, 2018) 2
Figure 2-1, Process of Kitchenhams Systematic Literature review, (Brereton, et al., 2007) ... 6
Figure 2-2, (Left-Right), Glass, Carbon and Kevlar Fibre, (Randjbaran, 2018) 11
Figure 2-3, Governing Equations for Various Physical Phenomena, (Dean, n.d.) 13
Figure 2-4, Example Mesh, (Symscape, 2010) 14
Figure 2-5, Winston Cup Stock Car Chassis 14
Figure 2-6, Initial Frame, (Ma, et al., 2003) 15
Figure 2-7, Optimised Frame, (Ma, et al., 2003) 16
Figure 2-8, Example of Upright Optimisation, (Wight, 2008) 16
Figure 2-9, Initial Structure 17
Figure 2-10, Optimised Structure 17
Figure 2-11, Optimised Implant 17
Figure 2-12, Camber, (Car-Engineer, 2019) 20
Figure 2-13, Toe, (Car-Engineer, 2019) 21
Figure 2-14, King-Pin Inclination, (Bengt, 2015) 22
Figure 3-1, Current Upright 23
Figure 3-2, Current Upright Lower View 23
Figure 3-3, Initial CAD Geometry, (UWTSD / Team MCR, 2017) 24
Figure 3-4, Twist Rig, (Katwa, 2018) 24
Figure 3-5, Brake Calliper Clearance 25
Figure 3-6, Lower Suspension Clearance 25
Figure 3-7, Non-Designable Region 26
Figure 3-8, Meshed Package Space 27
Figure 3-9, Package Space 28
Figure 3-10, Non-Designable Region 28

Figure 3-11, Simplified Package Space 28
Figure 3-12, Constraint Setup 29
Figure 3-13, Static Load Setup at Top Attachment Point 30
Figure 3-14, Loadcases for Optimisation 31
Figure 3-15, Example of a Loadcase 31
Figure 3-16, Comparison of First and Second Order Mesh, (Simscale, 2016) 33
Figure 3-17, Upright Shown in Separate Group 34
Figure 3-18, RBE Representing a Bolt 35
Figure 3-19, RBE Representing the Bearing 35
Figure 3-20, Example of Static Loads for FEA 36
Figure 3-21, Rig Constraints 36
Figure 3-22, Example FEA Loadcase 37
Figure 4-1, Axis for Road Vehicles, ISO Standard, (International Organization for Standardization, 2011) 38
Figure 4-2, Upright Testing Setup 38
Figure 4-3, Optimisation Result 40
Figure 4-4, High Isosurface Value 40
Figure 4-5, Low Isosurface Value 40
Figure 4-6, Results of Split Twice Mesh 41
Figure 4-7, Results of Split Once Mesh 41
Figure 4-8, Optimised Upright Design 42
Figure 4-9, Front View of Optimised Upright 43
Figure 4-10, Rear View of Optimised Upright 43
Figure 4-11, Side View of Optimised Upright 44
Figure 4-12, Optimisation Results Comparison 44
Figure 4-13, Optimised Upright Comparison 44
Figure 4-14, Comparison of Current and Optimised Upright Rear View 45
Figure 4-15, Comparison of Current and Optimised Upright 45
Figure 4-16, 3D Print Comparison 46
Figure 4-17, Calliper Fitment Check 46
Figure 4-18, Optimised Upright Rear 47
Figure 4-19, MCR Upright Rear 47
Figure 4-20, Steering Arm FEA Results in X Direction 50
Figure 4-21, Top Attachment Point FEA Results in Y Direction 50
Figure 4-22, Workshop Test of Top Attachment Point in Y Direction 51
Figure 4-23, FEA Result of Bottom Attachment Point Z Direction 51
Figure 4-24, Lower Attachment Point FEA Result X Direction 52

Figure 4-25, Brake Top Attachment Point FEA Result Y Direction 54
Figure 4-26, Lower Attachment Point FEA Result Z Direction 56
Figure 4-27, Sports2000 2019 Calendar, (Sports2000, 2019) 58
Figure 4-28, Brake Low FEA Result Current Upright 61
Figure 4-29, Brake Low FEA Result New Upright 61
Figure 4-30, Bottom Attachment Point FEA Result Current Upright 63
Figure 4-31, Bottom Attachment Point FEA Result New Upright 63
Figure 4-32, Bottom Attachment Point FEA Result Current Upright (Braking) 65
Figure 4-33, Bottom Attachment Point FEA Result (Braking) 65
Figure 4-34, Bottom Attachment Point 'Worst Case' Result Current Upright 68
Figure 4-35, Stress at Lower Attachment Point Current Upright 69
Figure 4-36, Bottom Attachment Point 'Worst Case' Result New Upright 69
Figure 4-37, Stress at Bottom Attachment Point New Upright 69

Table of Tables

Table 1, Gantt Chart Timings 3
Table 2, FEA Results for First and Second Order Meshes 33
Table 3, Aluminium 6061-T6 Properties 34
Table 4, X Direction Testing Results 39
Table 5, Y Direction Results 39
Table 6, Z Direction Results 39
Table 7, Mesh Comparison 41
Table 8, Aluminium 6061-T6 Heat Properties, (ASM Aerospace Specification Metals Inc, 2018) 48
Table 9, Current Upright FEA Results X Direction 49
Table 10, Current Upright FEA Results Y Direction 50
Table 11, Current Upright FEA Results in Z Direction 51
Table 12, Current and New Upright FEA Results X Direction 52
Table 13, Current and New Upright FEA Results Y Direction 54
Table 14, Current and New FEA Results Z Direction 56
Table 15, Forces at Contact Patch, (Meredith, 2018) 59
Table 16, Horizontal Forces 59
Table 17, Track Forces Linear FEA Results 60
Table 18, Track Forces Cornering FEA Results 62
Table 19, Track Forces Braking FEA Results 64
Table 20, Cornering Force Applied in Y Direction 66
Table 21, Braking Force Applied in Y Direction 66

Table 22, 'Worst Case' Loads 67
Table 23, Results of 'Worst Case' FEA 68

Table of Graphs

Graph 1, Project Gannt Chart 4
Graph 2, Graph Showing Elastic and Plastic Regions of Deformation, (Cyberphysics, 2018) 8
Graph 3, Comparison of FEA Results Between Current and New Upright X Direction 53
Graph 4, Comparison of Current and New FEA Results Y Direction 55
Graph 5, Comparison of Current and New Upright FEA Results Z Direction 57

Table of Equations

Equation 1, Matrix Example 13
Equation 2, Global Stiffness Equation 13

1 Introduction

1.1 Reasons

After spending 2 seasons as part of Team MCR, the universities race team, it has been observed that there are lots of opportunities for development of the car to try and help move forward on the grid. These development opportunities are areas that are not limited by the regulations of the championship, so this excludes engine development as the rules explicitly state the engine must be 'spec'. Therefore, the areas for development include aerodynamics and chassis.

Whilst at race weekends, it has been noted how the 'works' spec cars, i.e. cars run by MCR have different suspension uprights front and rear compared to the university car. This is due to a design update by MCR that has been applied to new chassis built after chassis number 14, built in 2014, which belongs to the university. This also suggests the current upright is over-engineered.



Figure 1-1, Current University Car Upright, (Katwa, 2018)



Figure 1-2, Updated MCR Upright, (Hughes, 2019)

Whilst there is more lap time to be potentially gained in aerodynamic upgrades, these upgrades are governed by a lot of regulations and are also costlier to produce and need thorough testing before they can be raced. Therefore, for this project, chassis development was the chosen option as the costs involved will not be as high and there will still be lap time gains on track.

1.2 Aims

The Sports2000 regulation 5.14.1 states that *'the car must weigh no less than 521kg with the driver not to be included in that weight and with no topping-up of fluids.'* (SRCC, 2018). As the MCR currently weighs 527.5kg a weight saving of over 6.5 kilos would allow the team to then use ballast to bring the car up to the championship regulated weight whilst optimising the weight distribution slightly.

With this in mind, the aim of this project was to design a new optimised front upright that was comparable in stiffness, and functionality of the current upright whilst being at least 0.5kgs lighter. This would lead to a 1 kilo weight reduction at least across the front axle in unsprung mass and bring the car closer to the minimum weight limit. This weight saving was targeted as a 1kg weight saving can decrease lap time by 0.03 seconds per lap (Mclaren, 2013). Based on a previous Sports2000 race at Brands Hatch this would save over 1 second during the race distance. Furthermore, the uprights should be designed to be able to take advantage of university facilities to allow them to be made in house.



Figure 1-3, University Sports2000 MCR, (UWTSD, 2018)

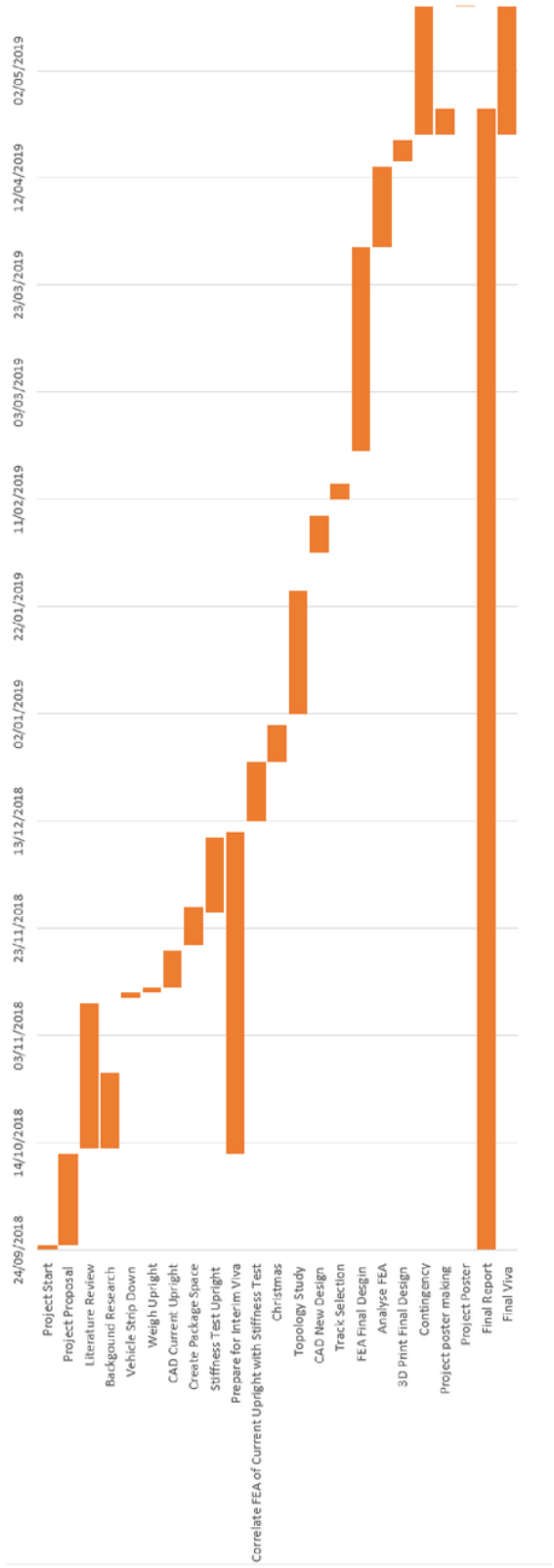
1.3 Timing

As with any project it is essential that a robust high-quality timing plan is followed, this allows the project to be delivered on time as regular checks can be carried out against the timing plan to track the projects progress and see if the timing needs to be updated to reflect any unexpected delays.

Below the initial Gantt chart can be found, with a table outlining the different tasks involved in the project and a projected duration for each task. This will be updated as the project advances and more tasks are added, such as looking at how to validate the FEA that is carried out, however the project must be complete by the 30th of April 2019. Weekly supervision meetings also took place, these can be found in the appendix.

Table 1, Gantt Chart Timings

Task	Start Date	End Date	Duration
Project Start	24/09/2018	25/09/2018	1
Project Proposal	25/09/2018	12/10/2018	17
Literature Review	13/10/2018	09/11/2018	27
Backgound Research	13/10/2018	27/10/2018	14
Vehicle Strip Down	10/11/2018	11/11/2018	1
Weigh Upright	11/11/2018	12/11/2018	1
CAD Current Upright	12/11/2018	19/11/2018	7
Create Package Space	20/11/2018	27/11/2018	7
Stiffness Test Upright	26/11/2018	10/12/2018	14
Prepare for Interim Viva	12/10/2018	11/12/2018	60
Correlate FEA of Current Upright with Stiffness Test	13/12/2018	24/12/2018	11
Christmas	24/12/2018	31/12/2018	7
Topology Study	02/01/2019	25/01/2019	23
CAD New Design	01/02/2019	08/02/2019	7
Track Selection	11/02/2019	14/02/2019	3
FEA Final Desgin	20/02/2019	30/03/2019	38
Analyse FEA	30/03/2019	14/04/2019	15
3D Print Final Design	15/04/2019	19/04/2019	4
Contingency	20/04/2019	14/05/2019	24
Project poster making	20/04/2019	25/04/2019	5
Project Poster	14/05/2019	15/05/2019	1
Final Report	24/09/2018	30/04/2019	218
Final Viva	20/04/2019	14/05/2019	24



Graph 1, Project Gannt Chart

1.4 Resources Needed

In order to complete this project, a number of different facilities will be needed, these include university facilities.

The race car will be needed after the end of the current season as to not disrupt the team's setup for the last round. The race vehicle workshop will be needed to allow the strip down and measurement of the current upright, the upright will then be reassembled onto the car ensuring it was left in the state it was found in. All workshop health and safety guidelines will be followed throughout to avoid any accidents or damage to the race car and upright.

The use of the race vehicle workshop flatbed and measuring equipment will be needed to allow accurate measurements of the current upright to be taken, this will allow an accurate CAD model to be made. Technician support will be needed in order to create a suitable testing rig to test the upright.

Different computer software packages will also be required in order to complete this project. Microsoft office will be used to write the report and to also hold relevant data and output any necessary graphs or tables. A computer aided design software package such as Solidworks will be used to create virtual models of the upright which can then be transferred into a Finite Element Analysis (FEA) package such as Genesis Design Studio, which will help to focus the design of the upright after carrying out a topology optimisation.

1.5 Partners

For this project, Team MCR will be partners as the current upright needs to be supplied to allow testing and measuring to take place. As this project is aimed at improving the performance of the university race car, there is no need for any industrial partners, this is because the university has the facilities to make the new upright if the team choose to. As racing is a competitive environment, if the manufacturer of the race car was involved in the project, the new upright would find its self on the 'works' race cars thus negating any potential advantage the university race car could gain over the 'works' run cars.

The cost of getting an external consultancy company to carry out FEA on a new upright design would also be prohibitive as the value of potential new uprights is not worth the budget it would take out of the race team budget.

2 Literature Review & Background Research

The purpose of the following literature review is to examine the underlining themes and aspects of race car component design. The review will be structured into four themes; material properties, suitable materials, Finite Element Analysis and design topology optimisation and upright design. These themes will help explore not only how a component of a race car can be designed, but also how to optimise the part for maximum performance gain.

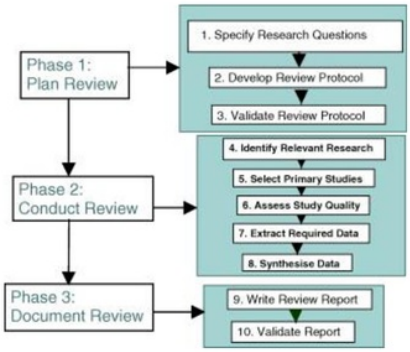


Figure 2-1, Process of Kitchenhams Systematic Literature review, (Brereton, et al., 2007)

The literature review below has been developed by following Kitchenhams systematic literature review, as shown in figure 2-1. The review consists of three different segments. The first segment is concerned with the planning of the review, this is where the topics to explore during the review are considered. Segment 2 is conducting the review; this involved the collection of multiple relevant references. Whilst the last segment is writing the review.

2.1 Material Properties

When designing new components, it is important to take into account the properties that can be useful to a designer. For example, it is expected that the upright will deform elastically when on track under certain loads so the new design must also behave the same way when on track and not experience plastic deformation.

2.1.1 Strength of materials

It is important to ensure that a component will not fail when in use, a component needs to have strength and stiffness.

2.1.1.1 Strength theory

Strength theory provides the basis for calculating the mechanical stresses seen within a material. There are two general questions answered with this theory;

- *'Distribution of the inner forces on the cross-sectional surface of a stressed machine part'*
- *'Changes in shape that are caused by these cross-sectional values'*

The first question gives the mechanical stress that is acting within the design and the second question allows the discovery of the deformations that take place in a machine part that are associated with the load applied, for example the change in length. (Schaeffler, 2014)

2.1.1.2 Stress

Perhaps one on the most famous physics terms, 'for every action (force) in nature there is an equal and opposite reaction' (Newton, 1686) can be used to help describe stress, as the external forces and moments acting on a body are balanced by the forces acting inside the same body. The stress state can be split in to two different stresses;

- *Normal stress = components perpendicular to the cross-sectional plane*
- *Shear stresses = two components in the cross-sectional plane*

If both of the shear stresses become zero as a result of the location of the cross-sectional plane, the normal stress can reach an extreme value which is given the name principal stress. (Schaeffler, 2014)

When a component is subject to a bending moment alone, the component will be subject to direct stress which will change through the material from tensile on one surface to compressive on the other. On the other hand, if a component is subject to a transverse force, this will cause shear stresses along with direct stress. (Matthews & Rawlings, 1994)

2.1.1.3 Deformation

Stresses always lead to a deformation of some sort, there is a clear distinction between the two different types of deformation, elastic and plastic and will be explored below.

2.1.1.4 Elastic deformation

Elastic deformation is where the deformation a body shows is no longer visible once the force or load applied to the body has been removed, that is to say that the body returns to its original state after having a load applied and then removed from it. It can be said that it follows Hooke's law, this is where elongations are proportional to the stress accompanying them. (Schaeffler, 2014)

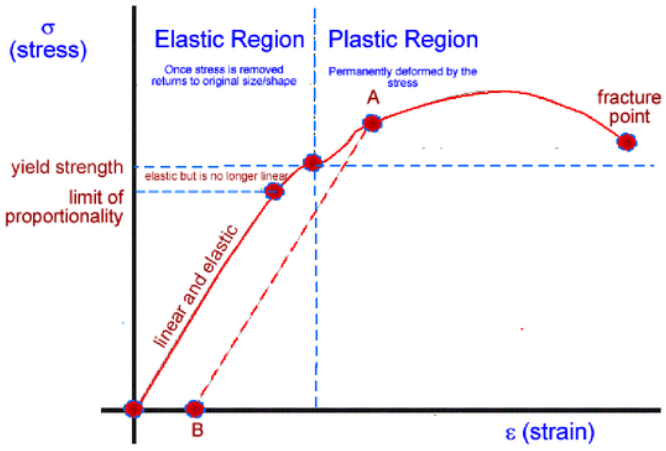
2.1.1.5 Plastic deformation

When the external forces acting on a body and therefore the inner stresses are greater than the intrinsic limit that a certain material possesses, one of two things can occur, the material can deform permanently, this is where once the load is removed, the material will not return to its pre-loaded state, or the material can break. (Schaeffler, 2014)

Usually, only the elastic range of materials is thought of when designing a component. However, the plastic deformation can also be useful, this was observed by (Smith, 1984) where it was stated that the plastic deformation range can be useful for forging metals into useful shapes.

2.1.1.6 Modulus of Elasticity & Strength

The modulus of elasticity can be thought of as the measure of the materials stiffness or the elasticity of the bonds within the material. The strength of a material however can be a relative measure of the amount of stress that is needed to rupture the bonds within the material. (Smith, 1984)



Graph 2, Graph Showing Elastic and Plastic Regions of Deformation, (Cyberphysics, 2018)

2.2 Suitable Materials

2.2.1 Aluminium (Currently Used)

Aluminium is in fact the earths most common metal however the price doesn't reflect that. This is due to the involved process that is required to take bauxite form ore into aluminium. Aluminium is often used in castings and due to its combination of mechanical characteristics that are beneficial to motorsport use, it its widely seen in paddocks across the globe, the fact that it is roughly 1/3rd the weight of steel but with tensile strengths higher than low carbon steels means the high price is worth paying. (Smith, 1984)

Some of the most common aluminium alloys are listed below;

- 1100
- 2024
- 3003
- 6061

With the exception of 1100, all find use in motorsport for many different things, from angle brackets to steering arms

2.2.2 Composite

The term composite within motorsport often tends to be people referring to a part that is exclusively made of carbon or Kevlar (aramid) fibres. However, the use of the term in this way is incorrect, as noted by (McBeath, 2000), the term is perhaps better defined as, 'made up of two or more parts or elements, and having better mechanical properties than the individual constituents'. However, (Matthews & Rawlings, 1994), state that the previous definition is inadequate and that there are other criteria with which to define a composite, these are;

- Both materials need to be present in greater quantities than 5%
- The composite properties have to be noticeably different than the individual constituents' properties
- A man-made composite is produced from mixing and combining the constituents by different means

Three of the most widely used composites in motorsport are;

- Fibre glass reinforced plastics
- Aramid fibre
- Carbon fibre

2.2.2.1 Glass Fibre

To use the proper terminology, fibre glass is actually glass fibre reinforced plastic, GFRP. It is a material that has been around since the end of the Second World War, where it was widely used in navy vessels.

The main use of fibre glass in motorsport is in the construction of bodywork, this results from its cheapness, and its strength to weight ratio being favourable. It is also very easy to repair, so any contact that happens out on track can quickly and easily be repaired at the circuit overnight rather than needing brand new components or bodywork, (McBeath, 2000). There are however drawbacks to the material noted by (Kaw, 2006), and this include a low elastic modulus, low fatigue strength and a sensitivity to abrasion, therefor it is important to consider these drawbacks when using it for bodywork.

2.2.2.2 Aramid Fibre

First becoming available in the early 1970's, aramid, aromatic polyamide fibres, are related to nylon but due to the slightly different chemical make-up, are used in body armour due to their high impact resistance. The most well-known type of this fibre is Kevlar which along with Twaron are actually brand names.

The advantages of this composite are high tensile strength along with a reasonably high stiffness with a relatively low density, this increase of stiffness is due to the extra benzene rings that are present in the polymer chain. (Matthews & Rawlings, 1994) Drawbacks of this composite are, the difficulty of cutting and therefore working with the material and low compressive strength which also leads to inter-laminar shear when placed in a laminate and exposed to high compressive force. This material is best used in structural applications that need high tensile strength and impact resistance, (McBeath, 2000). Another interesting property of aramid fibre noted in Mechanics of composite materials, (Kaw, 2006), is that they degrade in sunlight, which would limit the potential usefulness of the material.

2.2.2.3 Carbon Fibre

Perhaps the most well-known and popular composite that is seen not only in motorsport but also an increasing number of road cars is carbon fibre. Originally produced in the late 19th century, it wasn't until the 1960's that carbon fibre could be used as a structural material.

Carbon fibre is so widely used due to its high strength, stiffness, high tensile and compressive strength with a good resistance to corrosion and fatigue. In fact, carbon fibre has the highest specific stiffness of any currently commercially available fibre.

However, carbon fibre can be very brittle, especially in high modulus variants and the impact strength of carbon fibre is lower than both glass and aramid fibres, (McBeath, 2000). This is

also confirmed by (Kaw, 2006), where it is noted that carbon is brittle and much like ceramics, is flaw sensitive. Reinforcement of the carbon matrix allows for gradual fail and allows higher temperature resistance.

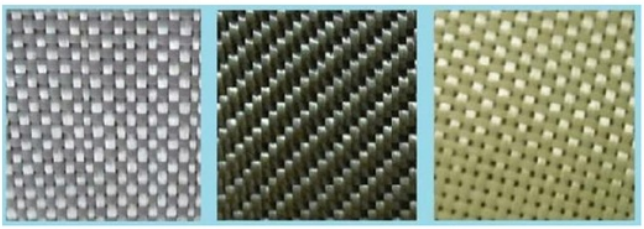


Figure 2-2, (Left-Right), Glass, Carbon and Kevlar Fibre, (Randjbaran, 2018)

2.2.3 Steel

Steels can be defined as iron that contains no more than 2% carbon that has dissolved within its matrix. Alloy steels are carbon steels that have been modified by adding tiny amounts of certain alloying materials so that certain characteristics of the steel can be improved. (Smith, 1984)

There are many different types of carbon steels, an exhaustive list would be too long to list so the most often used in motorsport are as follows (Smith, 1984);

- SAE 1010-1015
- SAE 1025
- SAE 4130
- SAE 4340

2.2.4 Material Choice

From the research carried out surrounding the current upright material and potential new materials, it has been decided that the new upright should be made out of the same aluminium 6061-T6 that the current upright is made from. This will also allow the new upright to be made in house using the universities manufacturing facilities.

This decision was made after considering the drawbacks of the other materials that had been researched and noted above.

2.3 Finite Element Analysis & Design Topology Optimisation

As the project relied on the use of FEA and topology optimisation, research was carried out into these areas to allow a better understanding of the processes and how they would be used in the project. Owing to the wide range of methods available for both, it is not practical to conduct a detailed analysis into every method, therefore, a summary of the key points can be found below.

As the university has access to VR&D Genesis Design Studio, and it is capable of carrying out FEA and topology optimisation, it was decided that it was the software package that will be used. The type of solver used will be a static linear analysis solver as Design Studio is based on Nastran which primarily uses the same method and was originally developed using U.S. government funding for NASA in the 1960's. (NASA Technology Transfer Program, n.d.)

2.3.1 FEA

Early FEA work was servery limited by the computing power of the day. As aircraft became quicker approaching and even passing supersonic speeds, the existing methods of FEA were unable to provide engineers the answers they needed. In the early 90's however, computing power grew such that the analytical capabilities are more advanced than senior stress engineers' knowledge. This has allowed even more complex and intricate FEAs to be carried out to help with race car design. (Bastow & Howard, 1993). These intricate and complex FEA methods were the *force matrix* method and the *stiffness* method. Thanks to (Turner, et al., 1956), the stiffness method went on to form what is used in the modern day (Mottram & Shaw, 1996). It can in fact now be said that FEA has become the key link between structural design and computer aided drafting. (Crolla, 2009).

In order to simplify the formula of the element stiffness equation, matrix methods are used as they can be used in long-handed solutions and easily inputted into a computer. This matrix notation provides an easy way of visualising and solving simultaneous equations. (Logan, 2012).

Equation 1 shows an example matrix that is commonly used. Where the subscript after F represents the node and direction of force. Displacements at nodes in each of x, y and z direction are represented by u, v and w. The number in subscript next to u, v and w represents the node.

$$\{F\} = \begin{Bmatrix} F_{1x} \\ F_{1y} \\ F_{1z} \\ F_{2x} \\ F_{2y} \\ F_{2z} \\ \vdots \\ F_{nx} \\ F_{ny} \\ F_{nz} \end{Bmatrix} \quad \{d\} = \begin{Bmatrix} u_1 \\ v_1 \\ w_1 \\ u_2 \\ v_2 \\ w_2 \\ \vdots \\ u_n \\ v_n \\ w_n \end{Bmatrix}$$

Equation 1, Matrix Example

There is an equation often used that can allow for the relationship of the global nodal forces (F) and the displacements at a global level (d). This is done through the use of the global stiffness matrix (K). The equation is not only the basic equation that the stiffness method of analysis uses but it also represents a set of simultaneous equations. (Logan, 2012)

$$\{F\} = [K]\{d\}$$

Equation 2, Global Stiffness Equation

As the finite element method (FEM) is a technique that is numerically based and can be used for solving a wide range of complex physical phenomena. It is used most often on problems that are not easily tackled. (Dean, n.d.) An overview of the governing equations is provided in figure 2-3.

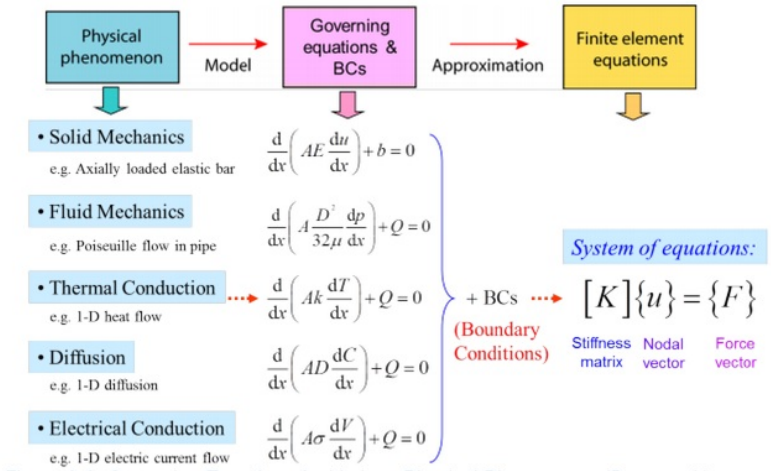


Figure 2-3, Governing Equations for Various Physical Phenomena, (Dean, n.d.)

Finite elements can possess many different and varied forms, it is dependent on the shape they are to represent. If a flat plate was to be modelled and represented, then the elements used will be of triangular or quadrilateral shape. Compare this to a solid where finite elements will usually be cubes or tetrahedrons. This is usually seen when a part has been meshed in the meshing program. (Ross, 1998). It is the mesh that is responsible for accurately representing the domain that is being tested. The elements of the mesh are thought to be interconnected at specified joints that are known as nodes. These nodes are usually found on the element boundary between two connected elements, therefore the size of the mesh used is important. This will be explored further in section 4.2.1 (Rao, 2004)

An example mesh can be found in figure 2-4.

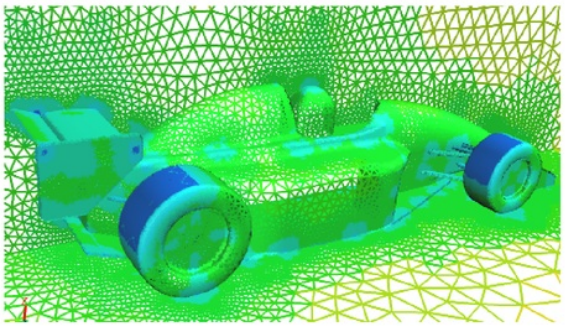


Figure 2-4, Example Mesh, (Symscape, 2010)

2.3.1.1 Practical Aspects of FEA

It is worth noting that FEA does not just refer to solely to the domain of structural mechanics, engineers use FEA in other areas such as heat conduction, fluid dynamics and electric and magnetic field areas of study. (Rao, 2004)

FEA can be used to validate the results of real-world testing and provide engineers with confidence in their designs. A study carried out on a BAJA SAE roll cage found that the error between the real-world testing and computational values was less than 20%. (Anand, 2017)

Race car design can also be improved through the use of FEA, for example, a study on chassis stiffness of a Winston cup stock car was carried out and thanks to the use of FEA, it was found that the chassis stiffness could be increased by over 70% (Crawford, 1994).

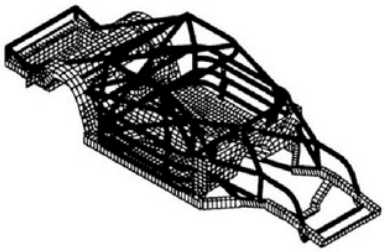


Figure 2-5, Winston Cup Stock Car Chassis

2.3.2 Design Topology Optimisation

Structure optimisation began in the 1960's and has developed rapidly since. Optimisation can simply be thought of as finding a set of design variable values that help to minimize the objective function but also satisfying all of the constraints and side constraints. (Leiva, 2013)

There are 3 main parameterisations for optimisation, these are sizing, shape and topology. Generally speaking, significant improvements can be achieved in performance metrics providing that the topology of the structure can vary. (MSC Software, 2007) An in-depth study of topology optimisation can be found in works by (Bendsoe, 2003).

Genesis is an analysis software package that will be used to carry out the FEA and optimisation. This software package is a fully integrated analysis and design optimisation package. Launched in 1984 the software had been written by leading structural experts. The analysis can be based on any number of methods such as static, normal modes, heat transfer and many more. (Vanderplaats, 2018)

The design optimisation within Genesis is based on the gradient-based solution techniques, in particular the Sequential Linear Programming (SLP), Sequential Quadratic Programming (SQP) and feasible direction methods. These methods are used as they approximate the problems generated using sensitivity and analysis information. The optimisation is then carried out by DOT or BIGDOT optimisers. Once the optimum of the rough problem has been discovered, the process is repeated with a new finite element analysis until the solution has converged. (Chang, 2015)

When carrying out a design topology optimisation, the designer will begin with the 'package space' that is, the area which is able to be designed in. This gets divided into a mesh of finite elements. Next the package space will be constrained and have loads applied so that the Optimisation programme will then use an iterative process to decide if an area within the design space should contain material. (Fiedler, et al., 2017)

An example of how optimisation can be used can be seen in a project carried out on a truck frame, the initial design can be seen, figure 2-6 and then the new optimised design can be seen, figure 2-7. (Ma, et al., 2003)

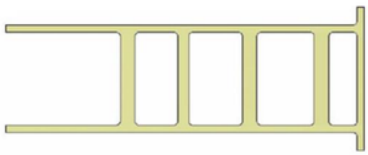


Figure 2-6, Initial Frame, (Ma, et al., 2003)

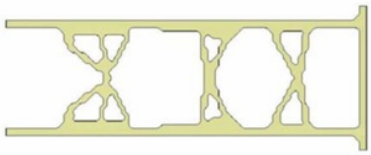


Figure 2-7, Optimised Frame, (Ma, et al., 2003)

Optimisation is a popular tool in chassis design, as seen from the above example and form a study carried out by (Bhardwaj, 2018), where it was found that optimisation could reduce the weight of a steering upright by over 18%.

A simple optimisation sequence can be seen in figure 2-8 from a project that was carried out by Luxon Engineering. (Wight, 2008) The steps are similar to what will happen in this project and this image is a good way to show what to expect from the project.

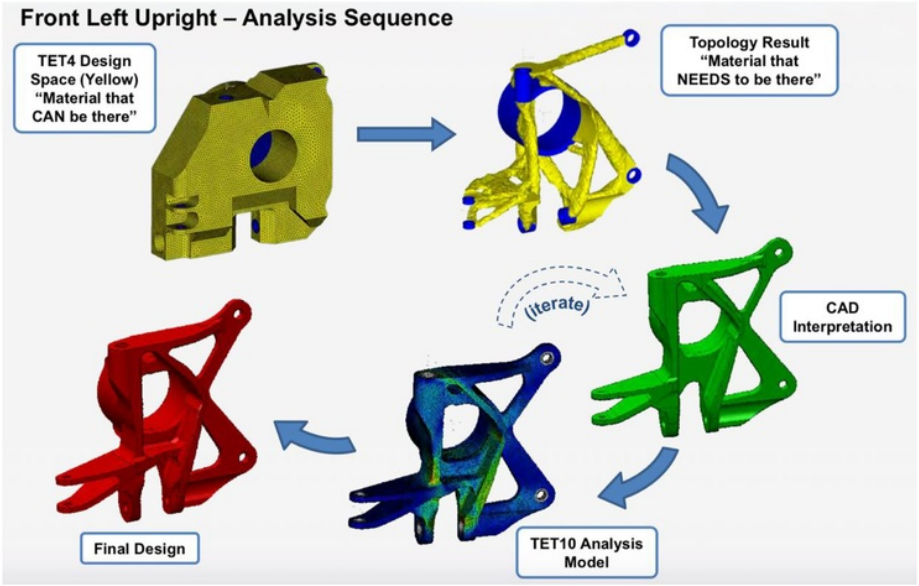


Figure 2-8, Example of Upright Optimisation, (Wight, 2008)

Optimisation is however not just used in automotive applications, work carried out by (Gao, 2019), shows how optimisation can be used in to help reinforce composite structures, figure 2-9, that are located near joints hinges and locks. Each layer of the lay-up was optimised figure 2-10, to help proved composite structures that are robust under nondeterministic loads.

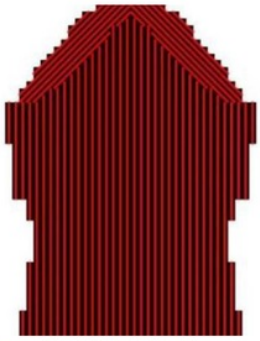


Figure 2-9, Initial Structure

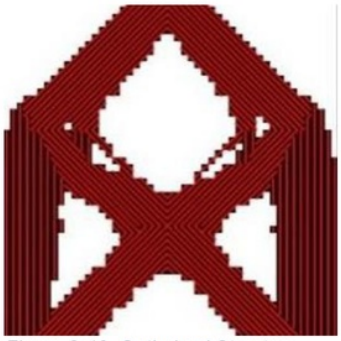


Figure 2-10, Optimised Structure

Optimisation has also been used to help with surgical implants, custom designed implants have been made for patients' thanks partly to the use of optimisation. Designs of implants have been freed up allowing more informed surgical decisions to be made. Any number of concept designs can be considered virtually before being made. (Coring Group, 360 Knee Systems, 2019) An optimised implant can be seen in figure 2-11.

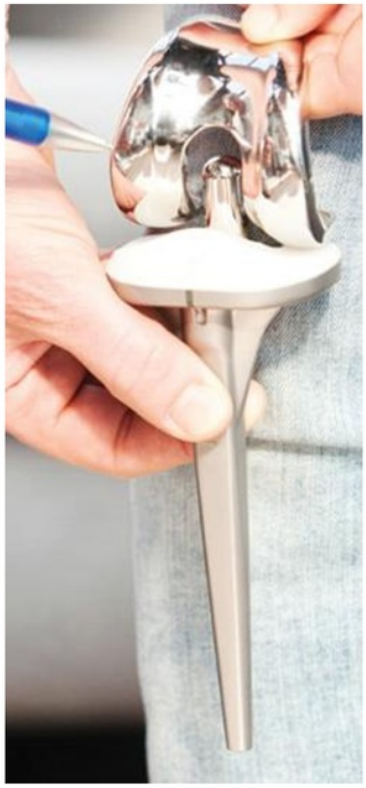


Figure 2-11, Optimised Implant

2.4 Upright Design

There are two key criteria, as explained by (Staniforth, 1994), that need to be considered when designing uprights;

- Do not come into contact with the wheel rim
- The further outboard they can be placed the less the wheel levers against the suspension links

It was also observed that the upright could, perhaps justifiably, be called more important than other items that make up a car's suspension. This is due to the upright needing to be able to withstand multiple loads, stress and strains whilst also having to have both suspension arms, brake callipers, steering arms and even brake ducts attached to it. All while keeping within the design constraint of the wheel's internal diameter. (Staniforth, 1994)

This was also noted in '*Design and Optimization of an Upright 2007*' (Wong, 2007) where it is stated that, as the upright can be exposed to shock loads as a result of the driver hitting a kerb, the upright must be stiff and strong enough to withstand these sudden abnormal loads. Whilst also being light and simple to install on the car.

The highest loads the upright can be expected to need to withstand when on track are shock loads as stated above, along with a 'worst case' scenario. The 'worst case' scenario would be when the car is braking during cornering. (Dhakar & Ranjan, 2016)

It is not only the forces that the upright is exposed to when on track that need to be considered. The suspension geometry will have a great influence on the path that the wheel will take when provoked away from its resting position. Because of this a good suspension system will have as little compliance as possible, as such the compliance within the upright itself must be considered critical. (Smith, 1978)

This point is further backed up in '*Fundamentals of Vehicle Dynamics*' (Gillespie, 1992). Gillespie states that the suspension must keep the tyres of the car in predictable contact with the track as otherwise the driver cannot perform to their maximum potential, thus highlighting the importance of control over the geometry through the suspension components, where the upright serves as a primary attachment point.

2.4.1 Weight Saving

As pointed out in Tune to Win, (Smith, 1978) the ability to accelerate faster than a competitor is the most important factor in racing. One of the factors that governs this is the gross weight of the vehicle. Therefore, it can be said that weight reduction is a key factor in racing, if the vehicle is lighter it will be able to out accelerate a competitor (assuming everything else being equal).

The same can be said for cornering power, again noted by (Smith, 1978), where it was stated that the cornering capacity of the tyres has a big influence on cornering power and again is influenced by the vehicles weight. This is not surprising as the benefit of the reduction of unsprung mass also helps to increase the mechanical grip available to the driver. (Bergrath, 2002).

As seen in competition car suspension, (Staniforth, 1994), it is important to reduce the unsprung mass as it can have a great effect on the heat generated into the suspension dampers and associated mountings.

Reducing mass can also lead to less weight transfer, assuming all other things being equal. The reduction of weight transfer is useful as it leads to higher traction which can lead to being able to deploy more power sooner than the competition. (Alexander, 1991).

2.4.2 Geometrical Considerations

When designing a new upright it is important to take into account the effect the upright could have due to placement of attachment points on the geometrical properties of the suspension. Some of these properties and their effect are explored below.

2.4.2.1 Camber

Camber is defined by the SAE recommended practice J670e as *'the outward angular lean of wheel relative to vehicle reference frame',* where outward lean is positive. (SAE, 1976)

Negative camber can help to increase the cornering power available. However, it is important to note that camber is relative to the surface of the road and not the chassis. Small amounts of camber give increases in cornering power due to a term known as 'camber thrust'. This occurs due to the straightening out of the tyres contact patch arc as the tread of the tyre rolls across the track. If positive camber is applied to the car then cornering power decreases as the camber thrust force acts away from the centre of curvature. (Smith, 1978)

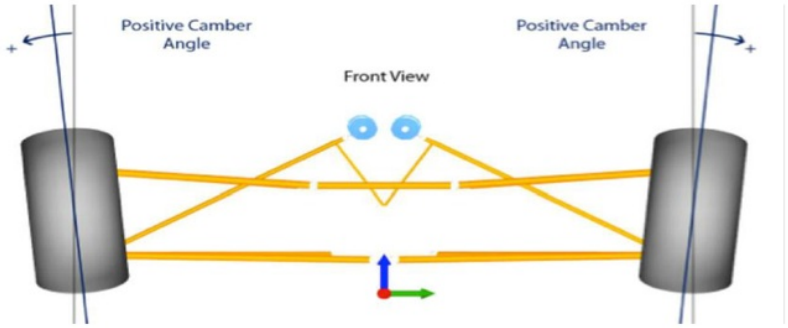


Figure 2-12, Camber, (Car-Engineer, 2019)

2.4.2.2 Toe

Toe is defined by the SAE recommended practice J670e as '*inward steer of wheel relative to the vehicle reference frame'*, where inward steer is positive. (SAE, 1976)

There can be thought of being two toe values, one when measured when the vehicle is parked in a workshop, and another value when the vehicle is on track undergoing movement. Therefore, toe angles can vary due to tyre forces and suspension bushings.

Zero toe would give low rolling resistance and minimal tyre wear, with a combination of toe-in on the front and toe-out on the rear a car will make a car stable and less prone to understeer. With the opposite setup the car would be more prone to oversteer. (Bengt, 2015)

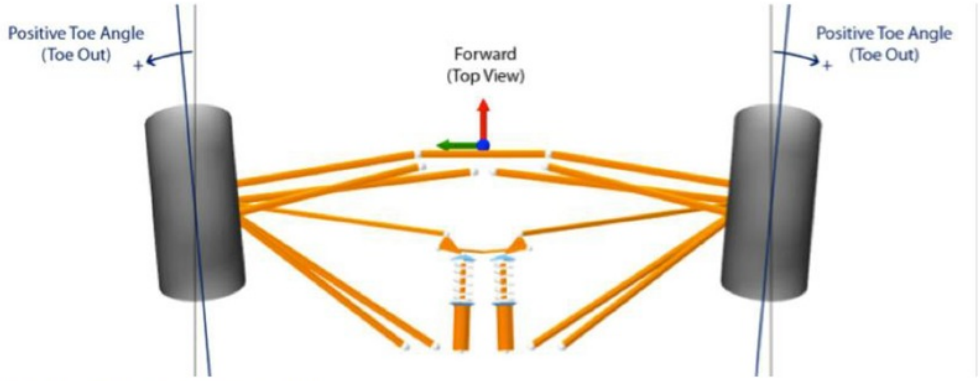


Figure 2-13, Toe, (Car-Engineer, 2019)

2.4.2.3 King-Pin Inclination

King-pin inclination is known as the angle in a front view between the steering axis (or Kingpin) and the vertical axis. (Bengt, 2015)

King-pin angle can have a big effect on the lift a wheel experiences during cornering. The grater king-pin inclination the higher the lift will be when the car is steered. Camber can also be affected as a result of king-pin inclination, as kingpin increases the wheel will lose camber with greater steering lock applied. This leads to positive camber on the outside wheel, whilst not disastrous, it is less than ideal on small tight technical tracks. (Milliken & Milliken, 1995)

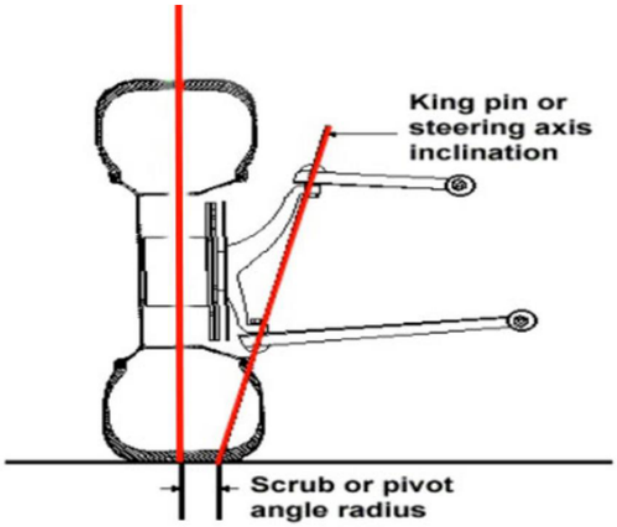


Figure 2-14, King-Pin Inclination, (Bengt, 2015)

2.5 Literature Review Conclusion

The literature review aimed to cover certain themes and aspects regarding race car component design, this has allowed a greater understanding of areas that were previously not very well understood.

For example, the grade of material chosen can have a big impact on the performance of a component and in some extreme cases could even be unsafe if used for the wrong application. After the research carried out and careful consideration, it has been decided to design the new upright using Aluminium 6061-T6. This is because the current upright is of this grade and a new upright could be machined from a block using university machines. The upright also displays no signs of fatigue over the 4 seasons that the university has raced the car.

This literature review has enabled the research and discovery of an important phenomenon with regards to suspension, in that the unsprung mass of a race car can has a great effect on the heat generated within the suspension dampers. This had not been considered in the project's initial benefits.

The themes covered in the above review will lead to a higher quality project being carried out, with the result of meeting the aims that have been stated previously.

3 Methodology

3.1 Attachment Points

To avoid confusion, figures 3-1 and 3-2 show each attachment point Circled. The attachment points are as follows:

- Top, figure 3-1
- Lower, figure 3-2
- Steering, figure 3-1
- Brake Top, figure 3-1
- Brake Lower, figure 3-2

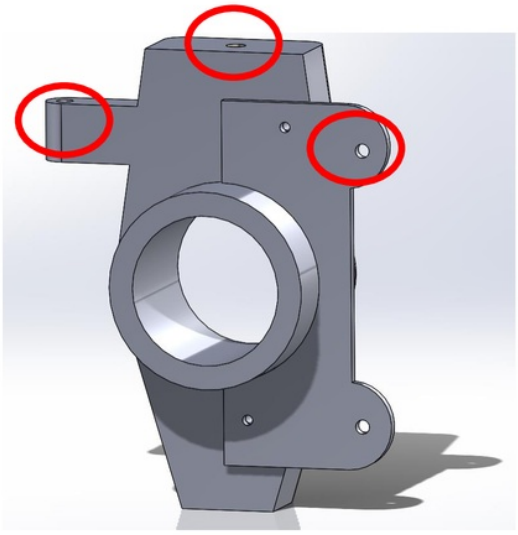


Figure 3-1, Current Upright

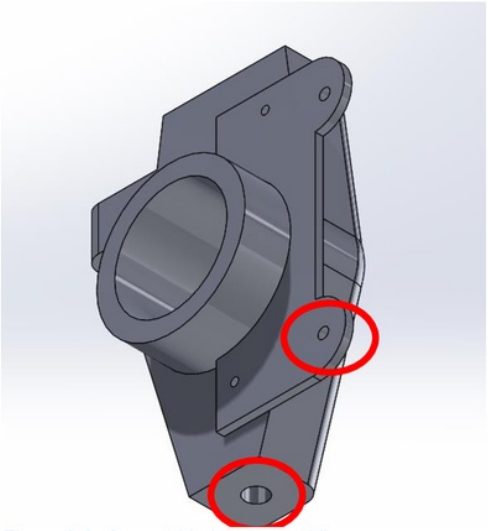


Figure 3-2, Current Upright Lower View

3.2 Initial CAD Model

The initial CAD geometry was provided by Team MCR and can be found in figure 3-3;

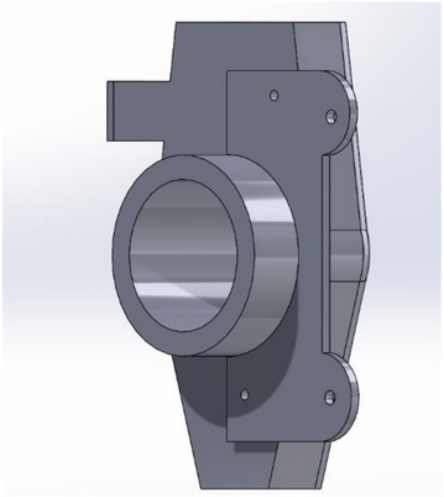


Figure 3-3, Initial CAD Geometry, (UWTSD / Team MCR, 2017)

The twist rig that the upright was tested on in the workshop was recreated in CAD and is shown below (Figure 3-4). This was created to allow the real-world experiments to be repeated in the FE package and correlated so that the newly optimised design could also undergo FEA and confidence could be had in the results.

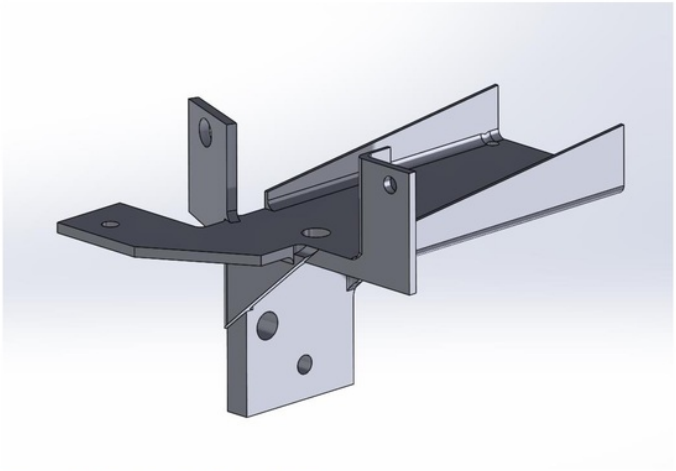


Figure 3-4, Twist Rig, (Katwa, 2018)

3.3 Package Space

In order to be able to carry out the design optimisation, the space available for the new upright design needed to be established. Therefore, the car was examined, and it was found that the upright would need to fit within the 13' front wheels. Another key point of note was the brake calliper location. As can be seen in figure 3-5, the brake calliper clearance is tight and currently has a measured clearance of 3.5mm. The lower suspension clearance is also shown for reference figure 3-6.

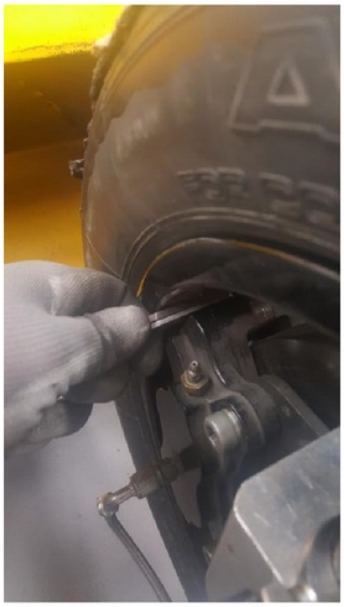


Figure 3-5, Brake Calliper Clearance



Figure 3-6, Lower Suspension Clearance

To allow for clearance of the wheel rim, the package space was sized at 320mm or 12.5'. This was created in the CAD software package to allow the optimisation software to 'know' where material can be for the new upright.

3.4 Non-Designable Region

Just as the optimisation package needs to 'know' where material can be, it also needs to 'know' where material cannot be located, and this is known as the non-designable region. The non-designable region is where material needs to be regardless of the new design. This is because the non-designable region includes the attachment points and the stub axle hole. A picture of the non-designable region can be seen below.

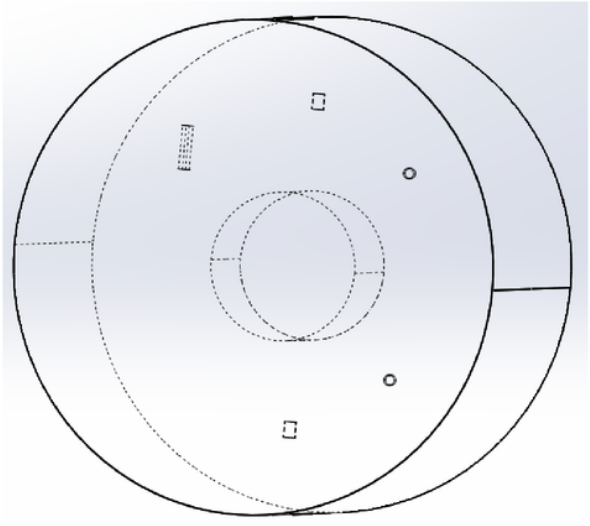


Figure 3-7, Non-Designable Region

3.5 Optimisation Setup

The package space had the non-designable region subtracted from it to leave cavities where the non-designable region was. This was then used as the model for the optimisation.

Most topology studies are carried out with the objective to minimize strain energy subject to mass fraction. This provides stiff structures whilst only using a pre-determined amount of material. (MSC Software, 2007)

3.5.1 Mesh

First the model was meshed in Solidworks using a fine draft quality mesh. The meshed model was then exported to Design Studio.

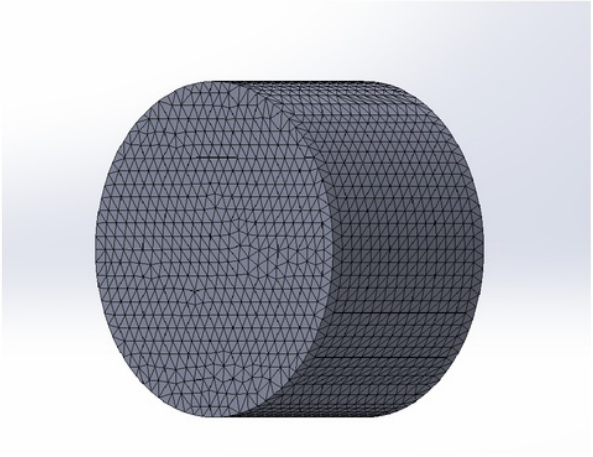


Figure 3-8, Meshed Package Space

3.5.2 Package Space Simplification

Once in Design Studio, a second skin of elements was created to allow the package space and non-designable region to be separate. The package space and non-designable region can be seen in figure 3-9 and figure 3-10 respectively below;

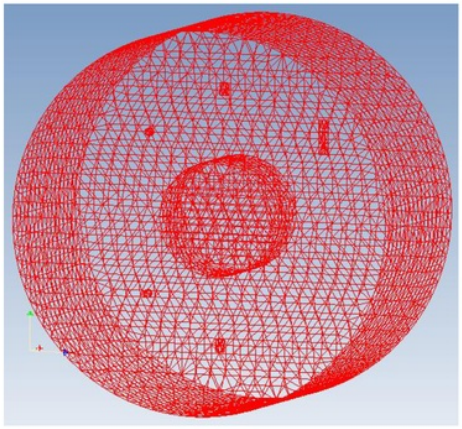


Figure 3-9, Package Space

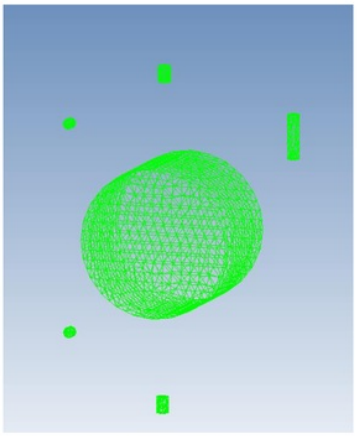


Figure 3-10, Non-Designable Region

Next, the package space needed to be simplified, this would allow a reduction of computing time needed to carry out the optimization and also limit where the optimisation will take place within the package space. The simplified package space can be seen below in figure 3-11.

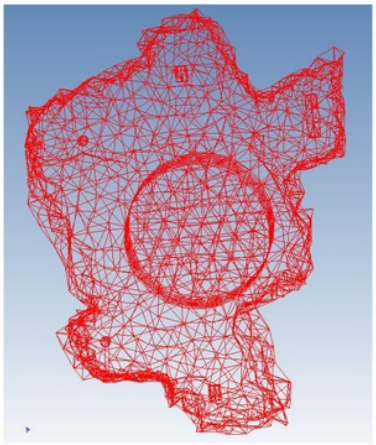


Figure 3-11, Simplified Package Space

3.5.3 Constraint Setup

Once the package space had been simplified, the topology constraints were set up. Without having and constraints applied, the structure would be free to move about in an unlimited fashion, thus meaning the solver would not be able to solve (Singiresu, 2004). Each test that was carried out in the workshop was named and setup. The model was constrained around the attachment points matching how it was constrained when tested. This can be seen in the figure 3-12 below, there are 15 tests setup matching the 15 tests carried out in the workshop, X, Y & Z for each attachment point.

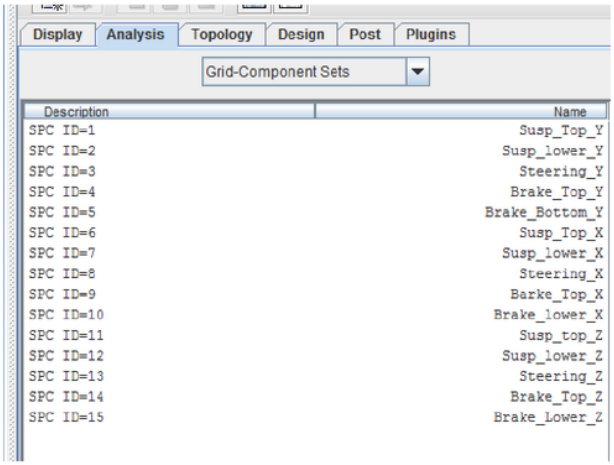


Figure 3-12, Constraint Setup

3.5.4 Static Load Setup

The static loads were setup to allow them to be added to the constraints to setup the individual load case. The load was applied directly to the attachment point, as the load used in the workshop testing was 15Kg, 150N was entered. This small load was used to prevent damage to the upright due to the lack of a spare. As seen in graph 2, this meant that any deformation was well within the elastic limit of the material. This load was divided by the number of grids that represented a particular attachment point. This load was placed in the direction that was loaded in the workshop and was represented by a 1 next to that particular vector in the setup table.

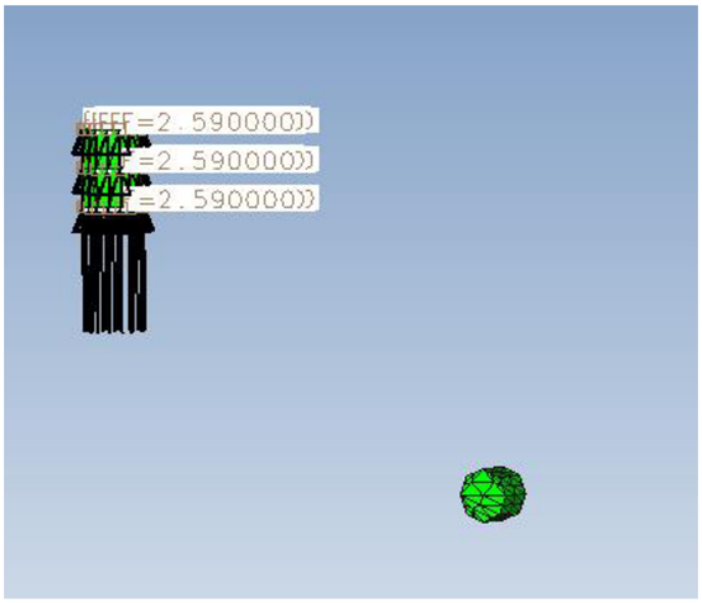


Figure 3-13, Static Load Setup at Top Attachment Point

3.5.5 Load Case Setup

With the constraints and static loads setup, the load case for each individual test could be setup. This was done by simply selecting the corresponding static load and constraint. Displacement and stress values were selected to be outputted as the results. This is so that the results can be looked at before running the optimisation and then be used for the optimisation. Figure 3-14 shows this was done for each of the 15 tests. This is shown below.

Loadcases

Description	Name
STAT ID=51	Susp_Top_Y
STAT ID=52	Susp_Top_X
STAT ID=53	Susp_Top_Z
STAT ID=54	Susp_low_Y
STAT ID=55	Susp_low_X
STAT ID=56	Susp_low_Z
STAT ID=57	Steering_Y
STAT ID=58	Steering_X
STAT ID=59	Steering_Z
STAT ID=60	Brake_top_Y
STAT ID=61	Brake_top_X
STAT ID=62	Brake_top_Z
STAT ID=63	Brake_Bottom_Y
STAT ID=64	Brake_bottom_X
STAT ID=65	Brake_bottom_Z

Figure 3-14, Loadcases for Optimisation

An example of a load case is also demonstrated by figure 3-15, showing the load applied and the relevant constraints.

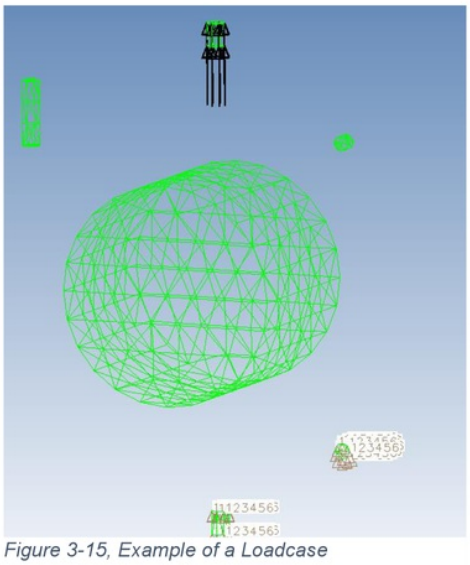


Figure 3-15, Example of a Loadcase

3.5.6 Optimisation Parameters

Firstly, the topology region needed to be setup. As the package space was the topology region, this was selected and modified to use an initial mass fraction of 0.05. This allows the solver to focus on the most important 5% of material (Vanderplaats Research & Development, n.d.). 5% was selected to allow the potential for a high weight saving in order to meet the aim of the project.

As the objective with the topology optimisation is to keep the same stiffness whilst losing mass, this objective needed to be setup in the solver, therefore the parameter strain energy – minimum was selected for all load cases. As previously stated, the constraint of the topology is to use the most important 5% of material so this was setup as the upper bound for the solver.

The optimisation was then ready to run.

3.6 FEA Model Setup

In order to carry out FEA on the upright, first a representative model had to be made. This was done using the CAD models of the upright and the twist rig. The upright was orientated as it was in the workshop against the twist rig and alloy steel Solidworks material characteristics were applied to the model to represent the twist rig and brake calliper plate.

The model was then meshed in Solidworks using the draft quality option with a 10mm mesh size. The model was then exported to allow use in Design Studio.

Once in Design Studio, to improve the accuracy of the results of the FEA, the mesh was split using Design Studio and the elements were also converted to second order elements. This was done as second order elements provide a better representation of the geometry that is being meshed due to the presence of mid nodes that allow deformation to be captured more accurately. (Simscale, 2016)

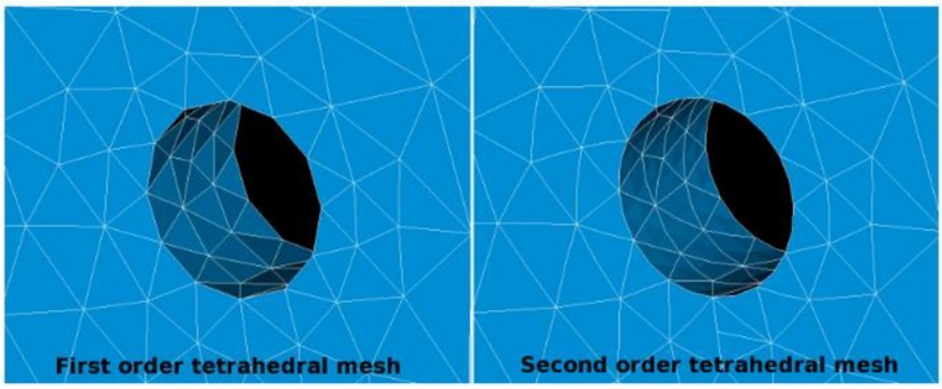


Figure 3-16, Comparison of First and Second Order Mesh, (Simscale, 2016)

FEA was ran with both first and second order elements and the results of the comparison can be seen below in table 2. (results in mm). When compared to the workshop result of 0.51mm, it can be seen that with second order elements, the deformation has been more accurately captured. Therefore, all future FEA was ran with second order element mesh.

Table 2, FEA Results for First and Second Order Meshes

Attachment Point	First Order	Second Order
Brake Low X	0.31	0.42

3.6.1 Material Selection

As alloy steel had been assigned to the model in Solidworks, the upright needed to be assigned the correct material independently of the rest of the model.

A new material group was made in Design Studio, and the following properties (Table 3), for Aluminium 6061-T6 were taken from Solidworks and added. The twist rig and brake calliper plate were left as alloy steel.

Table 3, Aluminium 6061-T6 Properties

E	Elastic Modulus	6.90E+10
G	Shear Modulus	2.60E+10
Nu	Poissons Ratio	0.33
Rho	Mass Density	2700
A	Thermal Expansion Coefficient	2.40E-05
St	Tensile Strength	3.10E+08

In order to assign the correct material properties, a new group was created for the upright and the material assigned to this group was Aluminium 6061-T6. Moving the upright to the new group was done by selecting all the elements of the mesh that represent the upright and selecting the modify tool to move the elements into the newly created group.

Figure 3-17 shows the upright in its own group.

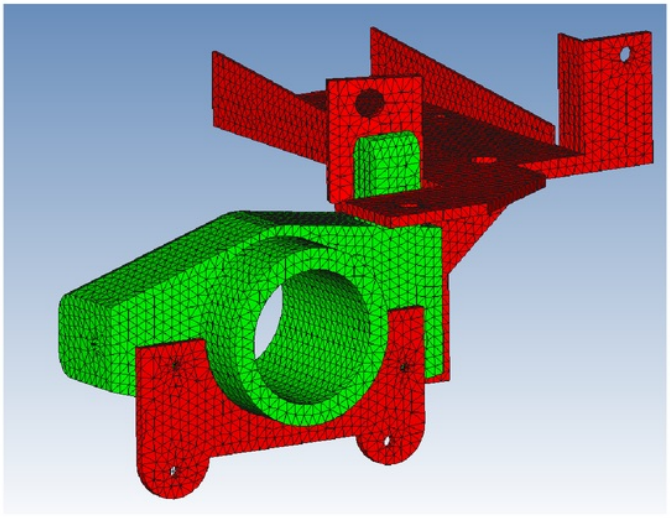


Figure 3-17, Upright Shown in Separate Group

3.6.2 Rigid Body Elements Selection (RBE)

In order to represent how the upright was bolted in the workshop, RBE elements were used. This is because an RBE can transfer stiffness as a rigid body and is always numerically stable for the solver. (Predictive Engineering, 2013). Therefore, it is ideal to not only represent bolts but also represent the stub axle bearing in the centre of the upright.

To setup the RBE elements in the model, independent and dependent elements needed to be selected. The independent element represents the bolt and the dependent elements represent what the bolt touches. To represent the bolt, a new element was created in the centre of the hole. As the dependent elements represent what the bolts touch, the elements within the attachment point on the upright, and the elements in the twist rig holes were selected. The elements selected varied depending on the test being carried out. The same method was used to represent the bearing. Figures 3-18 and 3-19 show examples of the RBE on the model.

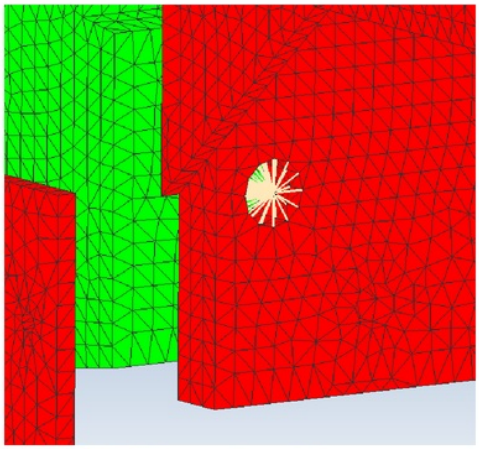


Figure 3-18, RBE Representing a Bolt

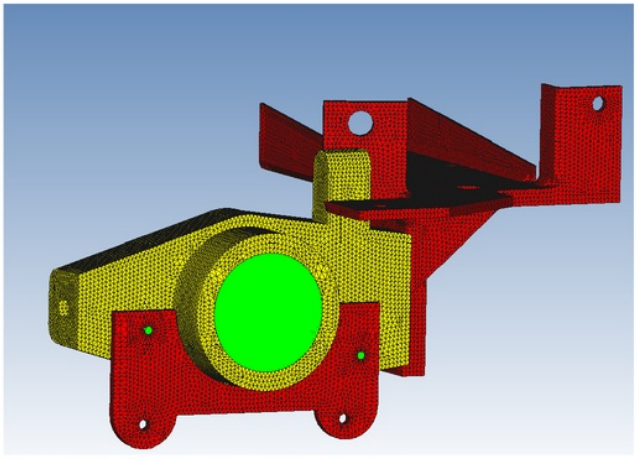


Figure 3-19, RBE Representing the Bearing

3.6.3 Static Load Setup

The loads were setup in much the same way as they were for the optimisation setup. However, as multiple attachment points were tested in one orientation in the workshop, this would be replicated by setting up multiple static loads to allow for multiple loadcases as appropriate. An example of this is shown in figure 3-20.

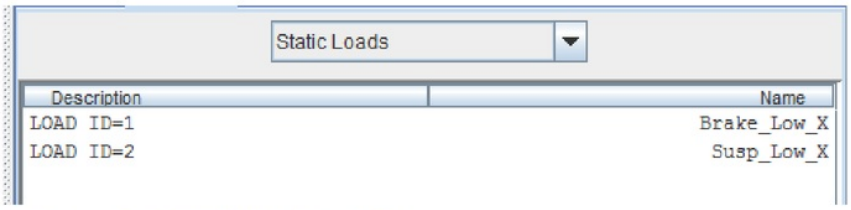


Figure 3-20, Example of Static Loads for FEA

3.6.4 Constraint Setup

As was the case with the static load setup, the constraints were setup a similar way, and each model was constrained as representatively to the workshop test as possible. The elements selected were the holes on the twist rig that were bolted to the worktop in the workshop. They were fixed in 6 degrees of freedom. The elements between the holes, (figure 3-21), were also constrained to represent the force of the bolts acting on them, therefore they were constrained in the positive Z direction. i.e. the elements were not free to move up of down and couldn't move in any other direction because of the constraints on the bolt hole elements.

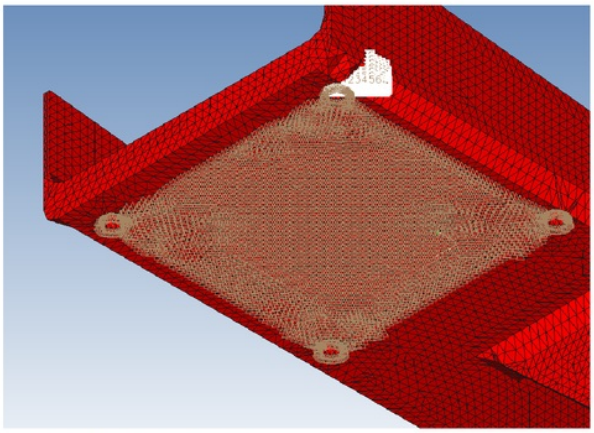


Figure 3-21, Rig Constraints

3.6.5 Loadcase Setup

The loadcases were setup in the same manner as they were setup for the optimisation. Again, displacement and stress were outputted, this would allow any stresses that occur to be seen and more importantly output the displacement seen by the upright. This is the data that would be correlated with the workshop testing.

An example of a loadcase can be found in figure 3-22.

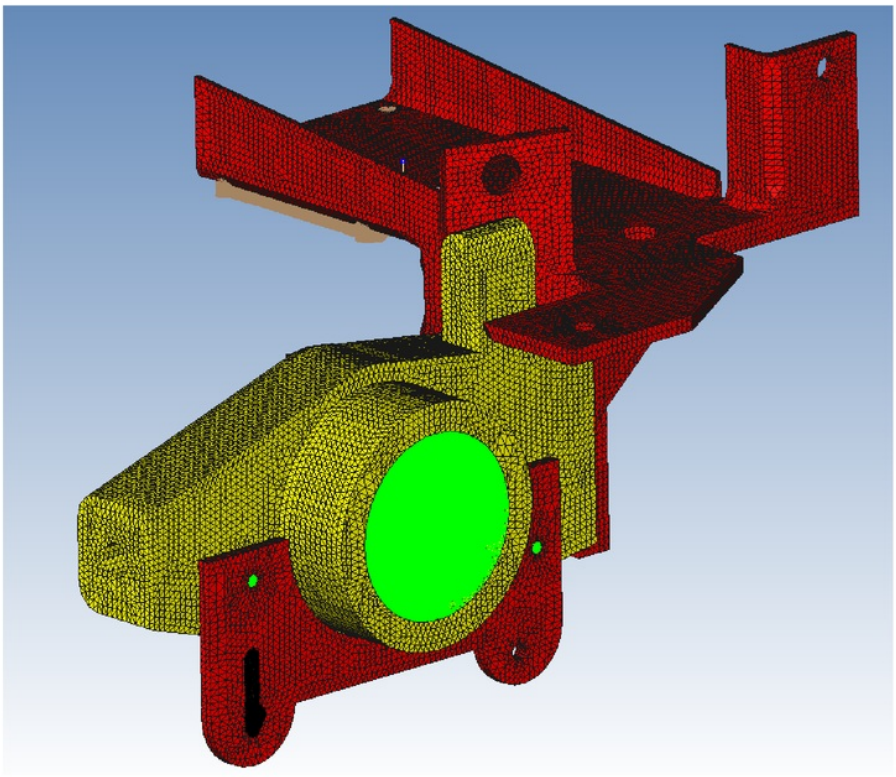


Figure 3-22, Example FEA Loadcase

4 Results

The testing was carried out following the axis used in international standard ISO8855 / SAE J670 for road vehicles. (International Organization for Standardization, 2011)

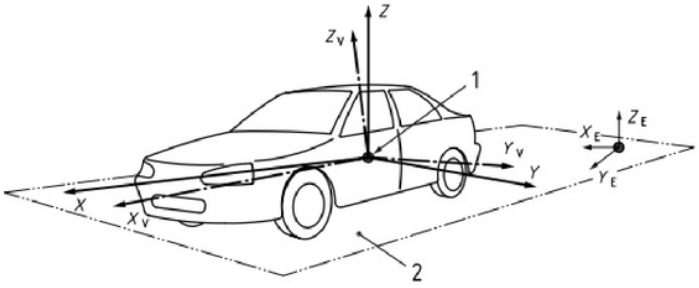


Figure 4-1, Axis for Road Vehicles, ISO Standard, (International Organization for Standardization, 2011)

4.1 Practical Testing Results

The practical testing was carried out in the university workshop. The upright was secured in two different places as best as possible for each test to ensure that it could not twist due to weight being added to the attachment point that was being tested.

Each attachment point was tested in 3 directions, X,Y,Z, to fully characterise the deflection experienced when loaded. Two DTI gauges were used to measure the deflection that occurred in the rig due to the loading. A third DTI gauge was used and placed as close to the attachment point as possible. This was conducted in order to record the deflection seen, when the load of 15kg was applied directly to the attachment point. The weight was hung on each attachment point's bolt. A picture of the test setup can be found below in figure 4-2. Contained in appendix 3 are pictures of each orientation the upright was tested in.

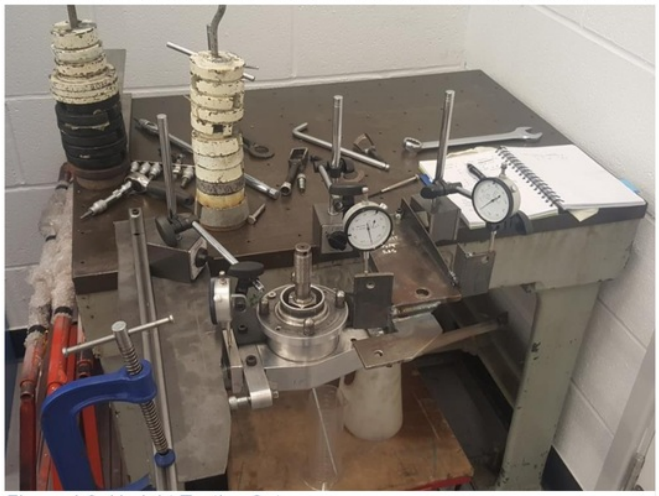


Figure 4-2, Upright Testing Setup

The results of the testing were tabulated and can be found below in tables 4, 5 and 6. The highlighted column displays the deflection at the attachment point whilst the 'Twist' columns display the deflection on both sides of the rig.

Table 4, X Direction Testing Results

Attachment Point	X	Possible Error	Possible Error	Twist Rig	Possible Error	Possible Error	Twist Rig	Possible Error	Possible Error
(All dim in mm)		+	-	L	+	-	R	+	-
Top	1.03	1.035	1.025	0.28	0.285	0.275	0.1	0.105	0.095
Bottom	0.26	0.265	0.255	0.19	0.195	0.185	0.02	0.025	0.015
Brake Top	1.01	1.015	1.005	0.29	0.295	0.285	0.03	0.035	0.025
Brake Bottom	0.51	0.515	0.505	0.13	0.135	0.125	0.01	0.015	0.005
Steering	0.62	0.625	0.615	0.3	0.305	0.295	0.08	0.085	0.075

Table 5, Y Direction Results

Attachment Point	Y	Possible Error	Possible Error	Twist Rig	Possible Error	Possible Error	Twist Rig	Possible Error	Possible Error
(All dim in mm)		+	-	L	+	-	R	+	-
Top	0.34	0.345	0.335	0.2	0.205	0.195	0.06	0.065	0.055
Bottom	0.27	0.275	0.265	0.19	0.195	0.185	0.05	0.055	0.045
Brake Top	0.67	0.675	0.665	0.19	0.195	0.185	0.02	0.025	0.015
Brake Bottom	0.59	0.595	0.585	0.16	0.165	0.155	0.03	0.035	0.025
Steering	0.23	0.235	0.225	0.22	0.225	0.215	0.02	0.025	0.015

Table 6, Z Direction Results

Attachment Point	Z	Possible Error	Possible Error	Twist Rig	Possible Error	Possible Error	Twist Rig	Possible Error	Possible Error
(All dim in mm)		+	-	L	+	-	R	+	-
Top	0.03	0.035	0.025	0.02	0.025	0.015	0.03	0.035	0.025
Bottom	0.02	0.025	0.015	0.02	0.025	0.015	0.01	0.015	0.005
Brake Top	0.03	0.035	0.025	0.01	0.015	0.005	0.02	0.025	0.015
Brake Bottom	0.4	0.405	0.395	0.08	0.085	0.075	0.02	0.025	0.015
Steering	0.12	0.125	0.115	0.05	0.055	0.045	0.09	0.095	0.085

As can be seen from the table 6, the smallest deflections were found when trying to 'stretch' the attachment points when loading in the 'Z' direction. Whilst the biggest deflection was found in the 'X' direction at the top suspension attachment point, table 4.

It is noted however that a potential error exists with using the available DTI gauges. This due to the resolution of the available gauges. The gauge could potentially read + or – 0.005mm on one increment so this margin for error was added into the tables. It is assumed the error is systematic. A systematic error is one that will be constant and repeatable. (Lartiga, 2001) Going forward, the measured values will be used to compare with the FEA results.

4.2 Optimisation Results

Once the optimisation software had ran, using the previously detailed methodology, the results were imported back into Design Studio to allow the results of the optimisation to be viewed. The optimisation had 6 design cycles. The result of the optimisation can be seen in figure 4-3 and is displayed within the package space (grey surrounding area);

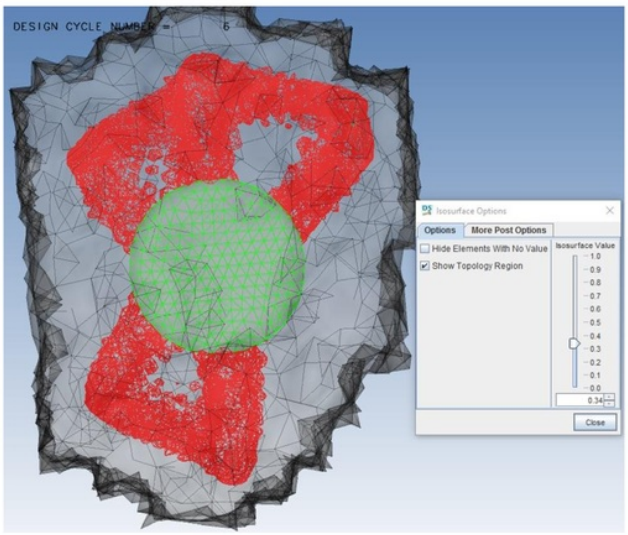


Figure 4-3, Optimisation Result

The optimisation of the upright shows where material can be lost and by changing the isosurface value, the important and non-important areas of the optimisation can be displayed. A high isosurface value shows where the most important areas for material to be are. Whereas a low value shows the opposite. The two figures below, 4-4 & 4-5 demonstrate this point.

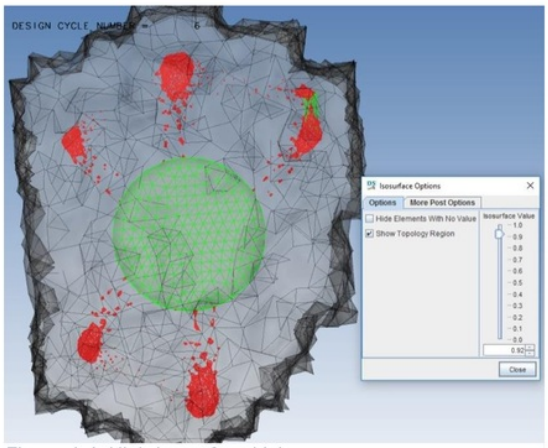


Figure 4-4, High Isosurface Value

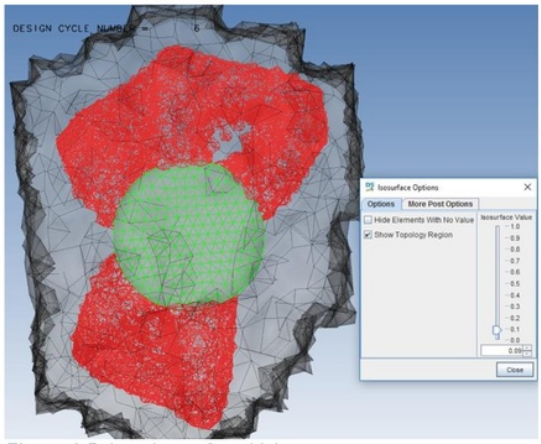


Figure 4-5, Low Isosurface Value

This optimisation result will form the basis of the new upright design, with the general shape of the optimisation result giving a good indication of the likely shape of the new upright. As to be expected, the key areas where material absolutely must be present in the new design is around the attachment points.

4.2.1 Mesh Study

After the optimisation was ran, it was decided to investigate the effect the mesh could have on the results of the optimisation this would allow an informed choice to be made on the mesh size going forward as well as seeing if different optimisation results would be obtained. Once imported into Design Studio, the mesh was split using the programs cutter. Table 7 shows the results of the study.

Table 7, Mesh Comparison

	Split Once	Split Twice
Avg Size	8mm	3mm
Grids	77,439	913,109
Elements	376,320	4,495,488
Time Taken	01:10	21:50

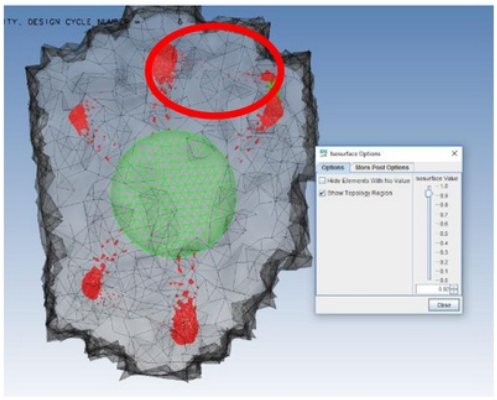


Figure 4-6, Results of Split Once Mesh

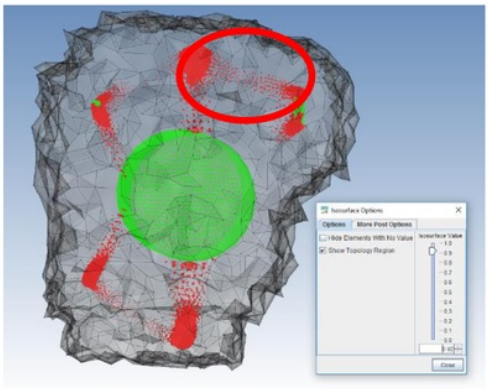


Figure 4-7, Results of Split Twice Mesh

As can be seen from circled areas in screenshots above, there is more detail in the results of the mesh that was split twice, figure 4-7 than there is in figure 4-6 which represents the mesh split once. The same basic feature outline can be seen in both, showing the mesh density has not yielded any significant influence over the design, giving additional confidence that the process has been conducted correctly. However, the extra 20 hours needed to run the optimisation with the finer mesh was deemed excessive when the results of the single split mesh were broadly as accurate. Especially given that the optimisation results are being used to inform future design, rather than form a definitive finalised version.

4.3 Optimised Upright Design

The results of the optimisation formed the basis for the new upright design. The current design was modified using the information learnt from the results of the optimisation.

The new design can be seen in figure 4-8. Using the mass properties feature of Solidworks, it was calculated that the new upright would be 0.95kg (26%) lighter than the current design. This weight saving is nearly double the initial aim of the project and would lead to a near 2kg saving across the front axle.

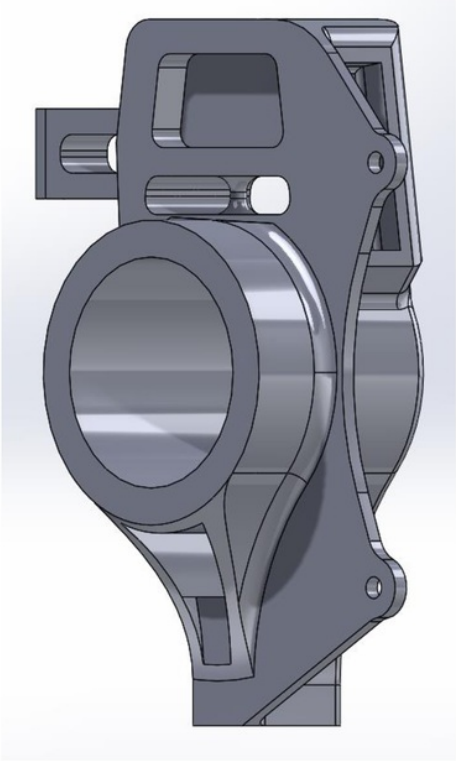


Figure 4-6, Optimised Upright Design

As can be seen from looking at the upright, the weight saving was achieved through the removal of material from the original upright. The brake bracket has also been integrated into one piece for the new design.

To ensure that the upright will not fail on track and to try and match the stiffness of the original upright, supports were added in the cut-outs where material had been removed. This is shown in figure 4-9. Figure 4-10 shows where material has been removed around the bearing hole helping to result in a light upright design. Figure 4-11 shows another cut out.

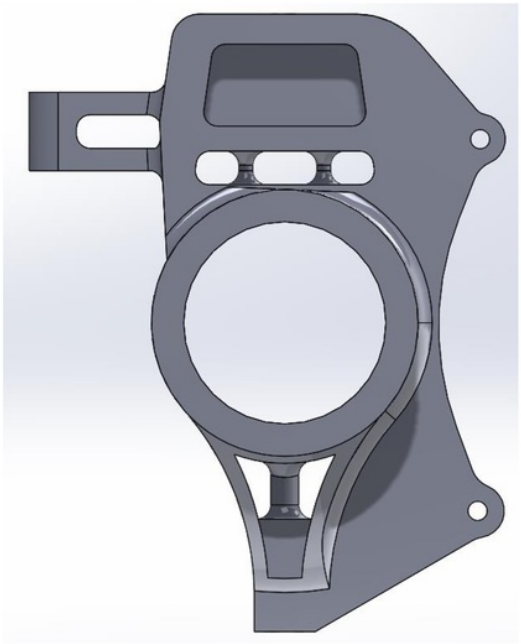


Figure 4-7, Front View of Optimised Upright

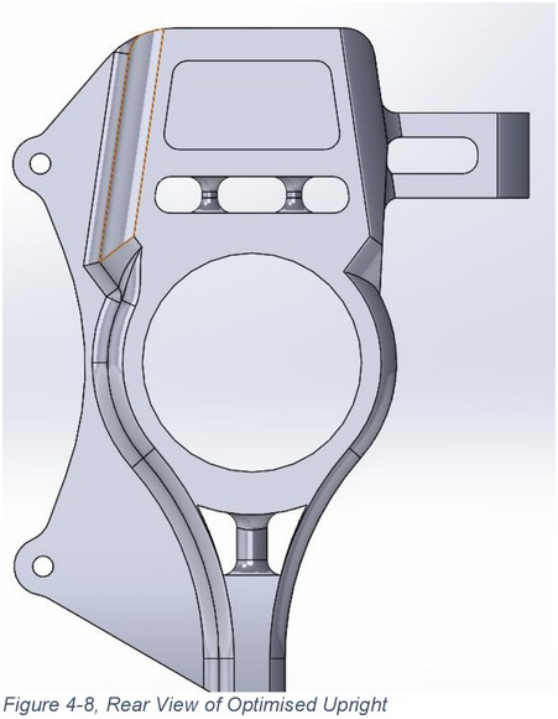


Figure 4-8, Rear View of Optimised Upright

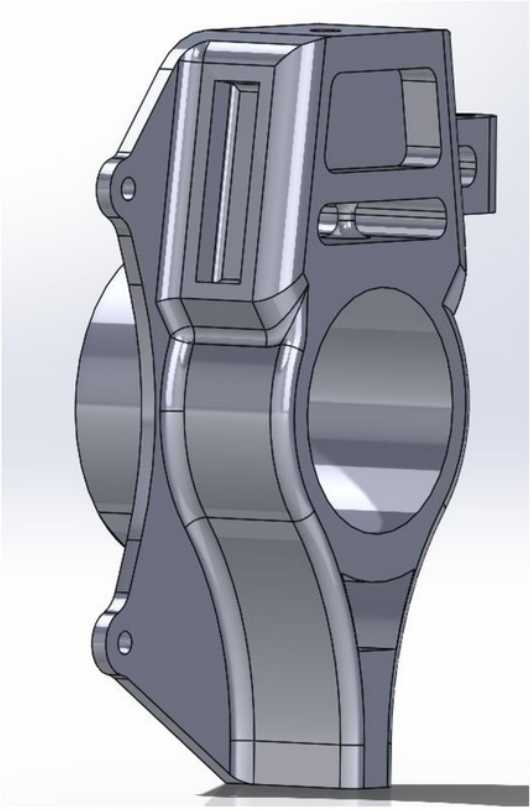


Figure 4-9, Side View of Optimised Upright

Looking at the optimisation results and the new design, the influence is clearly shown in figures 4-12 and 4-13, where it can be seen that the new design geometry correlates closely with the areas of critical material highlighted by the optimisation software.

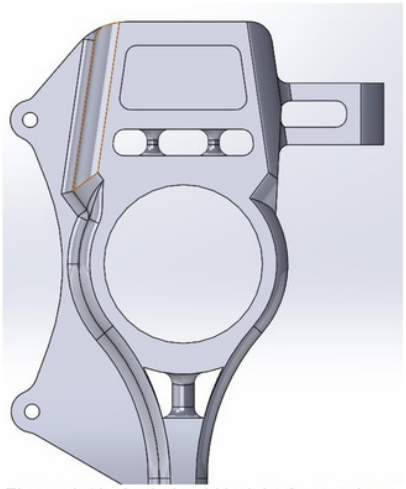


Figure 4-12, Optimised Upright Comparison

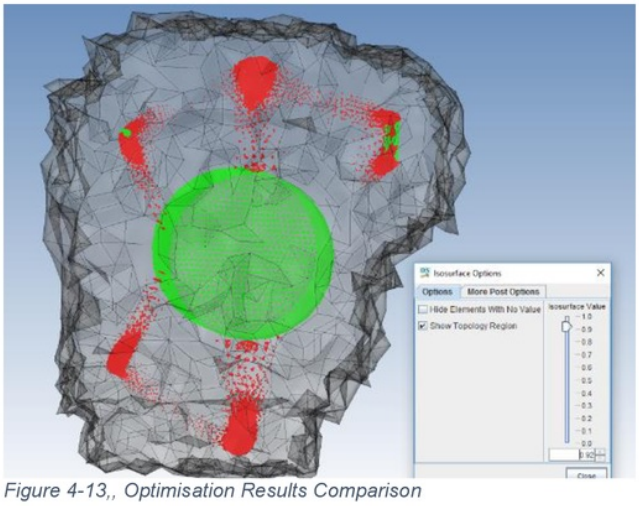


Figure 4-13,, Optimisation Results Comparison

When comparing the new and old designs side by side, figures 4-14 and 4-15, it is clear to see how the shape has been optimised, with significant areas of material having been removed, contributing to the mass reduction seen.

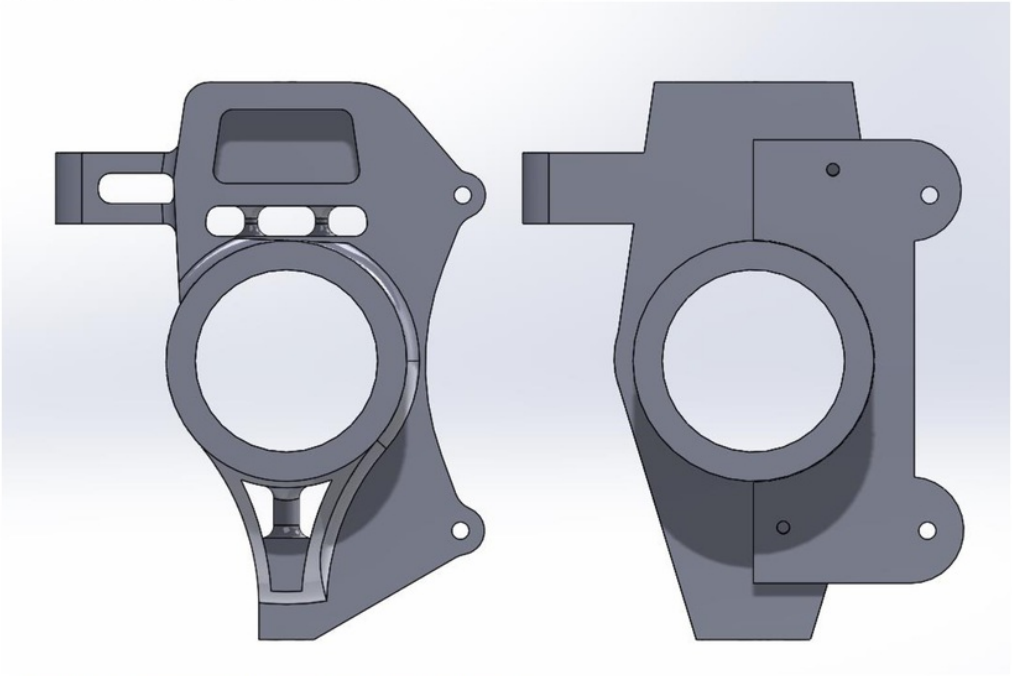


Figure 4-14, Comparison of Current and Optimised Upright

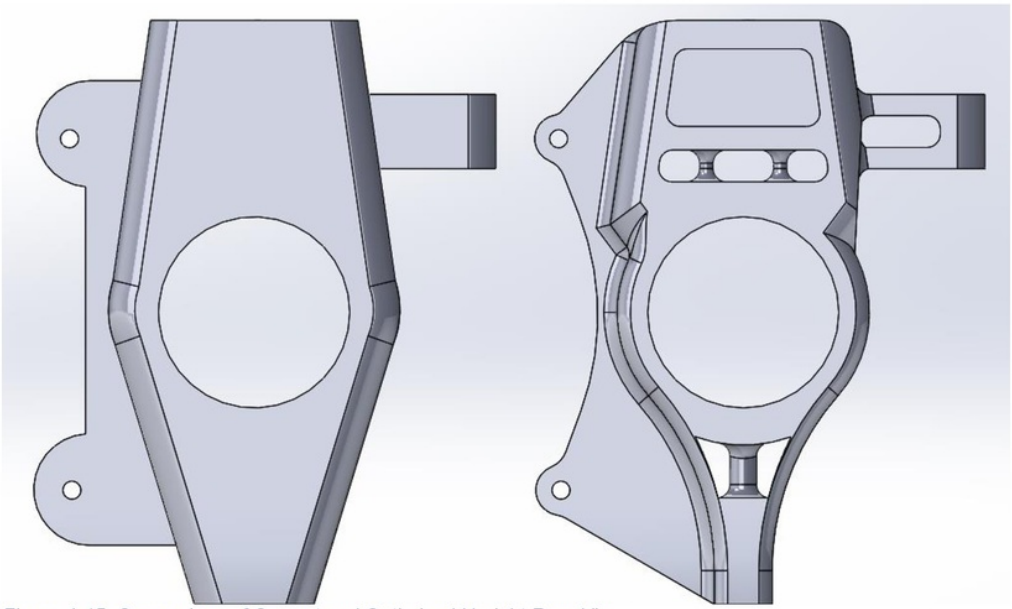


Figure 4-15, Comparison of Current and Optimised Upright Rear View

4.3.1 3D Printing

3D printing is a technology that is revolutionizing the automotive and aerospace industries. Scale models can be produced from CAD files within hours. It can help with feedback on designs and also help to show early stages of assembly. (Kumar, 2017)

The new upright design was 3D printed to allow a physical model to be handled and compared with the current upright physically.

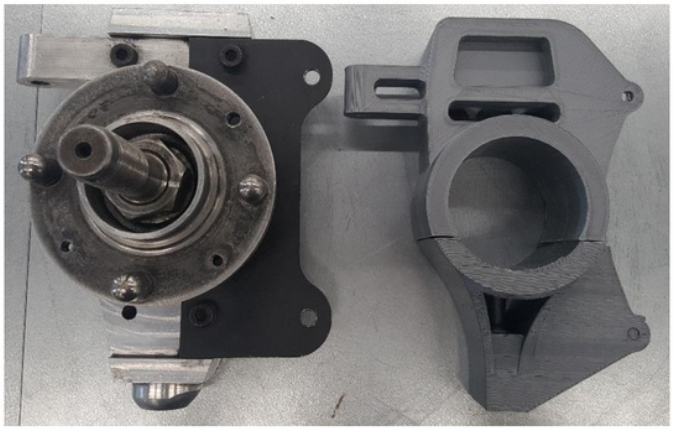


Figure 4-10, 3D Print Comparison

It can be seen from the figure 4-16, that the new design has undergone significant optimisation when compared to the current upright design. The prototype model allowed a fitment check of the brake calliper, figure 4-17, and it was found the calliper fits as required.



Figure 4-11, Calliper Fitment Check

4.3.2 MCR Upright

As stated previously, later built MCR chassis have an updated upright design, a photo of this upright was provided from John Hughes. (Figure 4-19)

As can be seen, the uprights look similar suggesting that MCR have also carried out a topology optimisation on the current upright for newer chassis. The key differences between the two uprights appear to be the triangulation of the steering arm bracket in the MCR design and the wider top half of the proposed new upright design.

The brake attachment points look similar between the 2 designs along with the weight saving measures around the bottom half of the upright. It can be said then, that as the MCR upright has ran without issue, the newly proposed upright should also be able to be ran without issue owing to the similar designs.

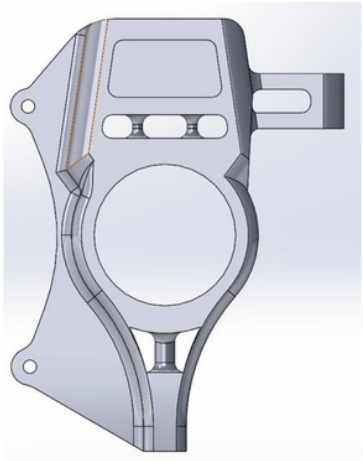


Figure 4-12, Optimised Upright Rear



Figure 4-13, MCR Upright Rear

4.3.3 Design Considerations

The positioning of the brake calliper mounting on the upright was not changed because there is limited space available to move the calliper. This is due to the already tight clearance thanks to the proximity of the inside of the wheel as seen in figure 3-5.

Therefore, this would also ensure that the new upright design met one of the projects original targets that the uprights should be interchangeable. The only other feasible place to move the brake calliper would be forward of the disc. However, this is not ideal as then the mass of the callipers, 1.75kg is being placed outside the wheelbase of the car and exposing the steering joint to a high heat zone which could cause failure. Furthermore, it has been found that the rear of the front wheel is ideal for brake cooling (Farias, 2015)

The effect of brake temperatures and heat cycles also needs to be considered when designing the new upright as aluminium's properties will change when heated. However, a limitation of the FEA carried out is that it is assumed that the test is happening at room temperature much like the workshop testing. AP Racing carried out a study on brake temperatures where it was found that *'brake temperatures should be maintained between 400-600 degrees Celsius for optimal performance'.* (AP Racing, 2011). Therefore, it would be beneficial to take this heat into consideration and re-test the new upright design, however due to time constraints this was not possible.

The heat properties of aluminium 6061-T6 can be found below. (ASM Aerospace Specification Metals Inc, 2018)

Table 8, Aluminium 6061-T6 Heat Properties, (ASM Aerospace Specification Metals Inc, 2018)

Thermal Properties			
CTE, linear 68°F	23.6 µm/m-°C	13.1 µin/in-°F	AA; Typical; Average over 68-212°F range.
CTE, linear 250°C	25.2 µm/m-°C	14 µin/in-°F	Estimated from trends in similar Al alloys. 20-300°C.
Specific Heat Capacity	0.896 J/g-°C	0.214 BTU/lb-°F	
Thermal Conductivity	167 W/m-K	1160 BTU-in/hr-ft²-°F	AA; Typical at 77°F
Melting Point	582 - 652 °C	1080 - 1205 °F	AA; Typical range based on typical composition for wrought products 1/4 inch thickness or greater; Eutectic melting can be completely eliminated by homogenization.
Solidus	582 °C	1080 °F	AA; Typical
Liquidus	652 °C	1205 °F	AA; Typical

The specification of the bearing was not considered, and a new bearing was not specified. This is because the bearing is a stock part and therefore there is a readily available supply of bearings from the manufacturer of the race car. There is also the possibility of needing to redesign supplementary components such as the stub axle. Team MCR did not want the current bearing being removed as it is a press fit and would be destroyed upon removal. This meant that the current bearing is unknown to the author and could not be researched further in order to calculate and specify a suitable new bearing recommendation.

4.4 FEA Results

The original upright was run through FEA in order to allow comparison with the new optimised upright. However, it would also allow validation of the workshop testing if the results were broadly similar. This would mean that confidence could be had in the new upright design if it showed similar deformations to the original upright when tested in FEA under the same conditions. The FEA results were retrieved in the post processing and taken in the same location as the DTI's were placed in the workshop. An average of the deflection around the area was taken. Results for all FEA tests can be found in appendix 4.

4.4.1 Workshop Vs FEA Results (Current Upright)

The results of the workshop testing compared to the FEA results for the current upright were tabulated and are displayed in the tables 9, 10 and 11. The percentages in red indicate that the FEA is over predicting the deflection compared to the workshop measured deflection.

4.4.1.1 X Direction

Table 9, Current Upright FEA Results X Direction

Attachment Point	Upright			Twist Rig					
X	Workshop	FEA	Difference	Workshop	FEA	Difference	Workshop	FEA	Difference
	mm	mm	%	L	L	%	R	R	%
Top	1.030	2.400	133	0.280	0.457	63.18	0.100	0.042	58.5
Bottom	0.260	0.170	35	0.190	0.049	74.05	0.020	0.028	4
Steering	0.620	2.170	250	0.300	0.421	40.33	0.080	0.039	51.88
Brake Top	1.010	1.760	74	0.290	0.415	43.41	0.030	0.037	23
Brake Low	0.510	0.160	68.63	0.130	0.051	60.62	0.010	0.020	103

Looking at the results for the X direction, table 9 it is clear to see some differences between the workshop results and the FEA. The differences were shown as a % as it was felt this would provide an easy indication of which results were different. The measurement of the rig deflection was also measured and compared to workshop testing.

As previously mentioned, the FE models were setup and constrained as close as possible to the workshop testing. However, where the FE model couldn't accurately replicate the real-world testing is clear to see. For example, the steering arm has a 250% difference, this could be due to the FE model not being constrained correctly as when tested in the workshop the upright also had a support resting underneath constraining it in 2 places. Figure 4-20 shows the result of the steering arm being tested in the X direction.

Although the % differences look high this is only down to the small load used and thus the small deflections that result. This means that any differences between the workshop and FEA results will give a high % difference.

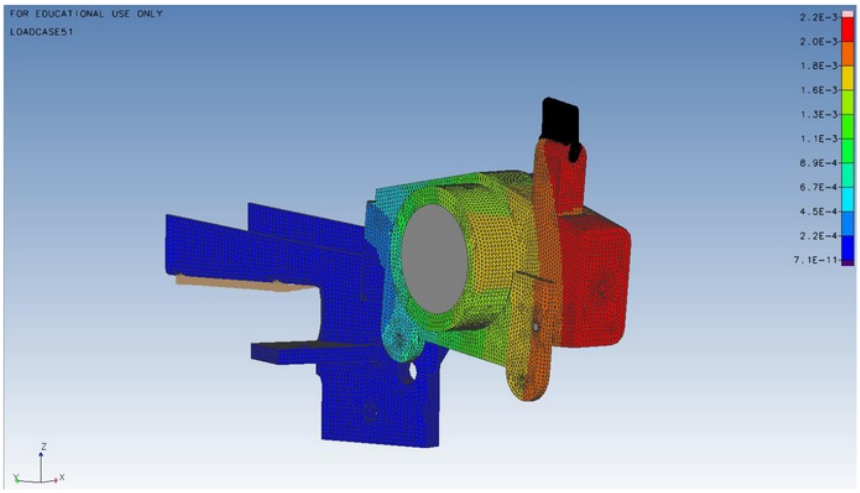


Figure 4-14, Steering Arm FEA Results in X Direction

4.4.1.2 Y Direction

When the uprights attachment points were tested in the Y direction, it is clear to see form table 10 that the FEA results are all lower than the workshop testing with the exception of the twist rig results for right side of the rig when tested for the steering arm and brake top. Figure 4-21 shows the results of the top attachment point being tested in the Y direction, and figure 4-22 shows the same test in the workshop.

Table 10, Current Upright FEA Results Y Direction

Attachment Point	Upright			Twist Rig					
Y	Workshop	FEA	Difference	Workshop	FEA	Difference	Workshop	FEA	Difference
	mm	mm	%	L	L	%	R	R	%
Top	0.340	0.162	53	0.200	0.048	76.15	0.060	0.020	66.83
Bottom	0.270	0.169	38	0.190	0.048	74.58	0.050	0.021	58.6
Steering	0.230	0.198	13	0.220	0.064	71	0.020	0.026	31
Brake Top	0.670	0.241	65	0.190	0.051	72.95	0.020	0.021	3
Brake Low	0.590	0.242	60	0.160	0.032	80	0.030	0.020	33

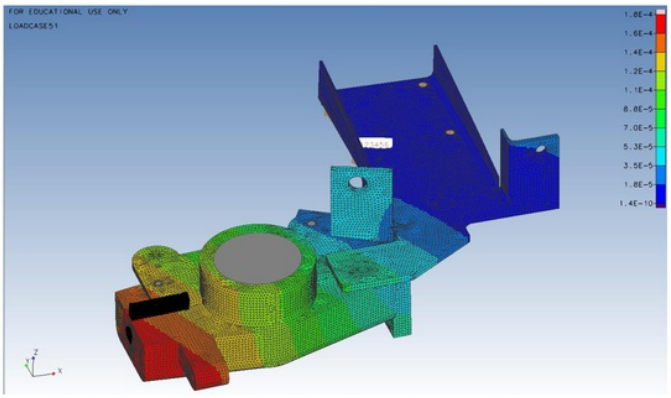


Figure 4-15, Top Attachment Point FEA Results in Y Direction



Figure 4-16, Workshop Test of Top Attachment Point in Y Direction

4.4.1.3 Z Direction

When considering the deflection in the Z direction, the result table, table 11, draws attention to the 500% difference in deflection of the bottom attachment point. This difference could again be attributed to the slight difference in constraining between the workshop and FE model. In the workshop testing the steering arm was rested against the bench to ensure that the upright could not rotate when the load was applied to the bottom attachment point. The results of the lower suspension attachment point can be found in figure 4-23.

Table 11, Current Upright FEA Results in Z Direction

Attachment Point	Upright			Twist Rig					
Z	Workshop	FEA	Difference	Workshop	FEA	Difference	Workshop	FEA	Difference
	mm	mm	%	L	L	%	R	R	%
Top	0.030	0.038	33	0.020	0.016	22	0.030	0.018	39
Bottom	0.020	0.124	500	0.020	0.025	26.50	0.010	0.011	7
Steering	0.120	0.050	58.4	0.050	0.021	58.4	0.090	0.036	60
Brake Top	0.030	0.063	100	0.010	0.014	42.00	0.020	0.037	83
Brake Low	0.400	0.163	60	0.080	0.032	60.38	0.020	0.015	25

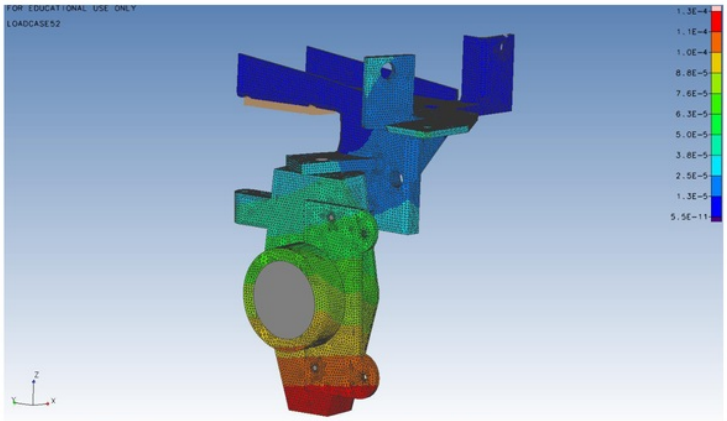


Figure 4-17, FEA Result of Bottom Attachment Point Z Direction

4.4.2 Current Design Vs Proposed Design FEA Results

The new upright underwent the same FEA as the original upright did to allow comparison with the old upright. Both uprights were then tested using loads from a previous seasons track data and then a 'worst case' scenario using calculated track data.

4.4.2.1 Workshop Loads

The new upright was tested and constrained in the same manner as the original upright was. The results were tabulated and can be seen in tables 12, 13and 14.

4.4.2.1.1 X Direction

Table 12, Current and New Upright FEA Results X Direction

Attachment Point	Upright		
X	Old	New	Difference
	mm	mm	%
Top	2.400	2.390	0.42%
Bottom	0.165	0.190	15.00%
Steering	2.170	2.120	2.36%
Brake Top	1.760	1.710	2.92%
Brake Low	0.157	0.180	14.00%

Looking at the X direction deflection, table 12, the new upright deforms less than the old upright apart from at the bottom and lower brake attachment points. However, the increase in deflection is not a huge amount as it is no bigger than 15% which was 0.025mm digger deflection. Figure 4-24 shows the lower suspension attachment point results.

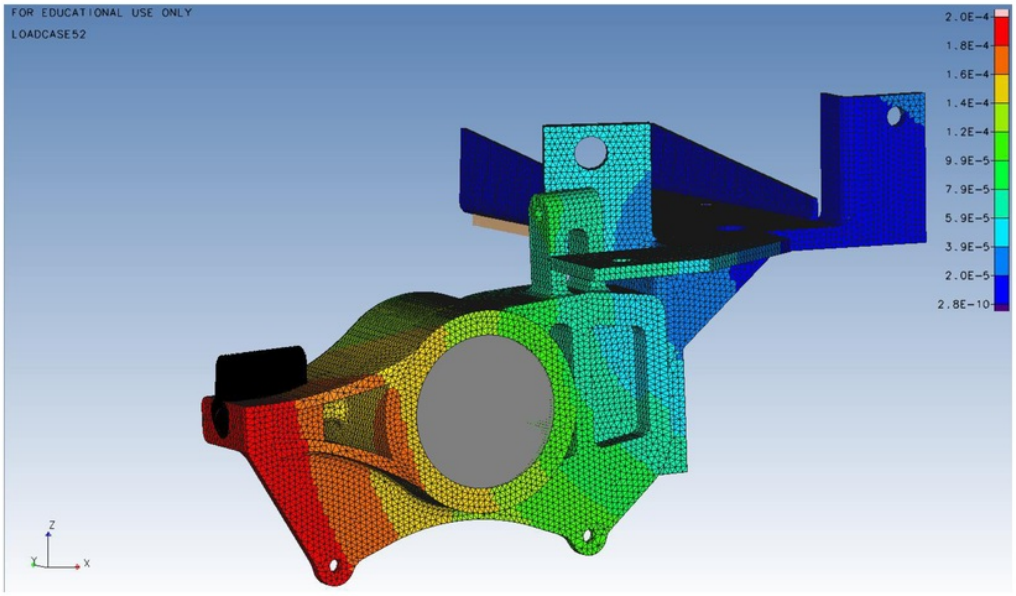
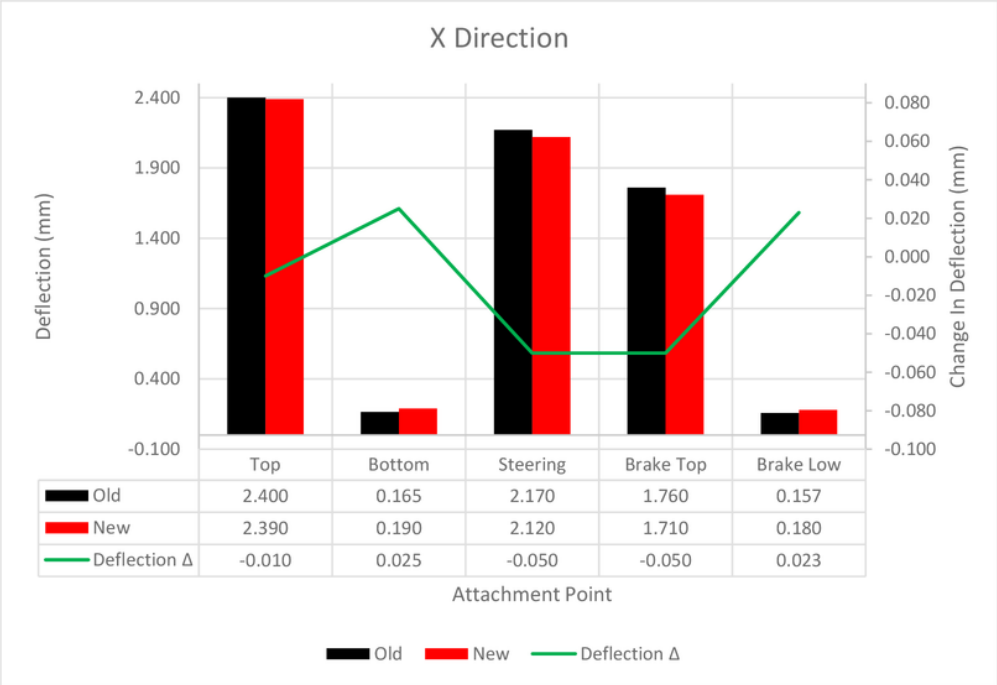


Figure 4-18, Lower Attachment Point FEA Result X Direction



Graph 3, Comparison of FEA Results Between Current and New Upright X Direction

The results were also plotted on graph 3 to help show the difference in the deflection between the old and new upright designs. The difference was changed from a % into a measurement to help the reader better picture the difference. It can be seen that generally the new upright deflects less than the old design when loaded in the X direction.

4.4.2.1.2 Y Direction

When looking at how the new upright deforms in the Y direction, table 13, it is clear to see that the brake attachment points in this direction are stronger than the current upright. This is because the deformation is less than the old design where the attachment points were located on a separate plate that was bolted to the upright. The reduction in deformation was 5% top brake attachment point and 10% bottom brake attachment point. Reductions of 0.11mm and 0.22mm respectively.

However, the other 3 attachment points all deform more than the original upright did. The highest increase in deformation was only 10% an increase of 0.11mm. The increases can be expected due to the removal of material near the respective attachment points compared to the original upright design potentially removing some strength leading to higher deflections.

Table 13, Current and New Upright FEA Results Y Direction

Attachment Point	Upright		
Y	Old	New	Difference
	mm	mm	%
Top	0.162	0.180	10.00%
Bottom	0.169	0.180	6.11%
Steering	0.198	0.220	10.00%
Brake Top	0.241	0.230	5.00%
Brake Low	0.242	0.220	10.00%

Results for the top brake attachment point can be found in figure 4-25.

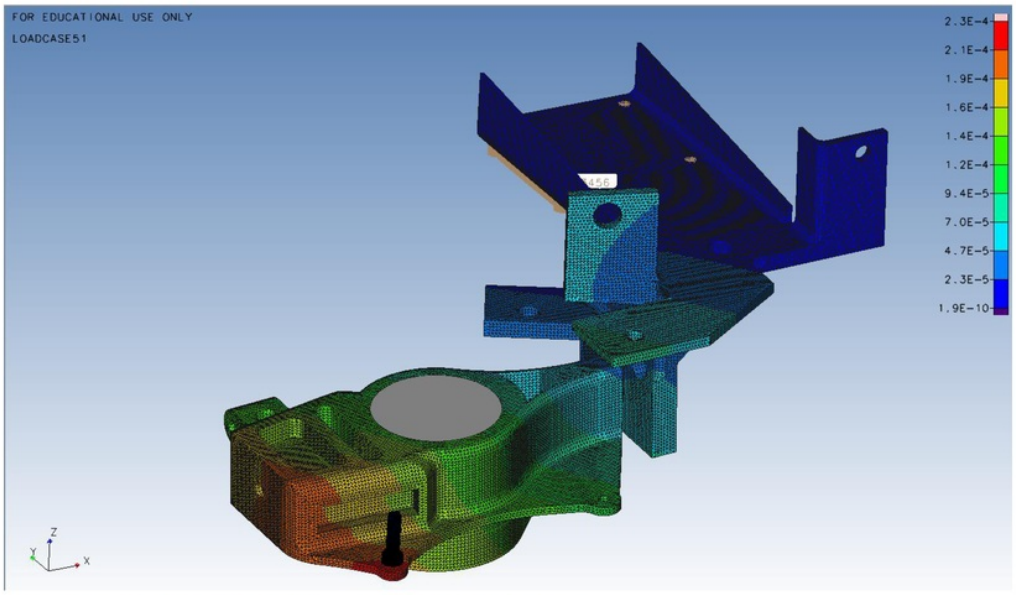
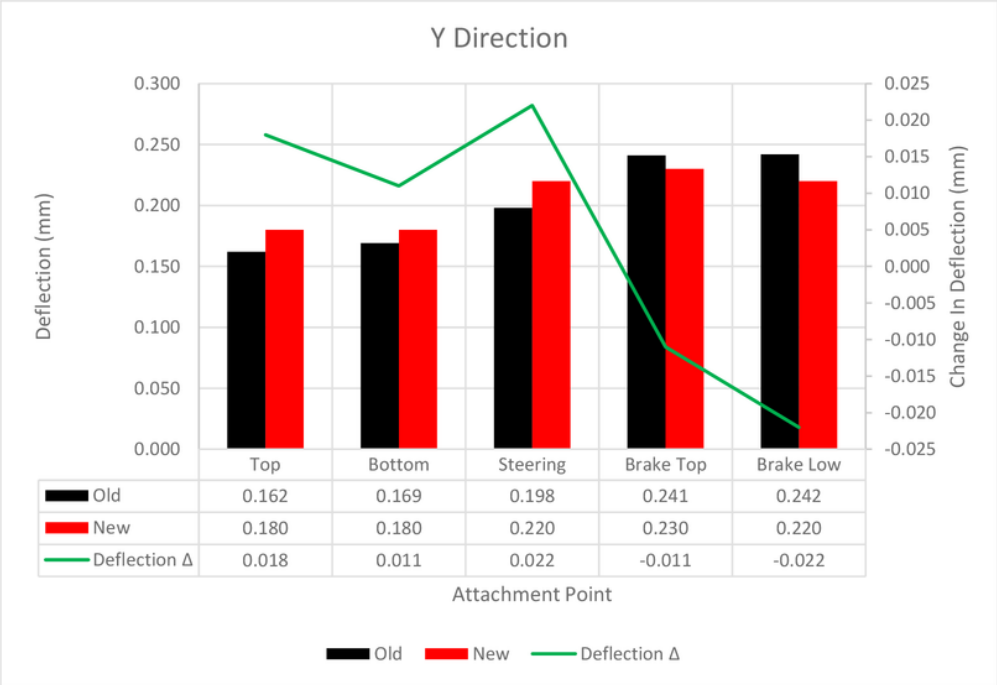


Figure 4-19, Brake Top Attachment Point FEA Result Y Direction



Graph 4, Comparison of Current and New FEA Results Y Direction

Graph 4 shows that the new upright deflects more than the old design at the top, bottom and steering arm attachments, however there is less deflection at the brake attachment points when compared to the old upright design.

4.4.2.1.3 Z Direction

The Z direction results show that only the lower brake attachment point deformed less than the original upright design. The decrease was small at 2%, which equates to 0.003mm. The other 4 attachment points all deformed more than on the original design, with the highest deformation being at the steering attachment point. The steering arm deformed 0.003mm more than with the old design, a 5% increase. Again, these slight increases can be attributed to the removal of material in the new upright.

Table 14, Current and New FEA Results Z Direction

Attachment Point	Upright		
Z	Old	New	Difference
	mm	mm	%
Top	0.038	0.039	2.06%
Bottom	0.062	0.065	4.62%
Steering	0.050	0.053	5.66%
Brake Top	0.063	0.064	1.56%
Brake Low	0.163	0.160	2.00%

The deformation of the lower suspension point is shown in figure 4-26.

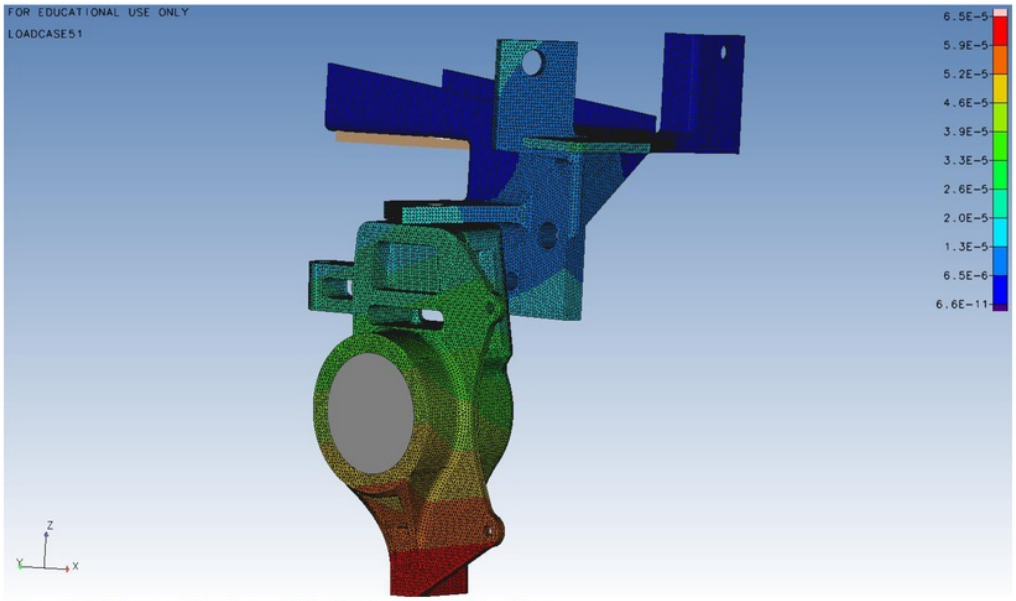
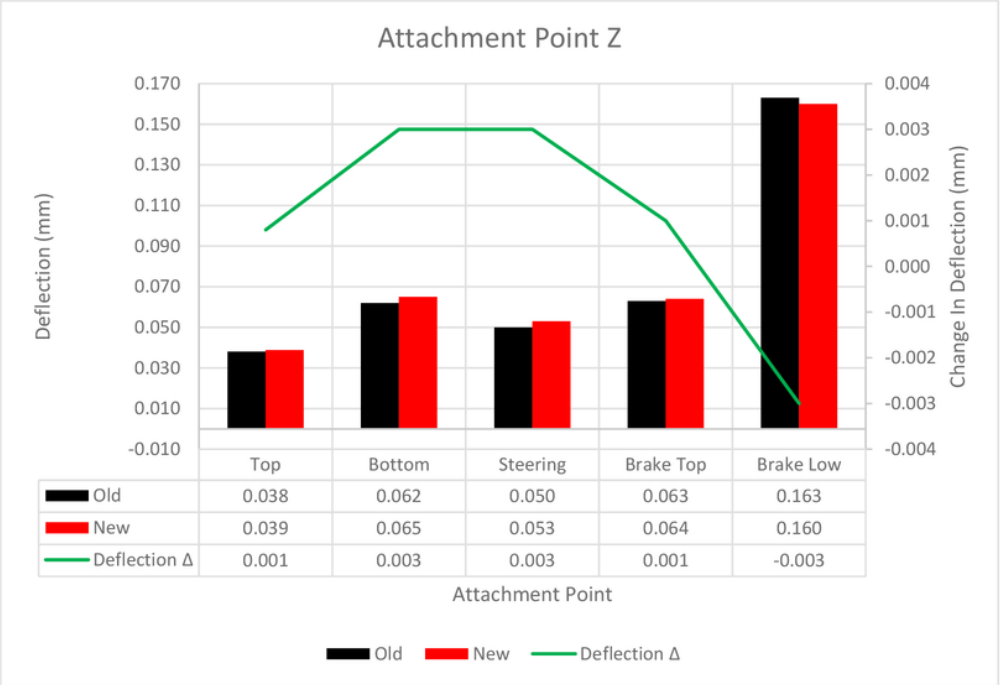


Figure 4-20, Lower Attachment Point FEA Result Z Direction



Graph 5, Comparison of Current and New Upright FEA Results Z Direction

When looking at graph 5, which shows the Z attachment point comparison, it is clear to see that there are only small differences between the old and new design, this shows that confidence can be had when the upright is exposed to loading in the Z direction.

Overall, when considering the results of the workshop loading of the old upright compared to the new upright, the biggest increase in deformation was found to be only 15% at the bottom suspension attachment point when tested in the X direction. An increase of 0.025mm. The biggest decrease in deformation was at the lower brake attachment point in the Y direction, a decrease of 10%, which was 0.022mm. This suggests that the new upright will perform in a similar way when on track, however, to prove this both upright will be tested using track calculated forces and the results compared.

4.4.2.2 *Track Loads*

To help fully assess and understand the new upright design, it was decided to test both uprights with forces calculated from Motec data.

4.4.2.2.1 Track Selection

In order to calculate the loads, an appropriate track needed to be selected. The race calendar was investigated and is shown in figure 4-27.

May 18/19th	Snetterton	Sprint (R1) F3/British GT
June 1/2nd	Thruxton	Double Header Sprint (R2 & R3) 50th Anniversary
July 6th	Oulton Park International	Double Header Sprint (R4 & R5)
July 21th	Donington Park National	Enduro
Aug 31/Sep1st	Brands Hatch GP	Enduro
Oct 5/6th	Silverstone International	Double Header Sprint (R6 & R7)
Oct 26/27th	Brands Hatch Indy Formula Ford Festival	Separate Races

Figure 4-21, Sports2000 2019 Calendar, (Sports2000, 2019)

Looking at the race calendar, it was decided to choose Oulton Park as it is a bumpy undulating track (Bike Sport News, 2017), with a good mixture of high and low speed corners with rapid direction changes. It is felt this will place some of the highest loads on the upright during the season.

The loads that were acting on the upright for Oulton Park were taken from a similar report *'The Potential Design Optimization of Automotive Upright, By Reducing Weight While Retaining Structural Integrity'* (Meredith, 2018).

The forces for Oulton Park are as follows in table 15, these are the initial contact patch forces. The vertical loads are applied directly to the upright and represent traveling along a straight (linear), cornering and during braking. However, the horizontal forces are at the contact patch, so moments were taken about the attachment point to calculate the horizontal forces applicable.

Table 15, Forces at Contact Patch, (Meredith, 2018)

	Vertical (N)	Horizontal (N)
Fcp force linear	1720	1580
Fcp force cornering	6205	4210
Fcp Breaking	1904	2005

The calculation of the horizontal forces can be found in appendix 5. Table 16 shows the horizontal forces calculated for Oulton Park.

Table 16, Horizontal Forces

	Horizontal Force (N)		
	Linear	Cornering	Braking
Top	340	905	430
Bottom	1920	5115	2705
Brake Top	514.7	1371.44	653.14
Brake Bottom	2094.7	5581.44	2658.14

4.4.2.2.2 Results

Both uprights were then tested with the calculated forces applied in the X and Z directions. The results of this testing can be seen in tables 17, 18 and 19.

Table 17, Track Forces Linear FEA Results

Attachment Point	Linear Force	Upright		
		Old	New	Difference
Top	N	mm	mm	%
Vertical	1720	0.00112	0.00278	148.00%
Horizontal	340	0.00055	0.00134	143.00%
Bottom	N	mm	mm	%
Vertical	1720	0.00093	0.00398	327.00%
Horizontal	1920	0.00385	0.01460	279.00%
Brake Top	N	mm	mm	%
Vertical	1720	0.02590	0.01843	29.00%
Horizontal	514.7	0.00630	0.00497	22.00%
Brake Bottom	N	mm	mm	%
Vertical	1720	0.02970	0.02479	17.00%
Horizontal	2094.7	0.03180	0.01964	39.00%

The biggest difference seen in deflection between the current and new designs when tested with the linear load applied is 327% at the bottom attachment point when loaded with the vertical force. This is a deflection increase of 0.00305mm. The lower brake bracket when applied with the horizontal force found a reduction of deflection by 39%, a 0.121mm decrease. Figures 4-28, old, and 4-29, new, visually show the difference in deflection for the lower brake attachment point.

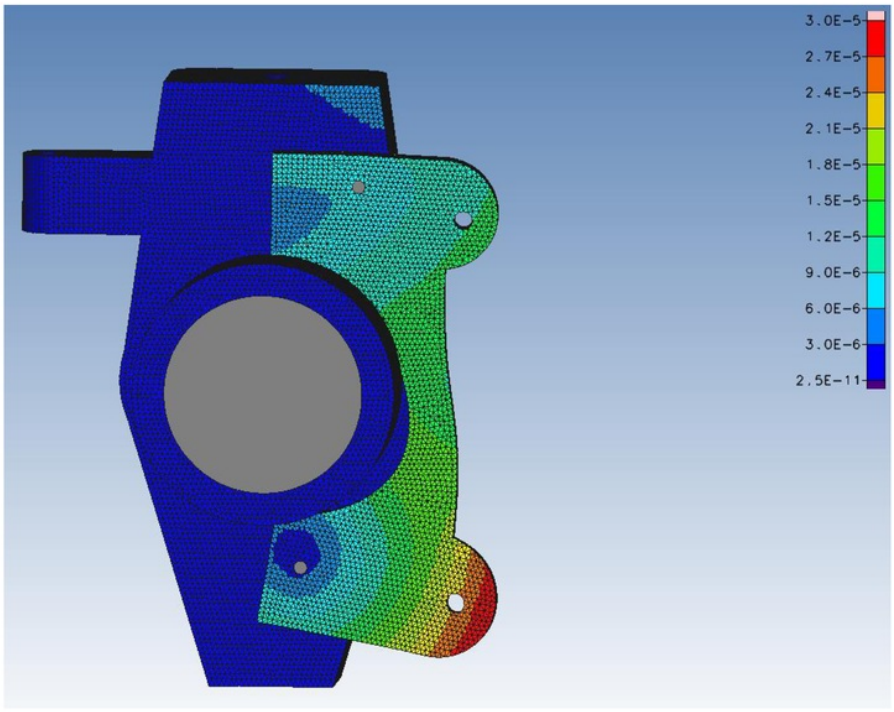


Figure 4-22, Brake Low FEA Result Current Upright

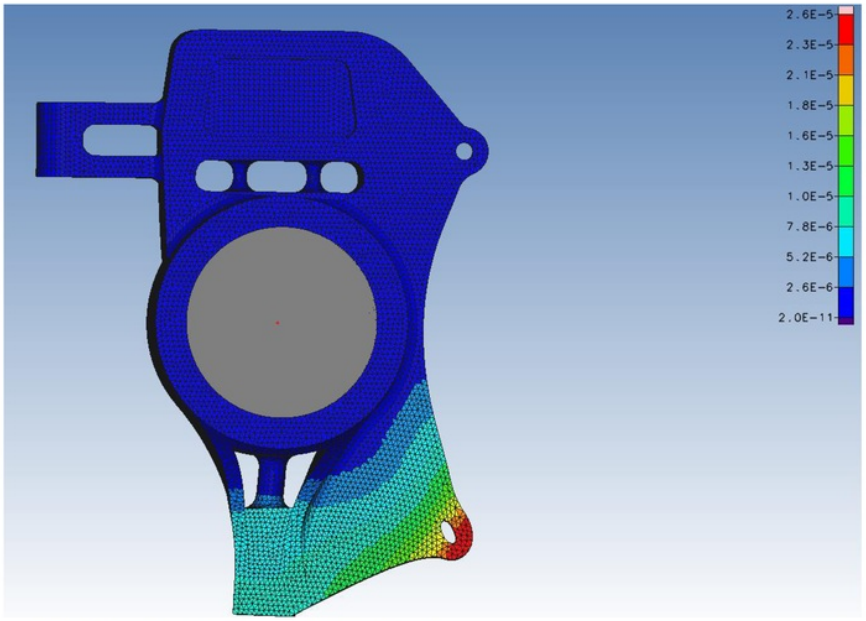


Figure 4-23, Brake Low FEA Result New Upright

The cornering forces and the corresponding deflections can be seen below. The results show a similar pattern to the linear force results in that the lower attachment point deflects the most when comparing new to old by 324%, 0.011mm when loaded vertically. The lower brake attachment point sees the biggest reduction in deflection when loaded horizontally, a 39% reduction or 0.0326mm.

Table 18, Track Forces Cornering FEA Results

Attachment Point	Cornering Force	Upright		
		Old	New	Difference
Top	N	mm	mm	%
Vertical	6250	0.00406	0.01040	156.00%
Horizontal	905	0.00147	0.00358	143.00%
Bottom	N	mm	mm	%
Vertical	6250	0.00339	0.01440	324.00%
Horizontal	5115	0.01010	0.03922	288.00%
Brake Top	N	mm	mm	%
Vertical	6250	0.09500	0.06799	29.00%
Horizontal	1371.44	0.01760	0.01325	25.00%
Brake Bottom	N	mm	mm	%
Vertical	6250	0.10800	0.09040	17.00%
Horizontal	5581.44	0.08500	0.05235	39.00%

Looking at the results visually, figures 4-30 and 4-31, it is clear to see the increase in the deformation between the old design and the new design. It is interesting to note that in the new design the deformation curves the upright to the right, this suggests that the lack of material above the attachment point is degrading the resistance to deflection in that area of the upright.

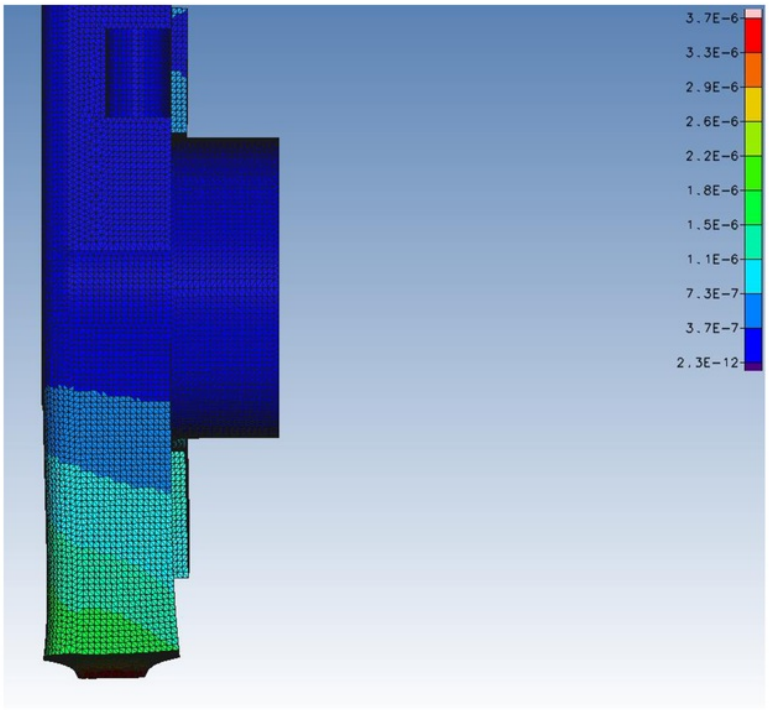


Figure 4-24, Bottom Attachment Point FEA Result Current Upright

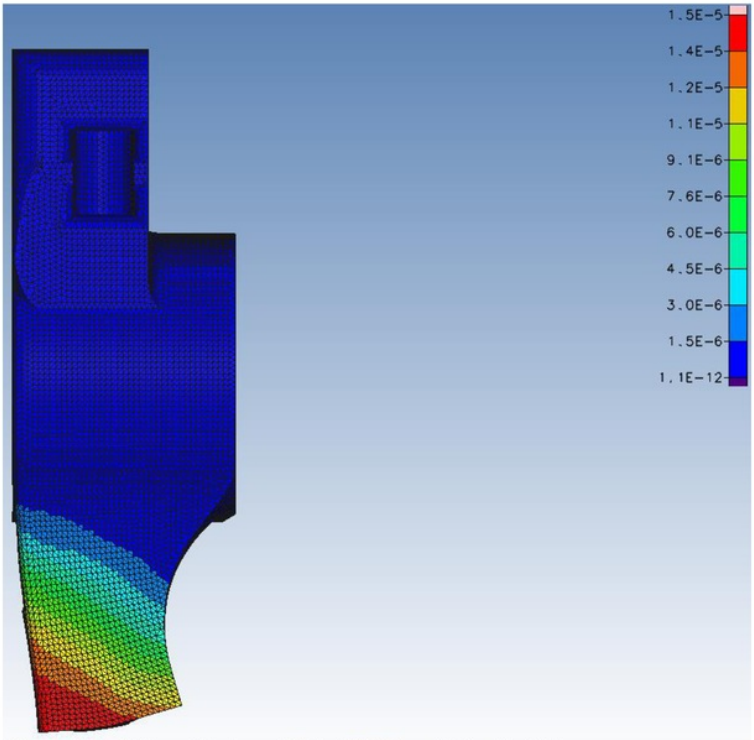


Figure 4-25, Bottom Attachment Point FEA Result New Upright

Lastly looking at the loads that the upright is exposed to under braking, it is again clear to see the same pattern as with the previous loads. This suggests that the new upright design needs to be modified further in order to strengthen the lower suspension attachment point. In this scenario, the deflection is 0.0033mm bigger, an increase of 329%. The lower brake attachment point has again seen the biggest reduction in deflection, deflecting 0.0159mm less with the new upright design, a 40% reduction.

Table 19, Track Forces Braking FEA Results

Attachment Point	Braking Force	Upright		
		Old	New	Difference
Top	N	mm	mm	%
Vertical	1904	0.00124	0.00310	150.00%
Horizontal	430	0.00070	0.00172	145.00%
Bottom	N	mm	mm	%
Vertical	1904	0.00103	0.00442	329.00%
Horizontal	2705	0.00536	0.02071	286.00%
Brake Top	N	mm	mm	%
Vertical	1904	0.03020	0.02040	33.00%
Horizontal	653.14	0.00834	0.00631	25.00%
Brake Bottom	N	mm	mm	%
Vertical	1904	0.03300	0.02737	18.00%
Horizontal	2658.14	0.04070	0.02472	40.00%

Figure 4-33 highlights the lack of material above the lower suspension attachment point, it can be said that after looking at the results and seeing that each test followed a similar pattern, further refining of that area of the upright needs to be done in order to reduce the deformation seen.

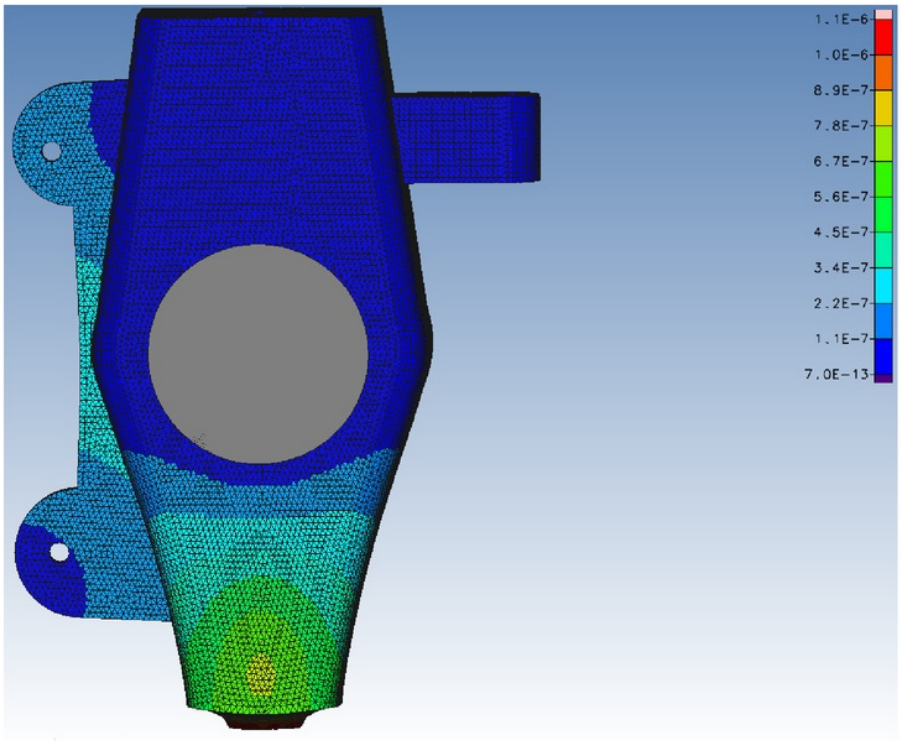


Figure 4-26, Bottom Attachment Point FEA Result Current Upright (Braking)

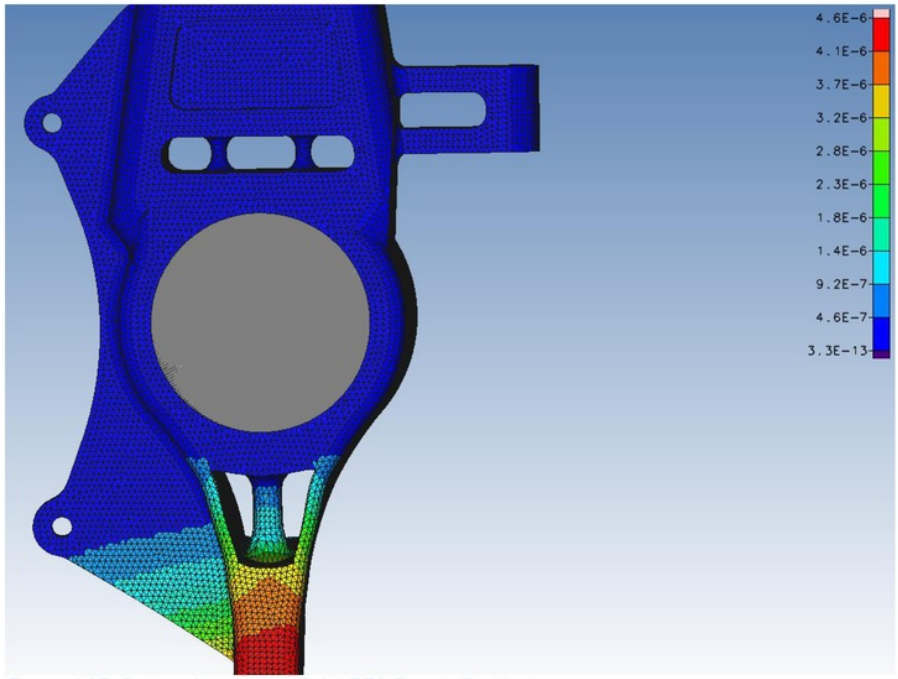


Figure 4-27, Bottom Attachment Point FEA Result (Braking)

4.4.2.2.3 Y Direction

After analysing the results from the upright being tested in the X and Z directions, it was decided to also test the upright in the Y direction with the horizontal forces to fully understand how the upright would deform.

The table of results can be seen in tables 20 and 21.

Table 20, Cornering Force Applied in Y Direction

		Upright		
Attachment Point	Cornering Force	Old	New	Difference
Top	N	mm	mm	%
Horizontal	905	0.00350	0.00966	176.00%
Bottom				
Horizontal	5115	0.02100	0.04698	123.00%
Brake Top				
Horizontal	1371.44	0.49210	0.09076	82.00%
Brake Bottom				
Horizontal	5581.44	0.00447	0.00442	2.00%

Table 21, Braking Force Applied in Y Direction

		Upright		
Attachment Point	Braking Force	Old	New	Difference
Top	N	mm	mm	%
Horizontal	430	0.00166	0.00458	175.00%
Bottom				
Horizontal	2705	0.01112	0.02481	123.00%
Brake Top				
Horizontal	653.14	0.23450	0.14640	38.00%
Brake Bottom				
Horizontal	2658.14	0.00214	0.00209	3.00%

When exposed to cornering and braking forces, the upper attachment point is the attachment point that experiences the biggest increase in deflection. 0.00616mm or 176% and 0.00292mm or 175% respectively for cornering and braking. This would suggest that the upper attachment point also needs to be modified further to help reduce the increase deflection seen under load.

The upper brake attachment point sees a drastic reduction in the deflection experienced under the cornering forces, it drops form 0.49210mm to 0.09076mm, a reduction of 82%. Under braking forces, the same attachment point also sees a 38% reduction of deflection, this along with the reduction of deflection in the other brake attachment point indicate that the integrated brake calliper bracket design is working effectively to reduce deflection.

4.4.2.2.4 'Worst Case' Loads

Once the track loads had been tested and the results analysed, it was decided to carry out a 'worse case' scenario FEA. As researched, this is when the car would be braking whilst cornering. Therefore, the loads seen at each attachment point vertically and horizontally were added together and applied to the upright attachment points. Table 22 shows the loads applied.

Table 22, 'Worst Case' Loads

Top	Oulton	Vertical	8154
		Horizontal	1335
Bottom	Oulton	Vertical	8154
		Horizontal	7820
Brake Top	Oulton	Vertical	8154
		Horizontal	2024.58
Brake Bottom	Oulton	Vertical	8154
		Horizontal	8239.58

The vertical load was applied in a downwards (Z) direction as per the previous FEA, and the horizontal load was applied in the Y direction. This is because the horizontal loads deformed the upright more in the Y direction when tested compared to when tested in the X direction. It was decided that because of this, the 'worst case' loads should be applied in the direction that deformed the upright the most as it gave the most destructive 'worst case' scenario.

Table 23 shows the results of the 'worst case' scenario FEA. Both uprights were tested and constrained in the same fashion. The % differences are high for the top and bottom attachment points which is to be expected given the small changes in deflection seen. For example, the bottom attachment point of the new upright deforms 1533% more than the old upright. However, this difference is in fact only 0.017mm when looking at the change in deflection between the two designs.

The brake attachment points both deflect less with the new upright design. As mentioned previously this can be attributed to the attachment points being one piece as part of the upright rather than being a separate plate that is bolted to the upright. The change from alloy steel to aluminium can also be expected to contribute to this decrease in deflection.

Table 23, Results of 'Worst Case' FEA

		Upright			
Attachment Point	Force	Old	New	Difference	Deflection Δ
Top	N	mm	mm	%	mm
Vertical	8154	0.00167	0.01317	688.00%	0.01150
Horizontal	1335	0.00168	0.01400	733.00%	0.01232
Bottom					
Vertical	8154	0.00114	0.01862	1533.00%	0.01748
Horizontal	7820	0.01072	0.06897	543.00%	0.05825
Brake Top					
Vertical	8154	0.09950	0.08439	16.00%	-0.01511
Horizontal	2024.58	0.66710	0.45220	33.00%	-0.21490
Brake Bottom					
Vertical	8154	0.10950	0.10677	3.00%	-0.00273
Horizontal	8239.58	0.00653	0.00645	2.00%	-0.00008

Figures 4-34 and 4-36 demonstrate the difference in deflection between the old and new upright for the bottom attachment point when loaded vertically. It can be clearly seen that the way the new upright would deform is completely different to the old upright. This can be attributed to the cut out above the bottom attachment point on the new upright design. The removal of material has meant that that area of the upright experiences higher Von Mises stress when compared to the standard design leading to higher strain. The modified design experiences a peak stress in that area of roughly 18.7MPa compared to 2.44MPa of the standard design. It is worth noting however that this is well below the elastic modulus of the specified aluminium, 69000MPa. The visible area of stress could also be reduced through the use of radii.

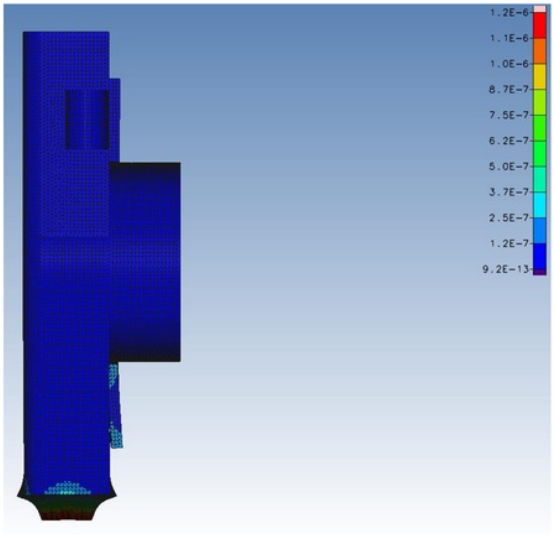


Figure 4-28, Bottom Attachment Point 'Worst Case' Result Current Upright

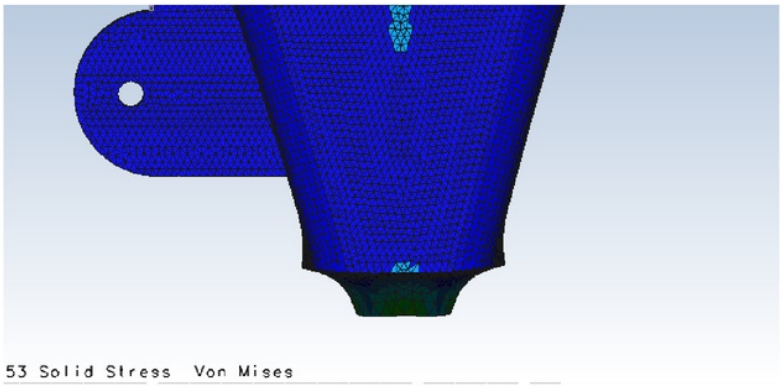


Figure 4-29, Stress at Lower Attachment Point Current Upright

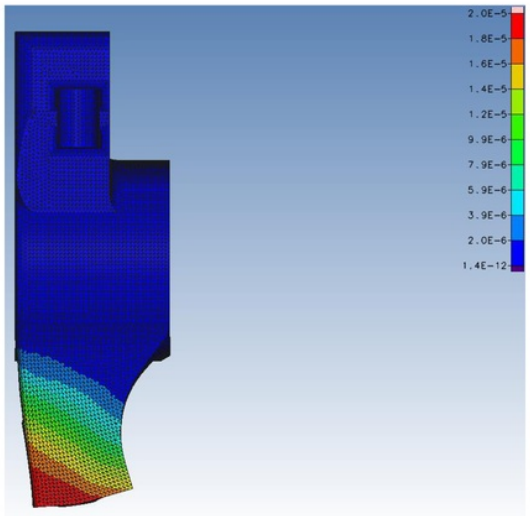


Figure 4-30, Bottom Attachment Point 'Worst Case' Result New Upright

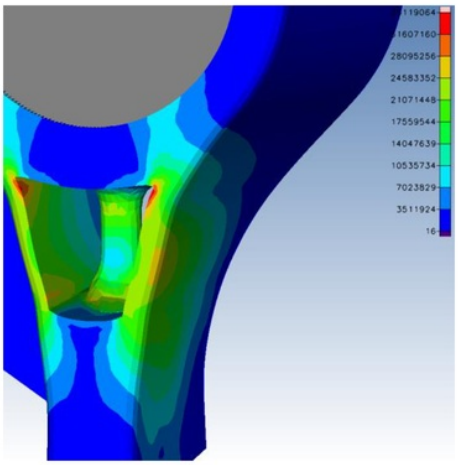


Figure 4-31, Stress at Bottom Attachment Point New Upright

5 Conclusion

The aim of this paper was to document the creation of a new, lighter, optimised front suspension upright that lost none of the functionality or stiffness of the current upright. This was done with the aid of computer software such as design topology optimisation and FEA. With the championship the university races in being so competitive, any improvements have the potential to have a big on track benefit.

When the proposed upright design was analysed against the current upright using track data, it was found that the biggest difference in deflection at any of the measured attachment points was 0.05825mm. This occurred under a worst-case scenario at the bottom suspension attachment point. The stress in this area increased marginally from 43MPa to 59MPa but was still within the elastic modulus of the aluminium grade specified.

The biggest decrease in deflection at the measured attachment points was found to be at the top brake attachment point when loaded in the Y direction. The reduction in deflection was 0.40134mm. The stress around this attachment point was also significantly reduced, from over 500MPa down to 28MPa.

Overall, it can be said that from the results, the proposed upright design reduced the deformation at the brake attachment points under all FEA tests. However, the upper and lower suspension attachment points deflected more than the current upright did when exposed to the same FEA. This could be down to the way the proposed upright was designed as the current upright model was modified by removing material rather than creating a new upright from scratch.

A small increase of deflection can be acceptable considering the weight saving made, in a similar project carried out by (Riordan, et al., 2010), where a 15% weight saving was made with the new upright design despite the small increase in deflection seen.

To help prove the proposed design would be safe to use on track, the compliance in top and bottom wishbone joints was measured and found to be 0.06mm in the Y direction, 0.12mm in the X direction and 0.8mm in the Z direction. As these values all exceeded the difference in deflection between the two upright designs, the increased deflection at the top and bottom attachment points can be ignored as the forces will take up the slack in the wishbone joints before acting on the upright.

The weight saving goal of this project (0.5kg) would equate to roughly 0.03 seconds per lap. However, with the proposed upright design being 26% lighter than the current upright, the weight saving that could be achieved was 0.95kg. This would lead to a potential lap time benefit of almost 0.06 seconds per lap. As stated previously, the added benefits of weight

saving are not just in lap time. The handling balance of the car can be improved as if the car is underweight then ballast can be used to optimise the handling behaviour to the driver's preference. The weight transfer that will occur will also be reduced meaning that the car will be settled sooner into the corner making the car easier to drive, (Alexander, 1991). The grip available to the driver is also increased thanks to a lower weight and this means that the car would be capable of out accelerating competitors, a point made in works published by (Bergrath, 2002) and (Alexander, 1991)

One of the other initial aims of this project was to match the stiffness of the current upright, however if the current upright is over-engineered then this could mean that the new upright design would also be over-engineered, and the deflections seen could be acceptable.

The decision on designing the upright for manufacturability and running the proposed new upright design will be left to Team MCR.

6 Recommended Further Work

Throughout the duration of any project there are always going to be areas that can be improved upon if the project was going to be carried out again. This project has been no exception.

Further research could be carried out into the use of different materials for the upright if price was no object. The use of composites could also be further explored, the lay-up process and how that impacts on the strength of the finished composite could be examined.

The workshop testing of the upright was also limited by the mass used, 15kg. It was seen from the results that only small deflections were seen. However, a greater mass couldn't be used as Team MCR only possess one upright for each side of the car and therefore did not want to risk damage to the upright during the testing. The FEA model of the current model could also be improved upon by adding a contact between the brake calliper plate and the bearing hole.

As mentioned previously in the report, the effect of brake temperature was dis-regarded for the FEA carried out. Further work should be undertaken to include the effect of heat in the setup of the FEA and even the topology optimisation.

The steering arm was also omitted from the analysis of the new upright, this is because the forces calculated were excessive and it is unknown what effect the steering rack would have on the forces the upright is being exposed to.

The specifying of a new bearing could also be researched, potentially leading to a lighter bearing to help save further weight on the car.

Further designs could be created and tested against the current upright. In this project, only one design was created and tested, however a better design that deflects less whilst still saving weight could be found with more initial concepts. Designs could also be studied with regards to aerodynamic performance, with the shapes being designed to help reduce drag as much as possible. Stress concentrations could also be considered, with radii added to reduce them.

The next stages of this project would be to look at manufacturability of the new upright design. It is one thing having a newly optimised design but if it is not feasible to make easily then the new design will never get made.

7 References

Alexander, D., 1991. *Perfromance Handling.* 1st ed. Osceola: Motorbooks Intl.

Anand, A., 2017. *Torsional analysis of the chassis and its validation through Finite Element Analysis.* Ranchi, Altair Technology Confrence .

AP Racing, 2011. *Disc Temperatures.* [Online]
Available at: http://www.apracing.com/Info.aspx?InfoID=36&ProductID=976
[Accessed 1 March 2019].

ASM Aerospace Specification Metals Inc, 2018. *Aluminum 6061-T6; 6061-T651.* [Online]
Available at: http://asm.matweb.com/search/SpecificMaterial.asp?bassnum=ma6061t6
[Accessed 18 April 2019].

Bastow, D. & Howard, G., 1993. *Car Suspension & Handling.* 3rd ed. London: Pentech Press Ltd.

Bendsoe, M. a. S. O., 2003. *Topology Optimization Theory, Methods, and Applications.* s.l.:Springer.

Bengt, J., 2015. *Vehicle Dynamics,* Gothenburg: s.n.

Bergrath, E. K. C. a. W. J., 2002. *Advanced Ceramics in Formula 1 Wheel, Clutch and Gearbox Rolling Bearings,* s.l.: SAE Technical Papers.

Bhardwaj, S. B. A. L. U. a. A. A., 2018. *Design and Optimization of Steering Upright to Reduce the Weight Using FEA,* s.l.: SAE Technical Paper .

Bike Sport News, 2017. *Oulton BSB test: Track return 'bit of a shock' for Guintoli.* [Online]
Available at: https://www.bikesportnews.com/news/news-detail/oulton-bsb-test-track-return-bit-of-a-shock-for-guintoli
[Accessed 13 04 2019].

Brereton, P., Budgen, B., Turner, M. & Khalil, M., 2007. *Lessons from Applying the Systematic Review Process within the Engineering domain.* s.l.:Journal of Systems and Software.

Car-Engineer, 2019. *Suspension Design Definitions and Effects on Vehicle Behaviour.* [Online]
Available at: http://www.car-engineer.com/suspension-design-definitions-and-effects-on-vehicle-behavior/
[Accessed 19 April 2019].

Chang, K.-H., 2015. *Design Theory and Methods using CAD/CAE.* Oxford: Elsevier.

Coring Group, 360 Knee Systems, 2019. *Customizing Implants With 3D Image Processing,* s.l.: Tech Briefs Media Group.

Crawford, J., 1994. *Finite Element Analysis of a NASCAR Winston Cup Stock Car,* s.l.: SAE Technical Papers.

Crolla, D., 2009. *Automotive Engineering, Pwertrain, Chassis System & Vehicle Body.* First ed. s.l.:Butterworth-Heinemann .

Cyberphysics, 2018. *The Youngs Modulus.* [Online]
Available at: https://www.cyberphysics.co.uk/topics/forces/young_modulus.htm

Dean, J., n.d. *Introduction to the Finite Element Method (FEM),* Cambridge: University of Cambridge.

Dhakar, A. & Ranjan, R., 2016. *Force Calculation In Upright Of A FASE Race Car,* Bamgalore: RV College of Engineering.

Farias, L. S. A. H. B. S. P., 2015. *Design of a Brake Caliper using Topology Optimization Integrated with Direct Metal Laser Sintering,* s.l.: SAE Technical Paper.

Fiedler, K., Rolfe, B. & De Souza, T., 2017. *Integrated Shape and Topology Optimization - Applications in Automotive Design and Manufacturing,* s.l.: SAE Int.

Gao, Y. X. Y. W. C. a. F. J., 2019. *Topology Optimization of Metal and Carbon Fiber Reinforced Plastic (CFRP) Structures under Loading Uncertainties,* s.l.: SAE Technical Paper .

Gillespie, T., 1992. *Fundamentals of Vehicle Dynamics.* Warrendale: Society of Automotive Engineers.

Hughes, J., 2019. *Updated MCR Upright.* Swansea: s.n.

International Organization for Standardization, 2011. *Road Vehicles - Vehicle dynamics and road-holding ability - Vocabulary.* [Online]
Available at: https://www.sis.se/api/document/preview/914200/
[Accessed 13 04 2019].

Katwa, K., 2018. *Twist Rig.* Swansea: s.n.

Katwa, K., 2018. *Uni Car Upright.* Swansea: s.n.

Kaw, A., 2006. *Mechanics of Composite Materials.* 2nd ed. Florida: CRC Press.

Kumar, P. K. N. M. S. a. B. H., 2017. *3D Printing Technique, An Effective Solution for Robust and Reliable Engineering of Trims,* s.l.: SAE Technical Paper .

Lartiga, C., 2001. *Development of a Rig and Testing Procedures for the Experimental Investigation of Horizontal Axis Kinetic Turbines,* s.l.: University of Victoria.

Leiva, J., 2013. *GENESIS Structural Optimisation: Current and Upcoming Key Features.* Warwickshire, VR&D.

Logan, D., 2012. *A First Course in the Finite Element Method.* 5th ed. Wisconsin: CengageLearning.

Matthews, F. & Rawlings, R., 1994. *Composite Materials: Engineering & Science.* 1st ed. Cambridge: Woodhead Publishing Limited.

Ma, Z., Wang, H., Kikuchi, N. & Pierre, C., 2003. *Substructure Design Using a Multi-Domain Multi-Step Topology Optimization Approach,* s.l.: SAE Technical Paper.

McBeath, S., 2000. *Competition Car Composites.* 3rd ed. Somerset: Haynes Publishings .

Mclaren, 2013. *Formula One Race Strategy.* [Online]
Available at: https://www.raeng.org.uk/publications/other/14-car-racing
[Accessed 12 March 2019].

Meredith, S., 2018. *'The Potential Design Optimization of Automotive Upright, By Reducing Weight While Retaining Structural Integrity' ,* Swansea: UWTSD.

Milliken, W. & Milliken, D., 1995. *Race Car Vehicle Dynamics.* Warrendale: SAE International.

Mottram, J. & Shaw, C., 1996. *Using Finite Elements in Mechanical Design.* Berkshire: McGraw-Hill Book Company Europe.

MSC Software, 2007. *User's Guide for Topology Optimisation.* Munich: MSC Software.

NASA Technology Transfer Program, n.d. *NASA STRuctrual ANalysis (NASTRAN).* [Online]
Available at: https://software.nasa.gov/software/LAR-16804-GS
[Accessed 11 04 2019].

Newton, I., 1686. *Principia Mathematica Philosophiae Naturalis.* 1st ed. s.l.:Benjamin Motte.

Predictive Engineering, 2013. *Small Connection Elements (RBE2, RBE3 and CBUSH) and How Amazingly Useful They Are For FEA Modeling,* Oregon: s.n.

Racing Circuits, 2019. *Silverstone.* [Online]
Available at: https://www.racingcircuits.info/europe/united-kingdom/silverstone/#.XLIq0khKiUk
[Accessed 13 04 2019].

Randjbaran, E., 2018. *Reasearch Gate.* [Online]
Available at: https://www.researchgate.net/figure/Left-to-right-Glass-carbon-and-Kevlar-fibre_fig1_261713262
[Accessed 09 November 2018].

Rao, S., 2004. *The Finite Element Method in Engineering.* 4th ed. s.l.:Elsevier Science & Technology Books.

Riordan, C., Tovar, A. & Renaud, J., 2010. *Topology Optimization of a Formula SAE Upright Using OptiStruct,* s.l.: SAE Technical Papers.

Ross, C., 1998. *Advanced Applied Finite Element Methods.* 1st ed. Chichester: Horwood Publishing.

SAE, 1976. *Vehicle Dynamics Terminology,* s.l.: SAE.

Schaeffler, 2014. *Technical Pocket Guide.* 1st ed. Herzogenaurach: Schaeffler Technologies.

Simscale, 2016. *When Should I use a second order mesh?,* s.l.: Simscale.

Singiresu, R., 2004. *The Finite Element Method in Engineering.* 4th ed. s.l.:Elsevier Science & Technology Books.

Smith, C., 1978. *Tune to Win.* Fallbrook: Aero Publishers.

Smith, C., 1984. *Engineer to Win.* 1st ed. Minnesota: Motor Books.

Sports2000, 2019. *Events.* [Online]
Available at: https://www.sports2000.co.uk/events/2019-events-entry-form/
[Accessed 18 April 2019].

SRCC, 2018. *Regulations.* [Online]
[Accessed 07 March 2019].

Staniforth, A., 1994. *Competion Car Suspension.* 2nd ed. Somerset: Haynes Publishing.

Symscape, 2010. *Open Wheel Race Car CFD Analysis.* [Online]
Available at: https://www.symscape.com/examples/rans/open-wheel-racecar-cfd
[Accessed 14 April 2019].

Turner, M., Clough, R., Matin, H. & Topp, L., 1956. Stiffness and Deflection Analysis of Complex Structures. *Journal of the Aeronautical Sciences,* 23(9).

UWTSD / Team MCR, 2017. *Current Upright CAD.* Swansea: s.n.

UWTSD, 2018. *MCR.* Swansea: s.n.

Vanderplaats Research & Development, n.d. *Topology: Bar subject to multiple torsional load.* [Online]
Available at: https://www.genesis-support.com/examples/topology-bar-subject-to-multiple-torsional-load
[Accessed 15 March 2019].

Vanderplaats, 2018. *vrand.com.* [Online]
Available at: http://www.vrand.com/products/genesis/
[Accessed 08 October 2018].

Wight, B., 2008. *Topology Optimization of Racecar Suspension Uprights.* California, Luxon Engineering.

Wong, A., 2007. *Design and Optimization of an Upright,* s.l.: s.n.

8 Appendices

8.1 Appendix 1…Supervision Meeting Notes

Below, copies of the supervision meetings throughout the project can be found.

PRIFYSGOL CYMRU
Y Drindod Dewi Sant
UNIVERSITY OF WALES
Trinity Saint David

Supervision Form	
MODULE: Dissertation (M6X00417)	
ASSIGNMENT: Optimisation of the MCR suspension upright	
STUDENT: Krishna Katwa	SUPERVISOR: Kelvin Lake
DATE: 15/10/18	Length: 30 mins
Objective of the meeting	
To discuss the aims and the objectives of the project	
Work Submitted by the student	
None	
Issues discussed at the meeting	
1. Proposal discussed. This is acceptable and clearly states the direction of the project. This lends itself to a simple Topology exercise to be carried out on this component. 2. The MCR is at Brands Hatch this weekend so the component will not be able to be taken off of the car until after this. 3. When the car is back from Brands the part can be taken off of the car with a view to measure and weigh the part so that a CAD/FE model can be built. Whilst this is happening the part will need to go back on the car for some straight line testing. KK to estabilish when this testing is due to happen so that this can be schedulled in. 4. In order to build the FE model it must be known what material (what alloy) the part is currently made from. KK to estabilsh this. 5. The regs state 'no composites'. This is hear-say. What do the regs actually say? 6. When the part is back from Brands, can the avaliable package space be estabilished? 7. Is the part handed/symmetrical. KK to estabilsh this. 8. KL to send KK design studio tutorials. Complete these this week whilst the car is being set up for Brands. 9. KK to research: Topology Optimisation, studies that have used this in different applications, why optimisating the uprights is important and similar studies that have been done (FSAE?) 10. KL to get racecar engineering article to KK. 11. KK to get a contents page together. 12. After the straight line testing the part can be taken off of the vehicle again and some simple stiffness tests can be set up to validate your baseline FE model	
Student action BEFORE next meeting	
- 4, 5, 7, 8, 9, 11	
Date of next meeting: 22/10/18	

PRIFYSGOL CYMRU
Y Drindod Dewi Sant
UNIVERSITY OF WALES
Trinity Saint David

Supervision Form

MODULE: Dissertation (M6X00417)	
ASSIGNMENT: Optimisation of the MCR suspension upright	
STUDENT: Krishna Katwa	SUPERVISOR: Kelvin Lake
DATE: 22/10/18	Length: 20 mins

Objective of the meeting

To discuss progress

Work Submitted by the student

1. car has not been unloaded from Brands yet.
2. composites ARE allowed, however it is felt that a machinable part would be better for this project.
3. straight line testing is in a 'couple of weeks', so that the part can be taken off and measured so that a CAD model can be built.
4. Current grade of Alu is believed to be AL6061 T6
5. Parts are handed, it has been decided that the LHS will be used going forward.
6. The wheel is 13", and current attachement points will remain the same. Existing package to be measured.
7. KK to research: Topology Optimisation, studies that have used this in different applications, why optimisating the uprights is important and similar studies that have been done (FSAE?)
8. KL to get racecar engineering article to KK.
9. KK to get a contents page together.
10. After the straight line testing the part can be taken off of the vehicle again and some simple stiffness tests can be set up to validate your baseline FE model

Student action BEFORE next meeting

- 3, 6, 9

Date of next meeting: 29/10/18

PRIFYSGOL CYMRU
Y Drindod Dewi Sant
UNIVERSITY OF WALES
Trinity Saint David

Supervision Form

MODULE: Dissertation (M6X00417)	
ASSIGNMENT: Optimisation of the MCR suspension upright	
STUDENT: Krishna Katwa	SUPERVISOR: Kelvin Lake
DATE: 05/11/18	Length: 30 mins

Objective of the meeting

To discuss the aims and the objectives of the project

Work Submitted by the student

None

Issues discussed at the meeting

1. Initial CAD model has been received, this is to be completed so that the stiffness tests can be correlated to this in FE.
2. Physical testing discussed. Stiffness at 5 attachment points to be estabilished in x, y and z. Design and rig so that this can be carried out. Get this rig manufactured.
3. Literature review discussed. This is to be completed this week.
4. Package space has been photographed, however this need to be measured so that the design space can be understood.
5. Contents page reviwed.
6. Topology exercise reviewed in Design Studio, this has been completed however the resolution of the results needed to changed to get the same results as the tutorial.

Student action BEFORE next meeting

- 1, 2, 3, 4

Date of next meeting: 08/11/18

PRIFYSGOL CYMRU
Y Drindod Dewi Sant
UNIVERSITY OF WALES
Trinity Saint David

Supervision Form

MODULE: Dissertation (M6X00417)	
ASSIGNMENT: Optimisation of the MCR suspension upright	
STUDENT: Krishna Katwa	SUPERVISOR: Kelvin Lake
DATE: 08/11/18	Length: 45 mins

Objective of the meeting

To discuss the aims and the objectives of the project

Work Submitted by the student

None

Issues discussed at the meeting

1. Initial CAD model has been received, this is to be completed so that the stiffness tests can be correlated to this in FE. Due to the fact that the part will still have the hub bearing in position, when you carryout your stiffness testing make sure that you clamp this area so that it does not deform. Stiffness at 5 attachment points to be estabilished in x, y and z. Design and rig so that this can be carried out. Get this rig manufactured.
2. Literature review discussed. Add aditional references to this. Large sections appear to be quoting a small number of sources, you need to put across an variety of viewpoints.
3. Package space has been photographed and measured. Use the exiting part to create your non-designable regions. Use your package space measurements to create your designable region. You can then combine these into a topology package space model that will be used in design studio for a topology run.

Student action BEFORE next meeting

- 1, 2, 3

Date of next meeting: 12/11/18

PRIFYSGOL CYMRU
Y Drindod Dewi Sant
UNIVERSITY OF WALES
Trinity Saint David

Supervision Form

MODULE: Dissertation (M6X00417)	
ASSIGNMENT: Optimisation of the MCR suspension upright	
STUDENT: Krishna Katwa	SUPERVISOR: Kelvin Lake
DATE: 12/11/18	Length: 10 mins

Objective of the meeting

To discuss the aims and the objectives of the project

Work Submitted by the student

None

Issues discussed at the meeting

1. Initial CAD model has been received, this is to be completed so that the stiffness tests can be correlated to this in FE.
2. Physical testing discussed. Stiffness at 5 attachment points to be estabilished in x, y and z. Design and rig so that this can be carried out. Get this rig manufactured.
3. Package space has been photographed, however this need to be measured so that the design space can be understood.

Student action BEFORE next meeting

- 1, 2, 3

Date of next meeting: 19/11/18

PRIFYSGOL CYMRU
Y Drindod Dewi Sant
UNIVERSITY OF WALES
Trinity Saint David

Supervision Form

MODULE: Dissertation (M6X00417)	
ASSIGNMENT: Optimisation of the MCR suspension upright	
STUDENT: Krishna Katwa	SUPERVISOR: Kelvin Lake
DATE: 19/11/18	Length: 45 mins

Objective of the meeting

To discuss the aims and the objectives of the project

Work Submitted by the student

None

Issues discussed at the meeting

1. Initial CAD model was lost and needed to be regenerated.
2. Initial CAD of the package space was reviewed.
3. The loading method of the existing part still needs to be estabilished so that the stiffness constraints can be set in the Topology study. This was reviewed in the workshop.
4. It is hoped that the stiffness of the existing part can be understood in time for the interim vivas.
5. Create and manufacture a rig so that the stiffness of the part can be understood. Carryout this testing.
6. Move all parts individually in Solidworks (not as an assembly) so that the package space can be created.

Student action BEFORE next meeting

- 5, 6

Date of next meeting: 26/11/18

PRIFYSGOL CYMRU
Y Drindod Dewi Sant
UNIVERSITY OF WALES
Trinity Saint David

Supervision Form

MODULE: Dissertation (M6X00417)	
ASSIGNMENT: Optimisation of the MCR suspension upright	
STUDENT: Krishna Katwa	SUPERVISOR: Kelvin Lake
DATE: 26/11/18	Length: 20 mins

Objective of the meeting

To discuss the aims and the objectives of the project

Work Submitted by the student

None

Issues discussed at the meeting

1. Create and manufacture a rig so that the stiffness of the part can be understood. Carryout this testing. This has not been done this week due to other commitments.
2. Move all parts individually in Solidworks (not as an assembly) so that the package space can be created. The designable space has now been estabilished. Add to this your non designable space. Once your testing has been carried out you can then set-up your DS model. We can set this up next week.
3. create your slides for your viva. We can review these next week.

Student action BEFORE next meeting

- 1, 2, 3

Date of next meeting: 03/12/18

PRIFYSGOL CYMRU
Y Drindod Dewi Sant
UNIVERSITY OF WALES
Trinity Saint David

Supervision Form

MODULE: Dissertation (M6X00417)	
ASSIGNMENT: Optimisation of the MCR suspension upright	
STUDENT: Krishna Katwa	SUPERVISOR: Kelvin Lake
DATE: 10/12/18	Length: 20 mins

Objective of the meeting

To discuss the aims and the objectives of the project

Work Submitted by the student

None

Issues discussed at the meeting

1. Testing complete
2. Initial topology set up, this will be reviewed on Monday 17th dec
3. Viva slides reviewed
4. work over christmas reviewed. It is hoped that the initial topology run can be run on Tuesday. The initial CAD can then completed over christmas.

3

- prepare fpr your viva

Date of next meeting: 17/12/18

Y Drindod Dewi Sant
Trinity Saint David

Supervision Form

MODULE: Dissertation (M6X00417)	
ASSIGNMENT: Optimisation of the MCR suspension upright	
STUDENT: Krishna Katwa	SUPERVISOR: Kelvin Lake
DATE: 28/01/19	Length: 20 mins

Objective of the meeting

To discuss the next steps and the progress of the project

Work Submitted by the student

None

Issues discussed at the meeting

1. FE model of the existing upright still needs to be complete. Test this in EXACTLY the same way that the test was carried out in the workshop, including the rigs so that the deformation of these can be seen and compared to test.
2. The initial topology run is being set up. However, it was questioned how to load the models where the part (not one of the fixing points) was constrained. When you do this you have two options. 1. Ignore these loadcases and optimise the structure using the remaining loadcases as the inclusion of these parts of the original model in the optimisation run will opbiously ensure (wrongly) that these are in the final design. 2. Optimise the structure and constrain the part using the closest fixing point to the surface that was constrained in test. Try options 1 and 2 and see what difference it makes.
3. The design volume, the mesh size and the constraint of the amout of material remaining all need to be reduced to expose the loadpaths needed.

Work to be carried out before the next meeting

- 1, 2, 3

Date of next meeting: 04/03/19

PRIFYSGOL CYMRU
Y Drindod Dewi Sant
UNIVERSITY OF WALES
Trinity Saint David

Supervision Form

MODULE: Dissertation (M6X00417)	
ASSIGNMENT: Optimisation of the MCR suspension upright	
STUDENT: Krishna Katwa	SUPERVISOR: Kelvin Lake
DATE: 11/02/19	Length: 15 mins

Objective of the meeting

To discuss the next steps and the progress of the project

Work Submitted by the student

None

Issues discussed at the meeting

1. The FE model of the original upright needs to be assessed with the jig as tested in the workshop. This to be reviewed on Thursday.
2. Initial topology has been completed. This runs on the C drive. Try re-running this with a finer mesh.
3. Create your new design using the topology results to drive this design. You will then be able to assess your new design in the same way that the original was tested to show that the response is the same.
4. Calculate the loads that would be seen by this part in use. You can then show that your new part is fit for purpose.

Work to be carried out before the next meeting

- 1, 2, 3

Date of next meeting: 18/02/19

PRIFYSGOL CYMRU
Y Drindod Dewi Sant
UNIVERSITY OF WALES
Trinity Saint David

Supervision Form

MODULE: Dissertation (M6X00417)	
ASSIGNMENT: Optimisation of the MCR suspension upright	
STUDENT: Krishna Katwa	SUPERVISOR: Kelvin Lake
DATE: 11/03/19	Length: 30 mins

Objective of the meeting

To discuss the next steps and the progress of the project

Work Submitted by the student

None

Issues discussed at the meeting

1.The initial FE models were not running due to the fact that the boundary conditions were over constraining the model. This was discussed and then rectified. Repeat this for all of your models so that correlation with test can be achieved.

Work to be carried out before the next meeting

- 1

Date of next meeting: 18/03/19

PRIFYSGOL CYMRU
Y Drindod Dewi Sant
UNIVERSITY OF WALES
Trinity Saint David

Supervision Form

MODULE: Dissertation (M6X00417)	
ASSIGNMENT: Optimisation of the MCR suspension upright	
STUDENT: Krishna Katwa	SUPERVISOR: Kelvin Lake
DATE: 18/03/19	Length: 30 mins

Objective of the meeting

To discuss the next steps and the progress of the project

Work Submitted by the student

None

Issues discussed at the meeting

1.The FE models for the baseline part have now been completed so that these can be compared to test. However, there is some penetration between the jig and the part. Fix this by trimming back the jig and re-running the model.
2. The model has been run with coarse and fine meshes. The finer mesh gives a more accurate result and the run time is still acceptable, therefore use the finer mesh moving foward. Repeat this exercise with second order elements.
3. Once the FE model of the original model has been completed you can create a model of your new design and compare the stiffnesses at the attachement points as well as carrying out a strength test using secondary research (based on oulton park as this is an undulating track). Repeat these loading calculations using a different circuit to show how the forces seen at a different track would compare to those seen at oulton.

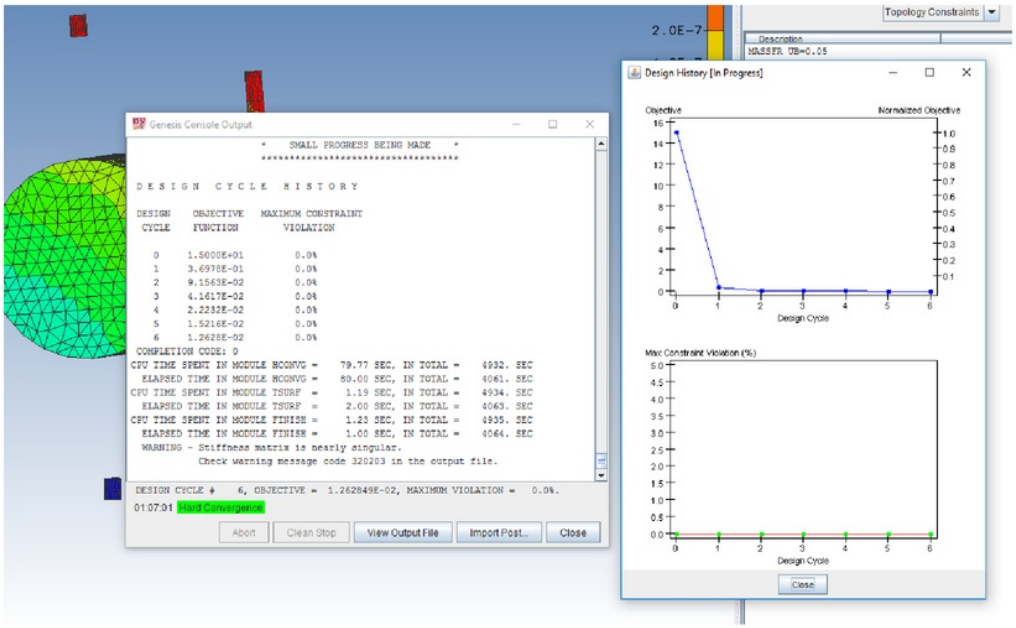
Work to be carried out before the next meeting

- 1, 2, 3

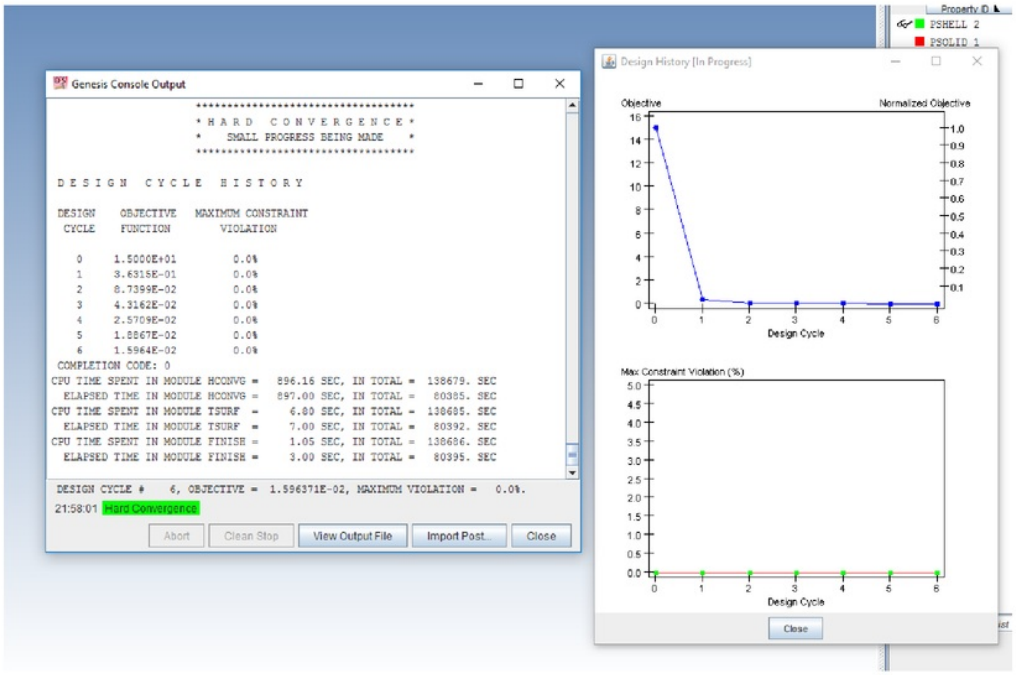
Date of next meeting: 25/03/19

8.2 Appendix 2… Optimisation Mesh Study Time Taken

Split once



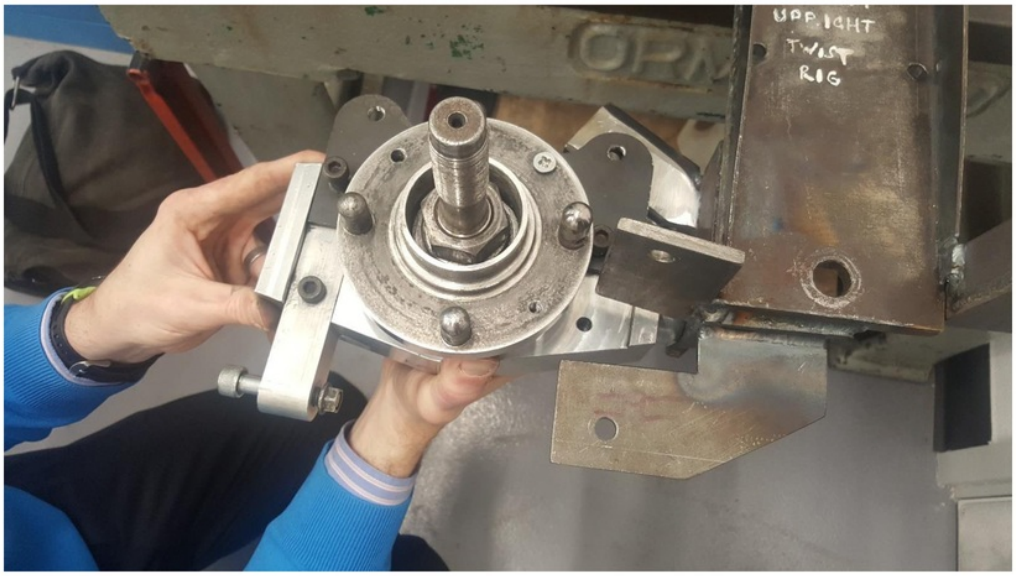
Split twice



8.3 Appendix 3…Upright Testing Pictures

The following pictures show how the upright was restrained when certain attachment points were tested.

Suspension top and steering in the Y direction.



Suspension low and brake low in the Y direction.



Steering in the Z direction.



Suspension top and brake top in the Z direction, the rig was rotated 180 degrees.



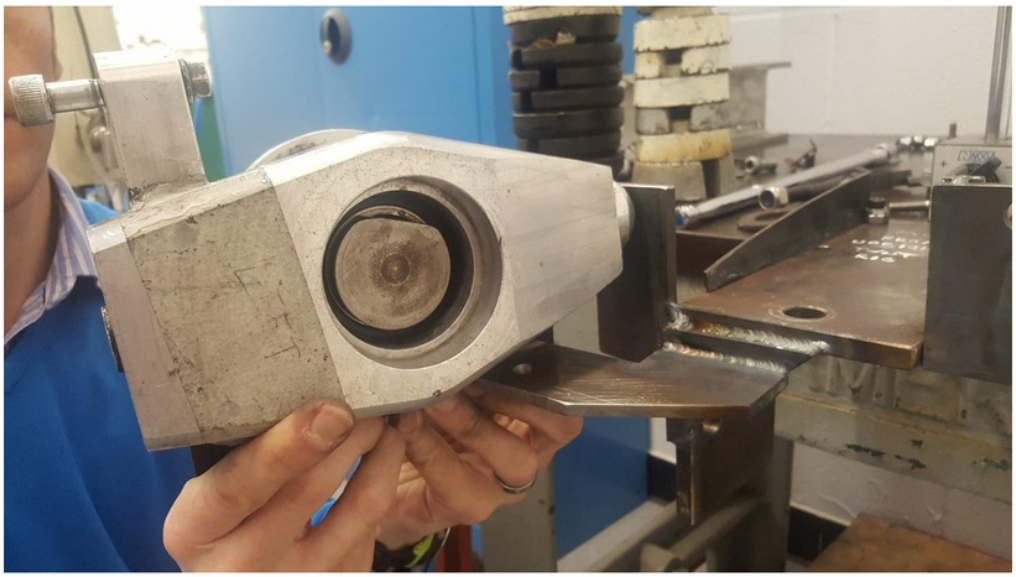
Suspension low in Z



Brake top in the Y direction



Suspension top, steering and brake top in the X direction.



Brake low and suspension low in the X direction.



Suspension lower and brake lower in the Z direction.

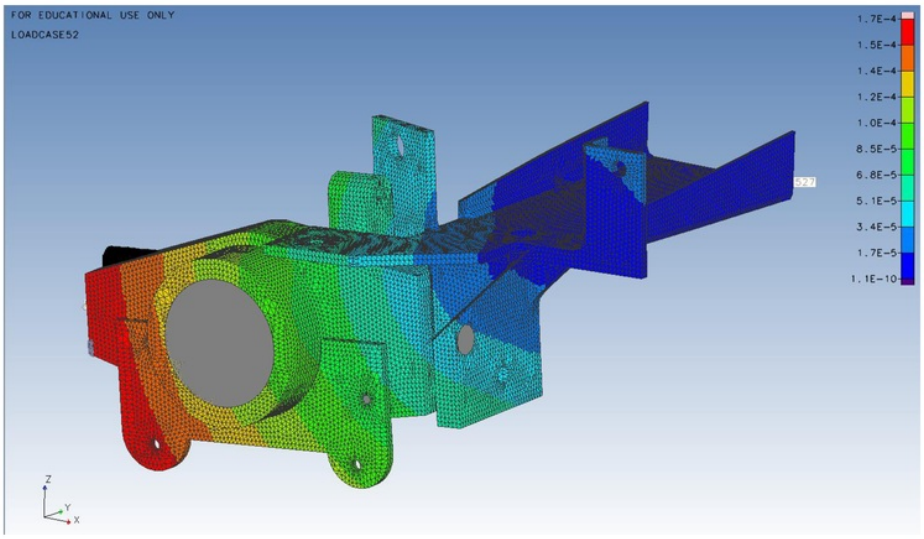


8.4 Appendix 4…FEA Screenshots

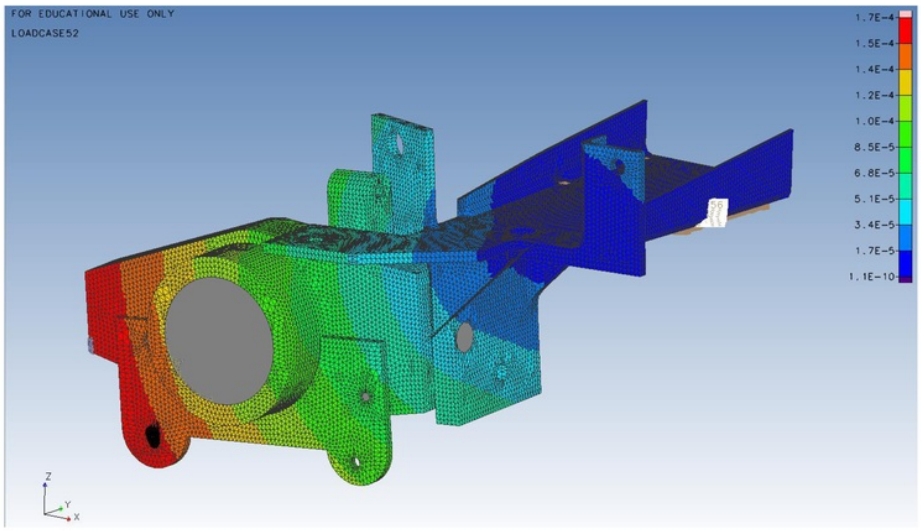
Below the results of each FEA test can be found.

The following are the standard upright workshop results:

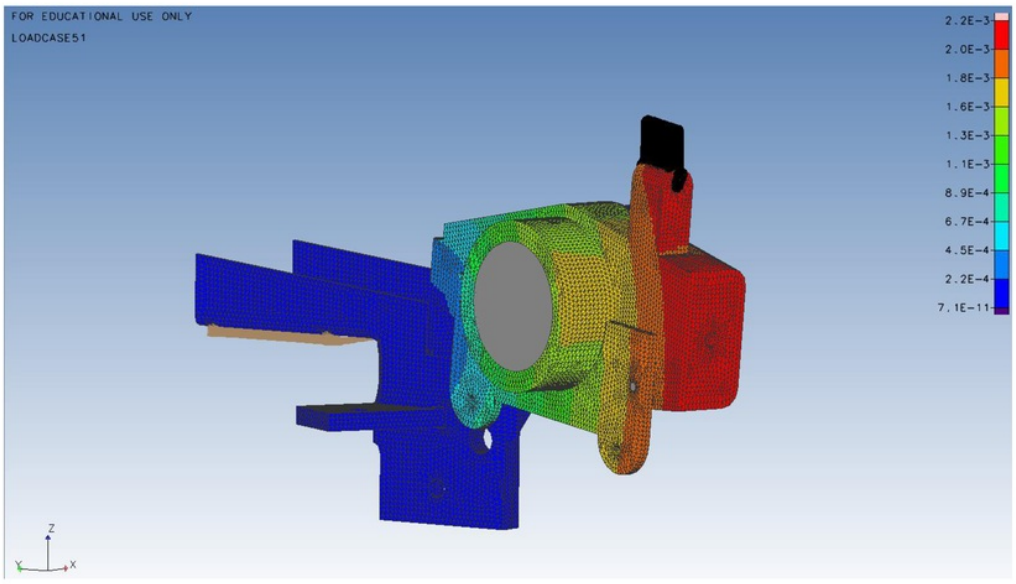
Suspension low X



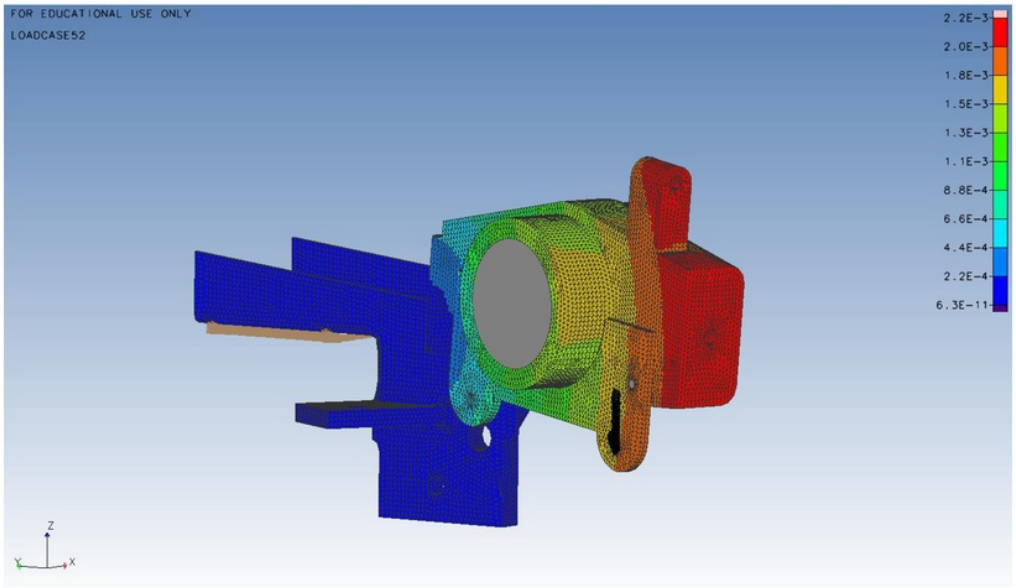
Brake Low X



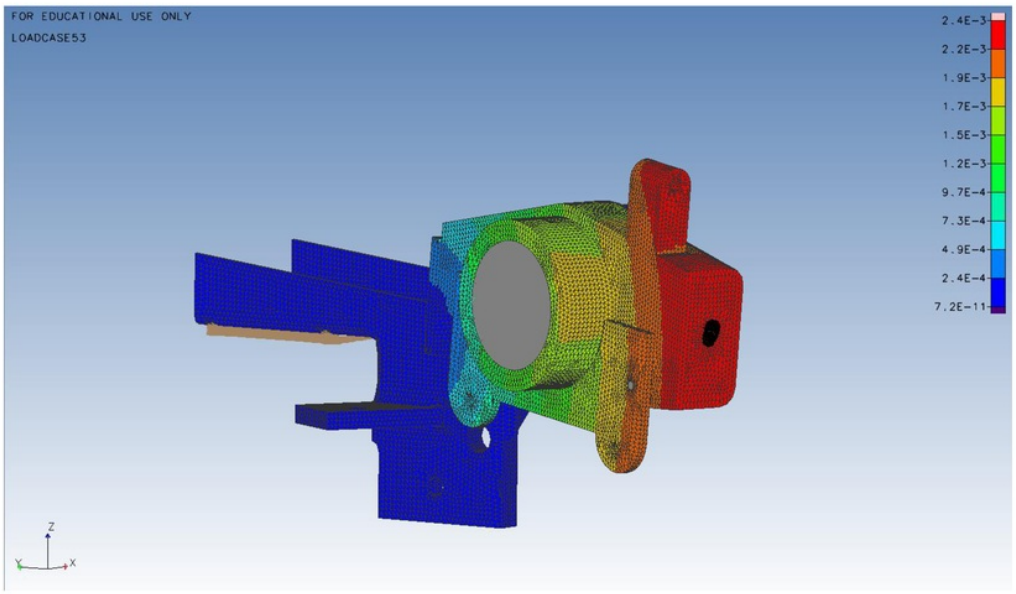
Steering X



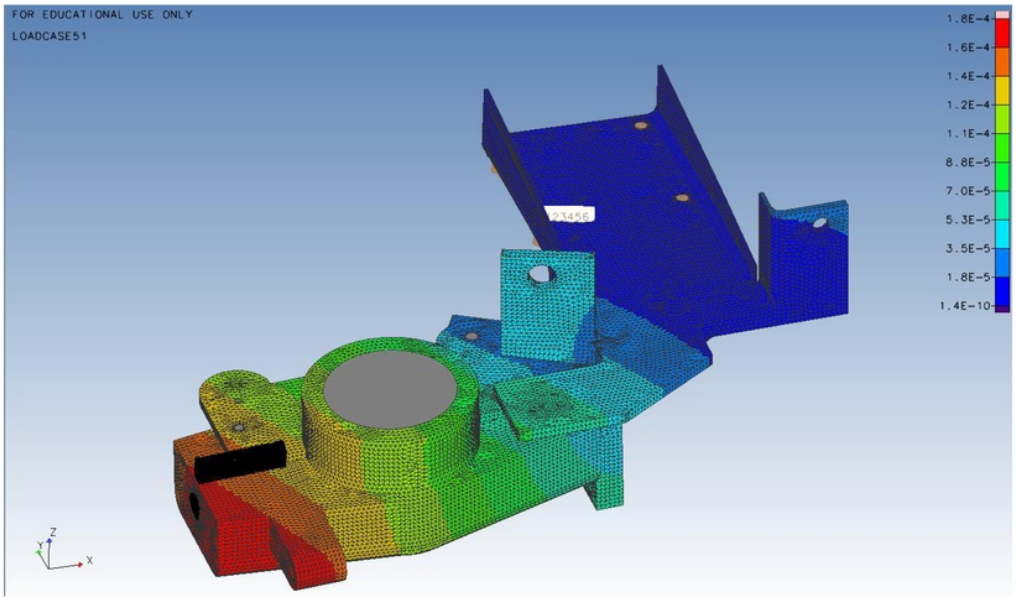
Brake top X



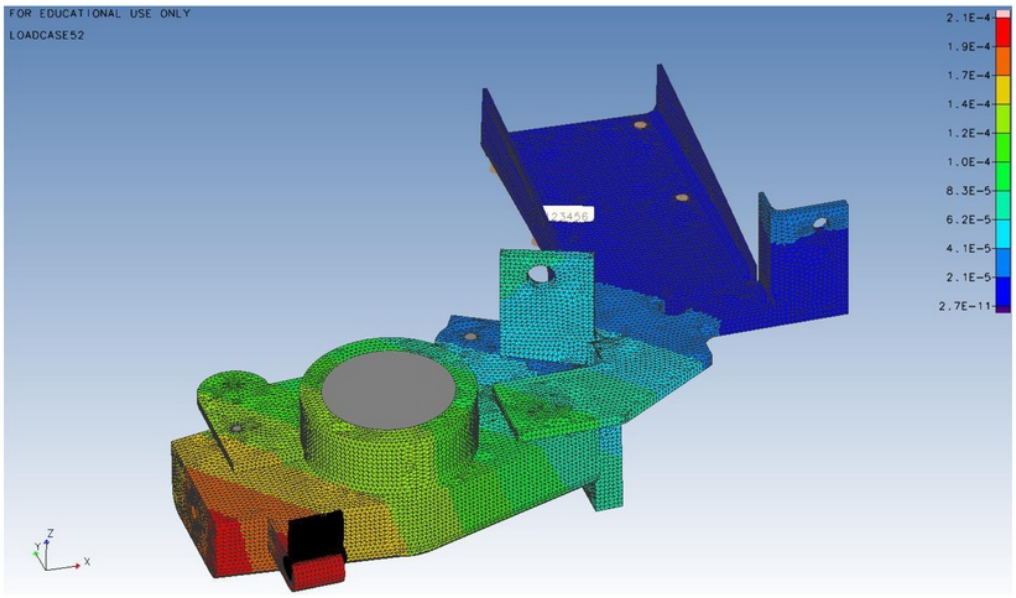
Suspension top X



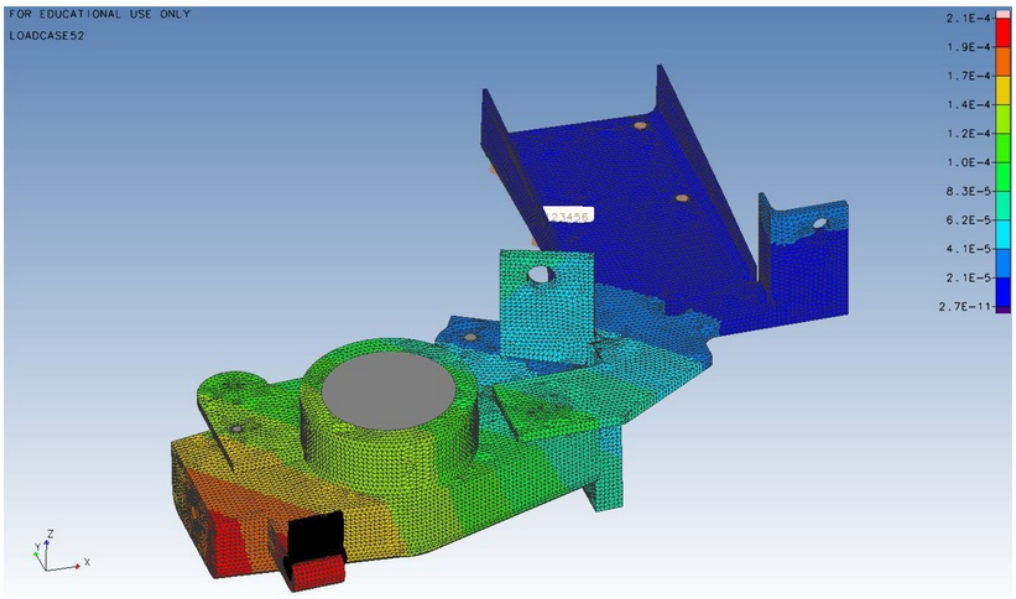
Suspension top Y



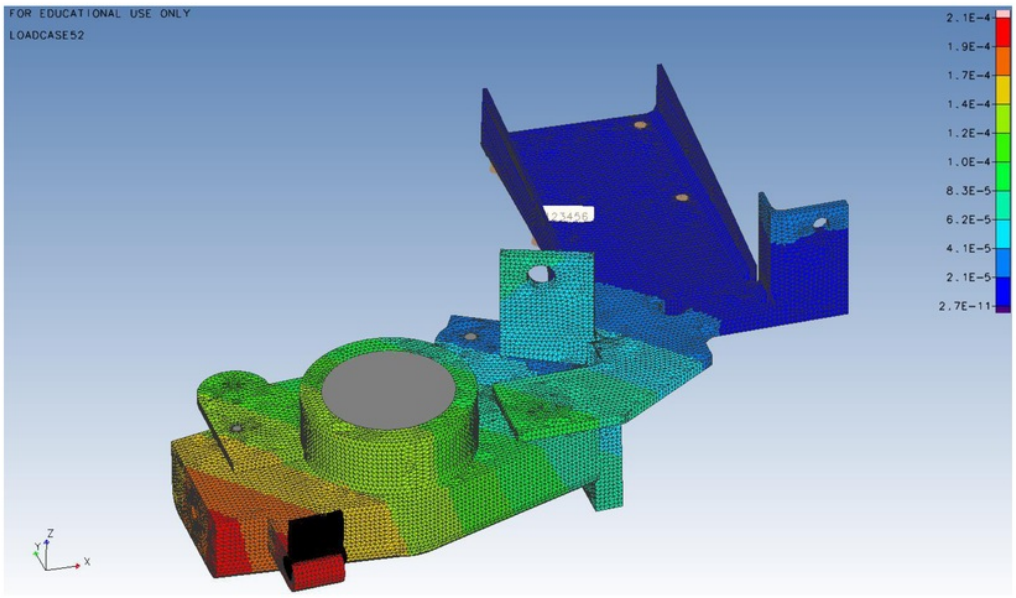
Steering Y



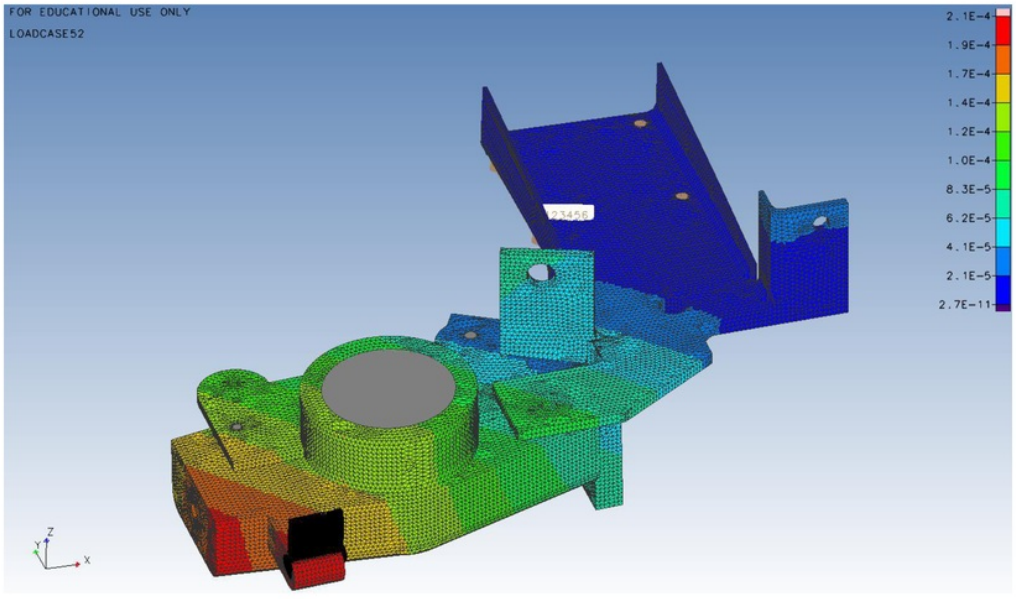
Brake low Y



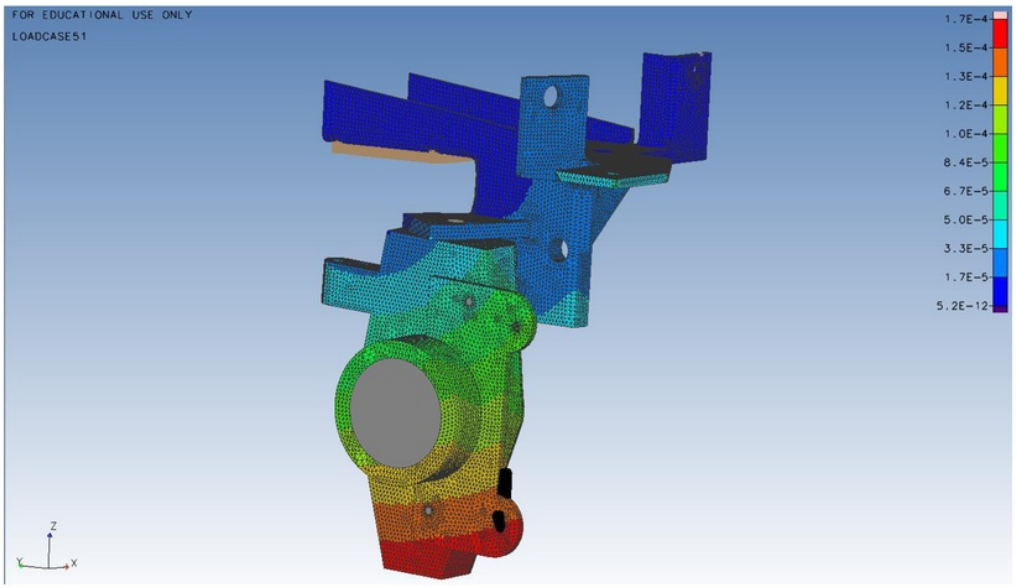
Suspension low Y



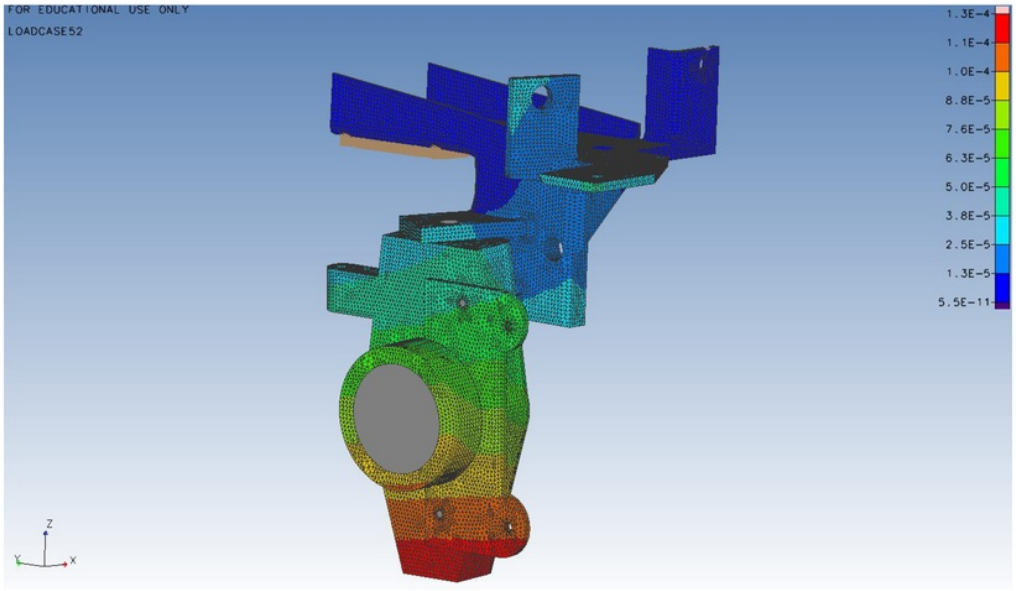
Steering Z



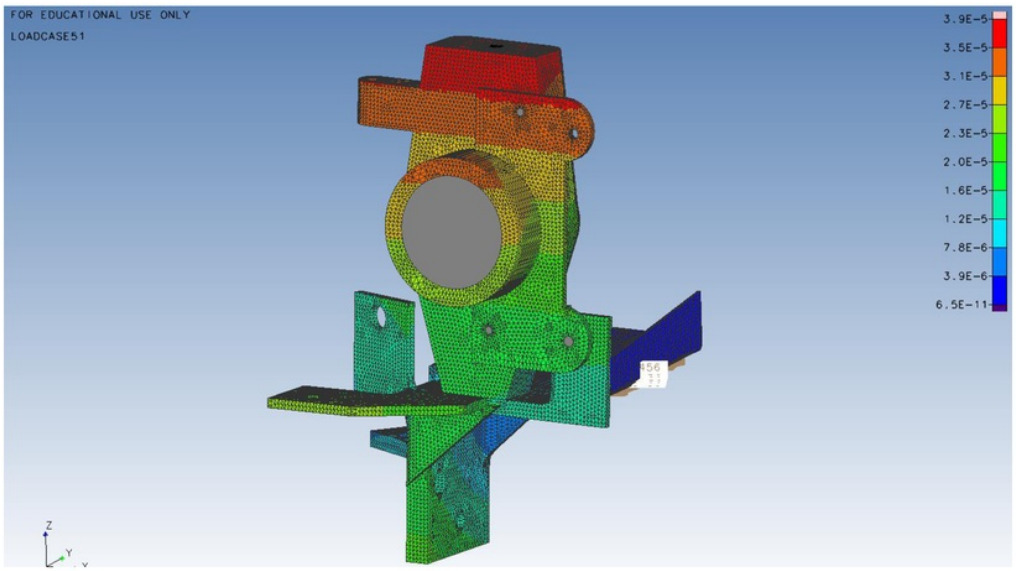
Brake low Z



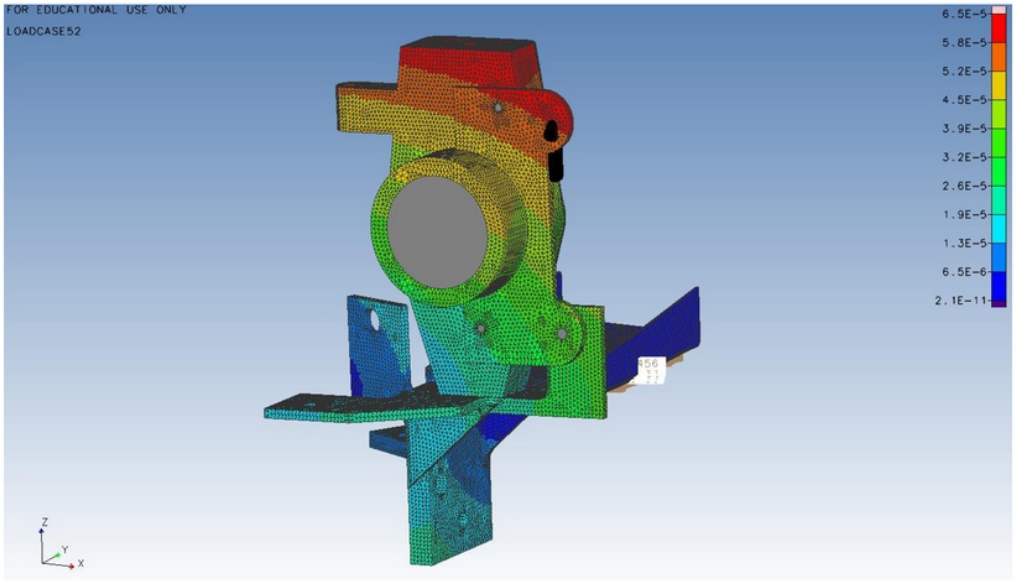
Suspension low Z



Suspension top Z

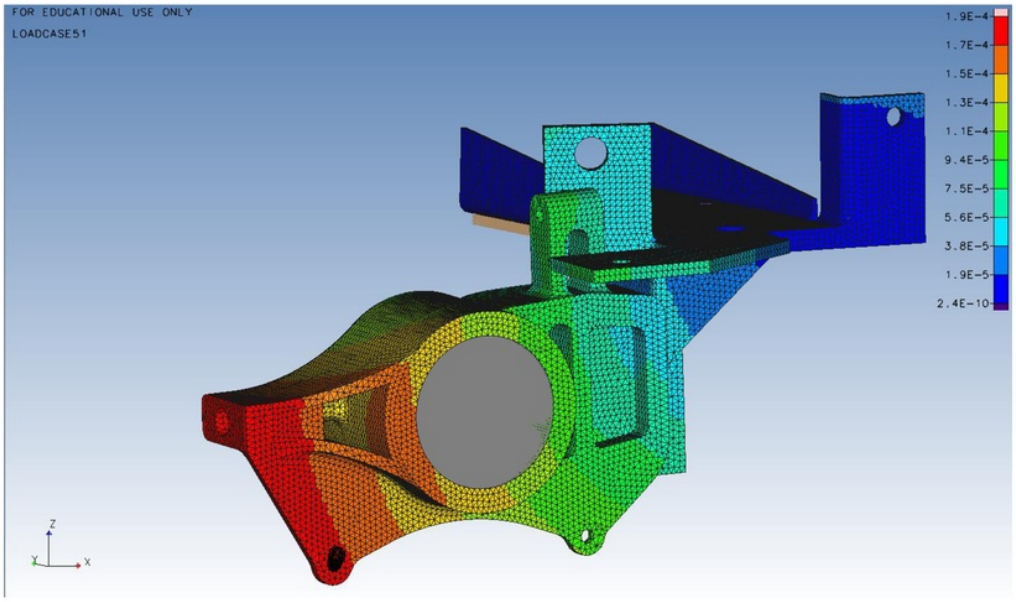


Brake top Z

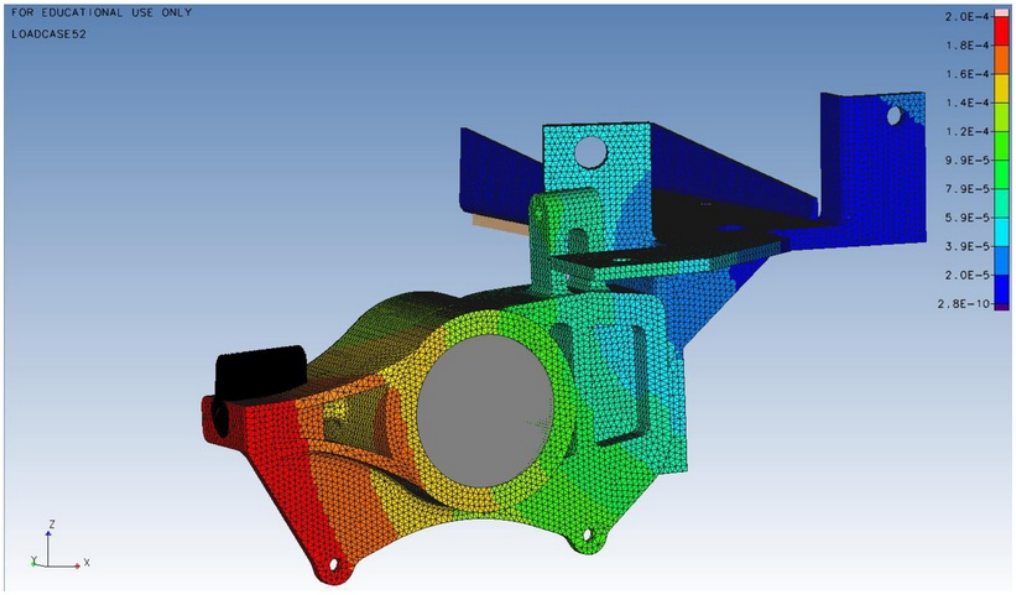


The following screenshots are from the new upright design being tested under the same workshop loads and constraints at the current upright.

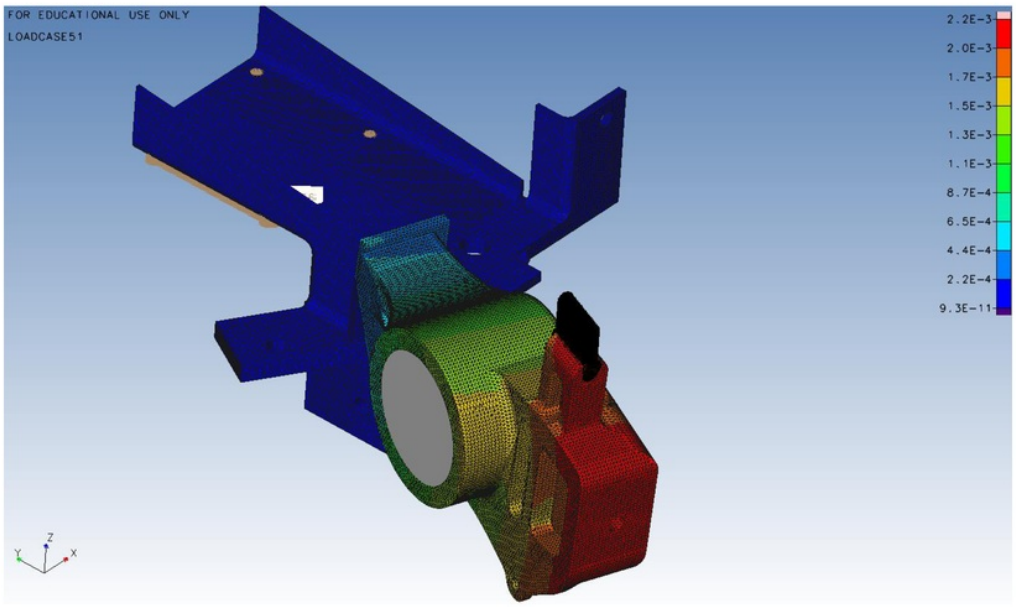
Brake low X



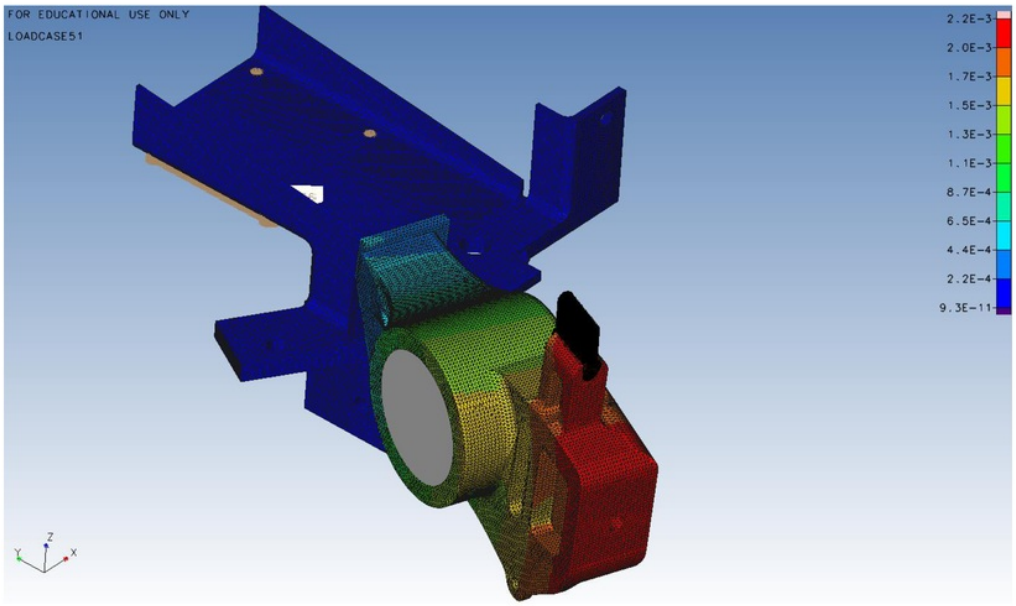
Suspension low x



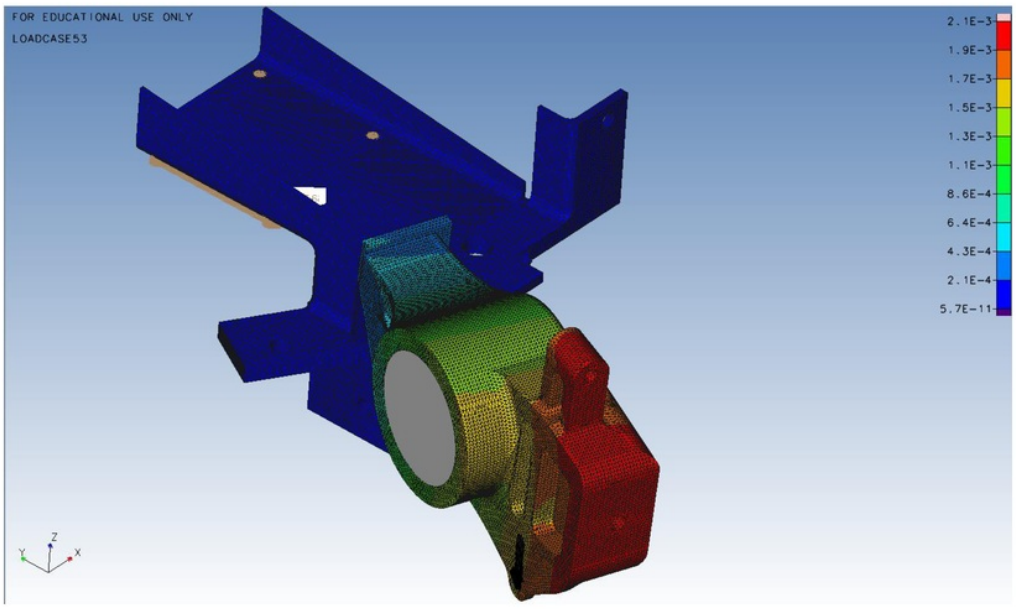
Suspension top X



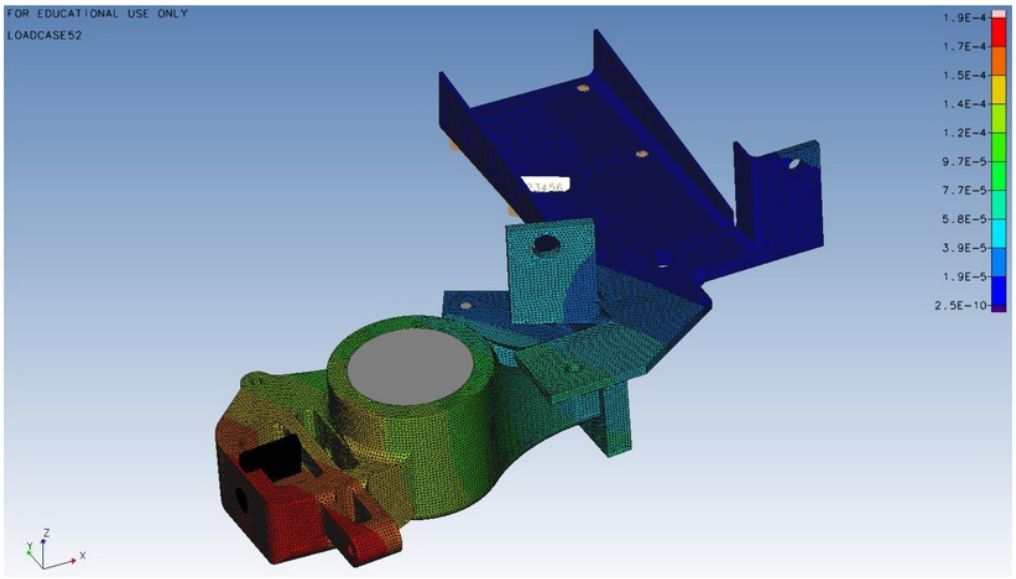
Steering X



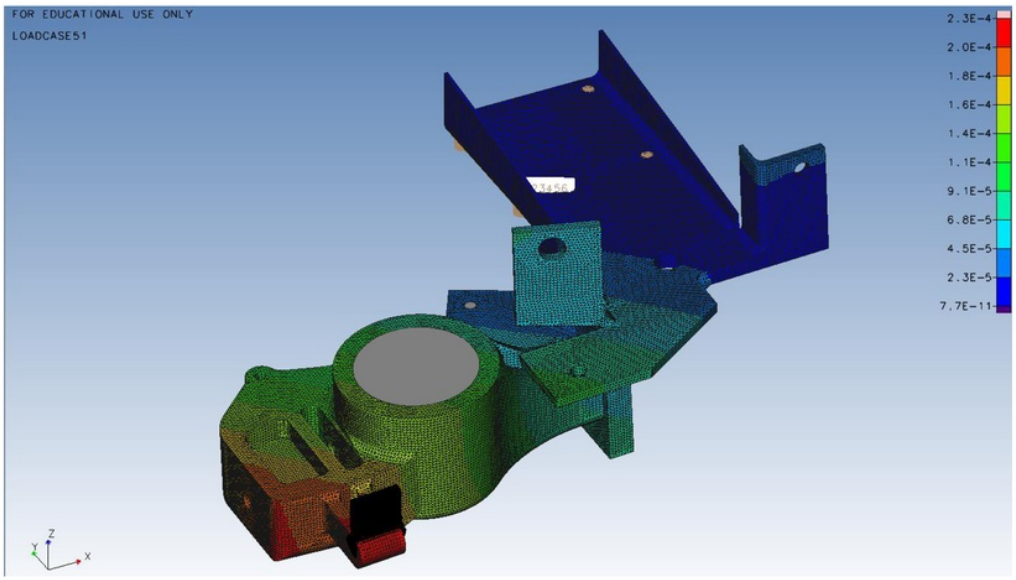
Brake top X



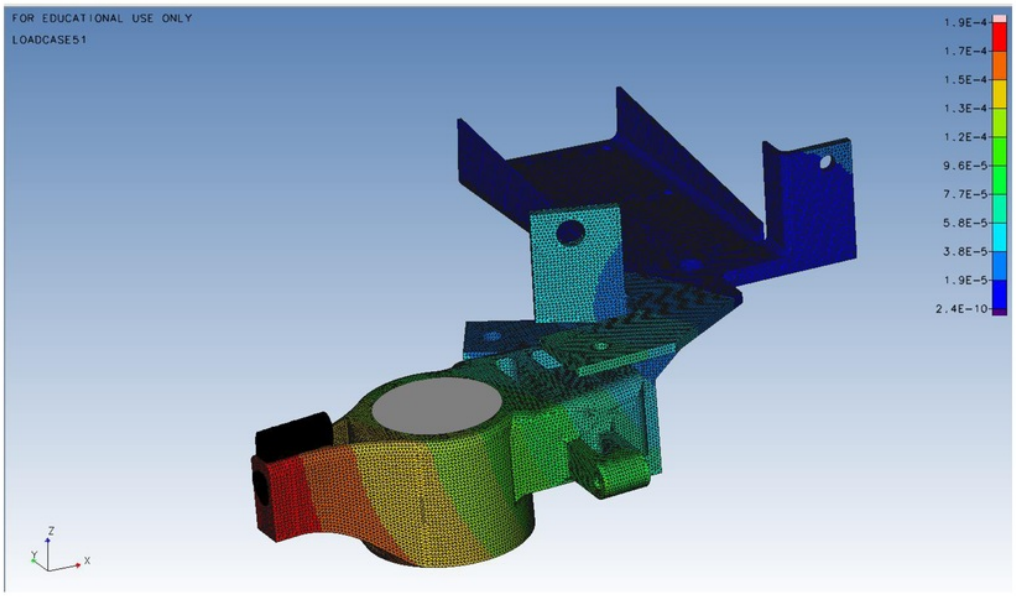
Suspension top Y



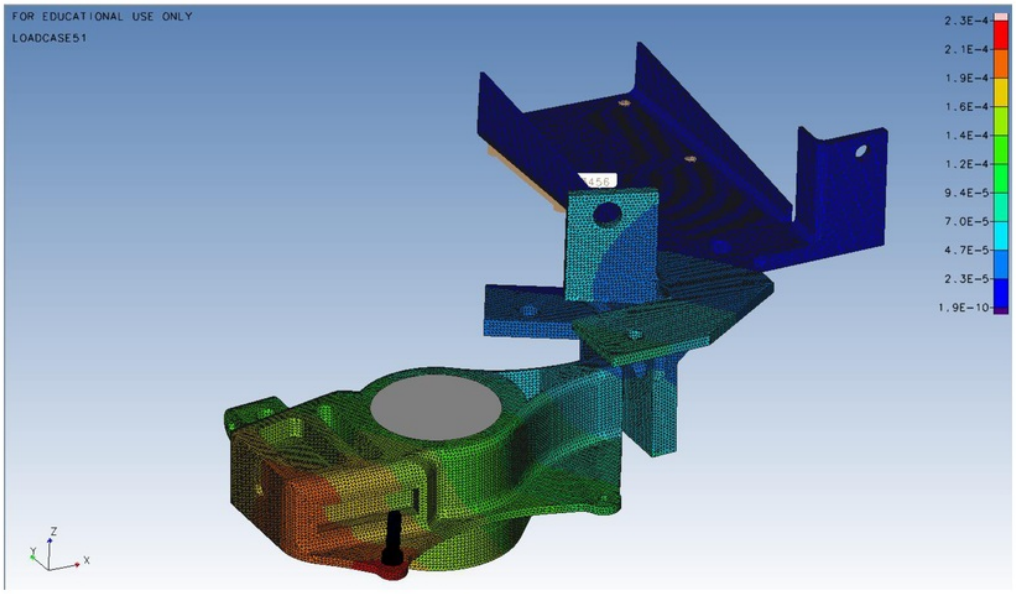
Steering Y



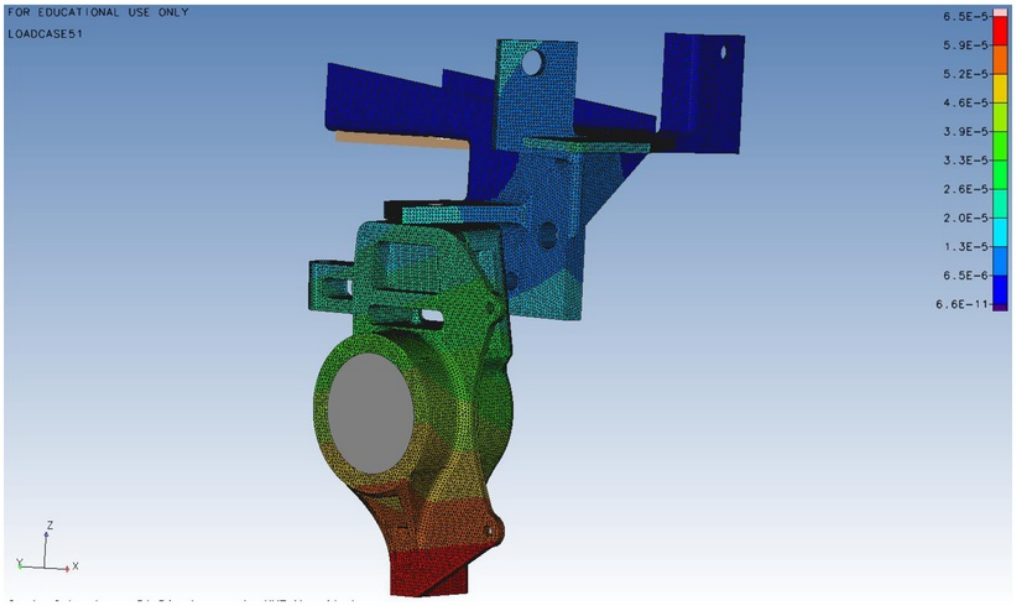
Suspension low Y



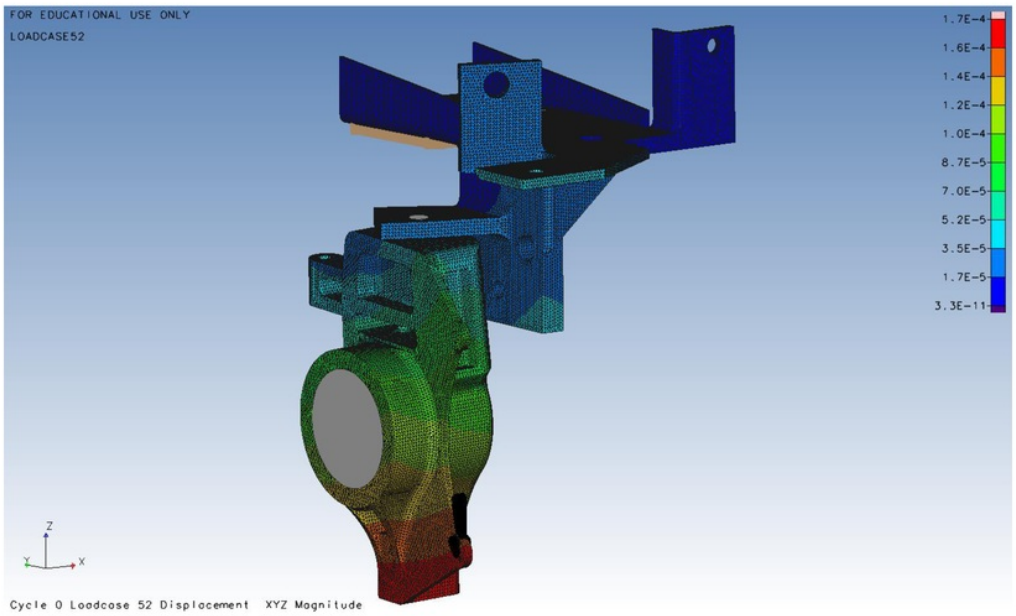
Brake top Y



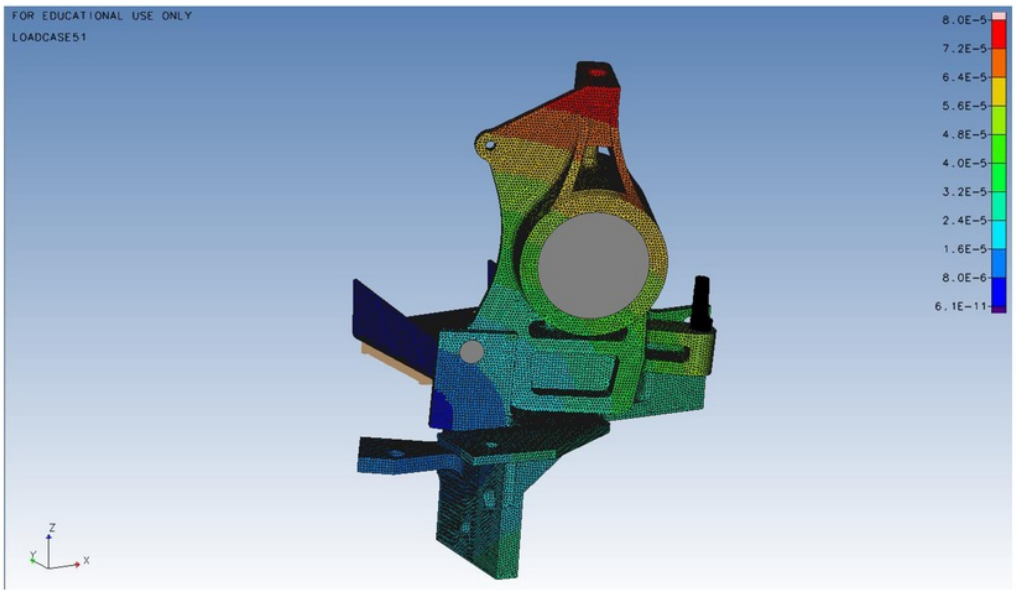
Suspension low Z



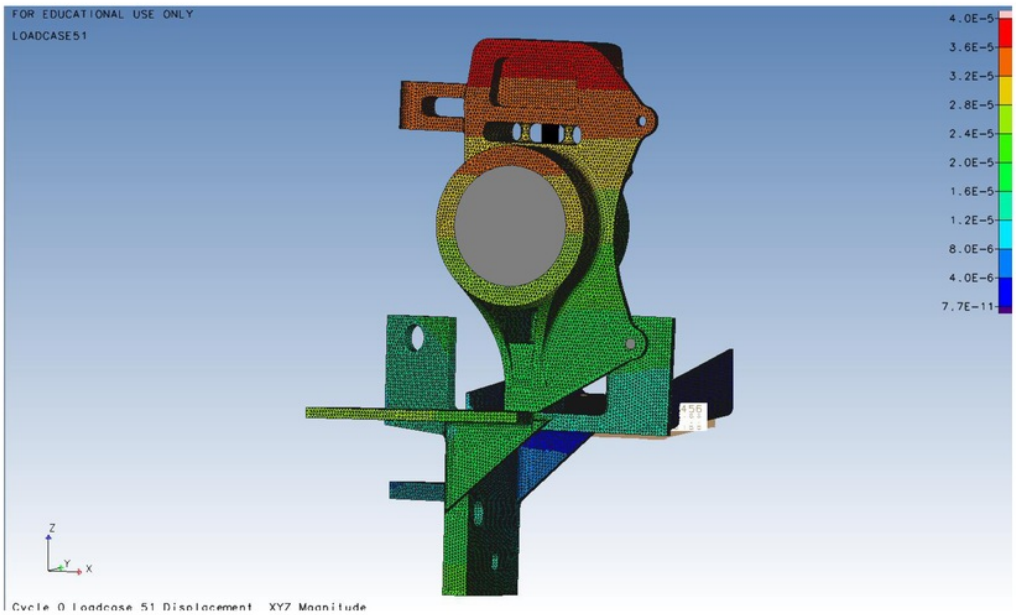
Brake low Z



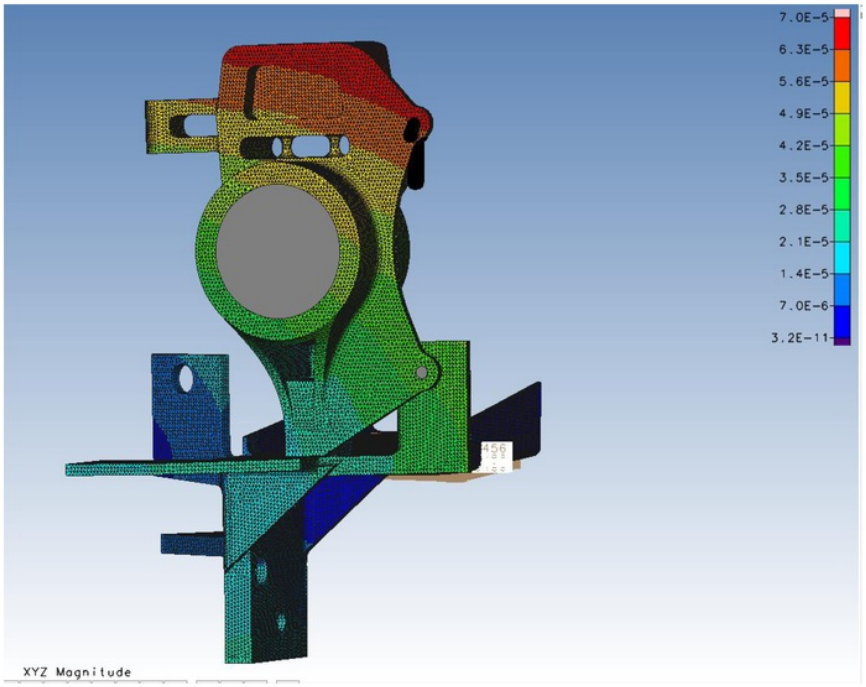
Steering Z



Suspension top Z



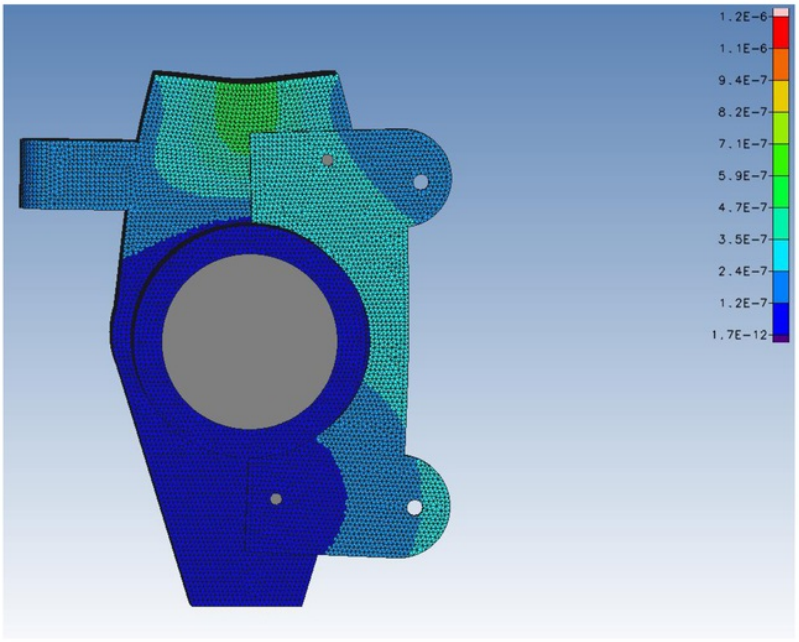
Brake top Z



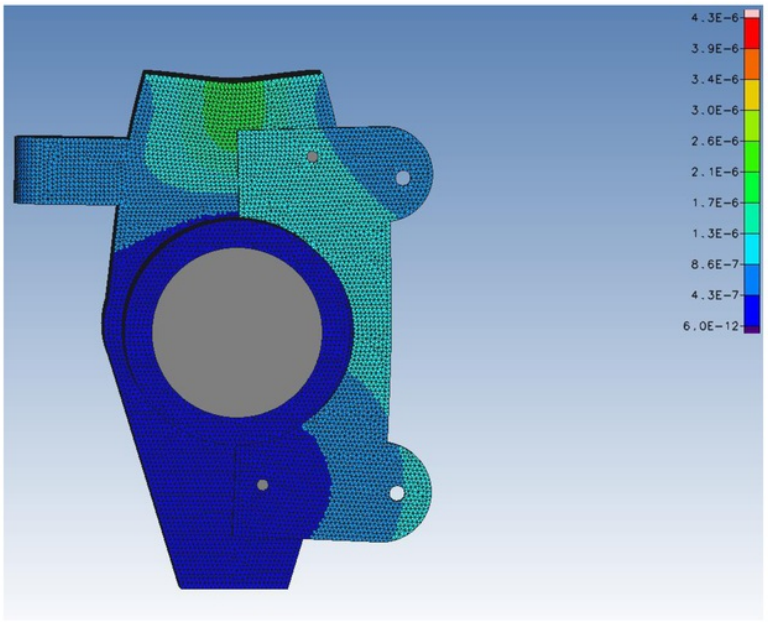
The following show the results of the FEA on the current and new upright when loaded with track forces.

Current

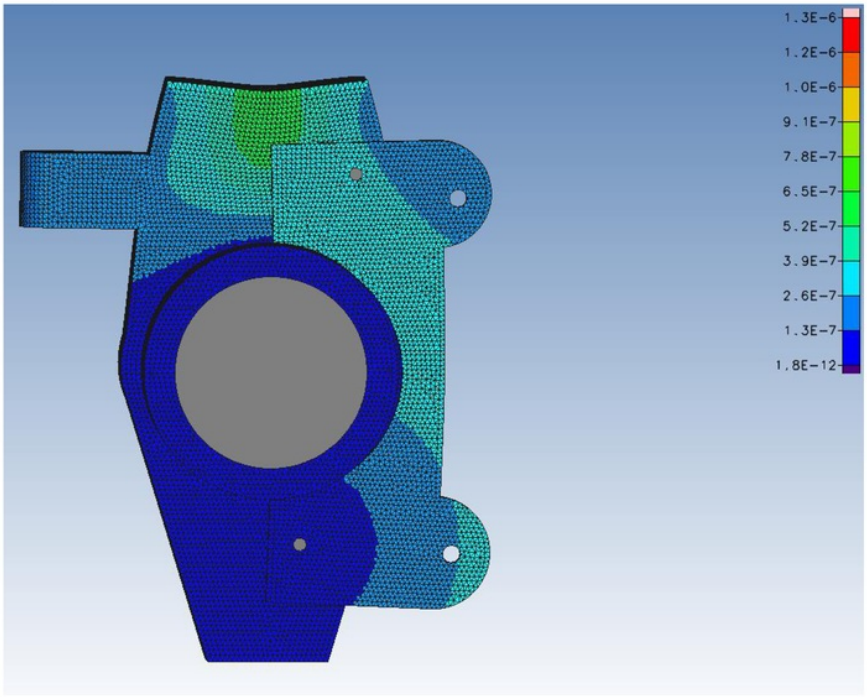
Top linear vertical



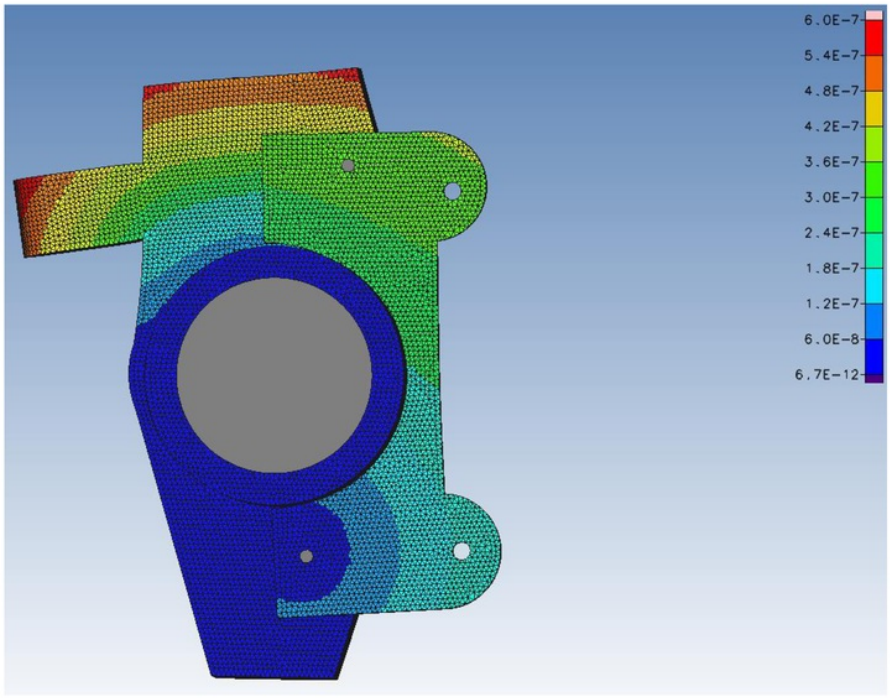
Top cornering vertical



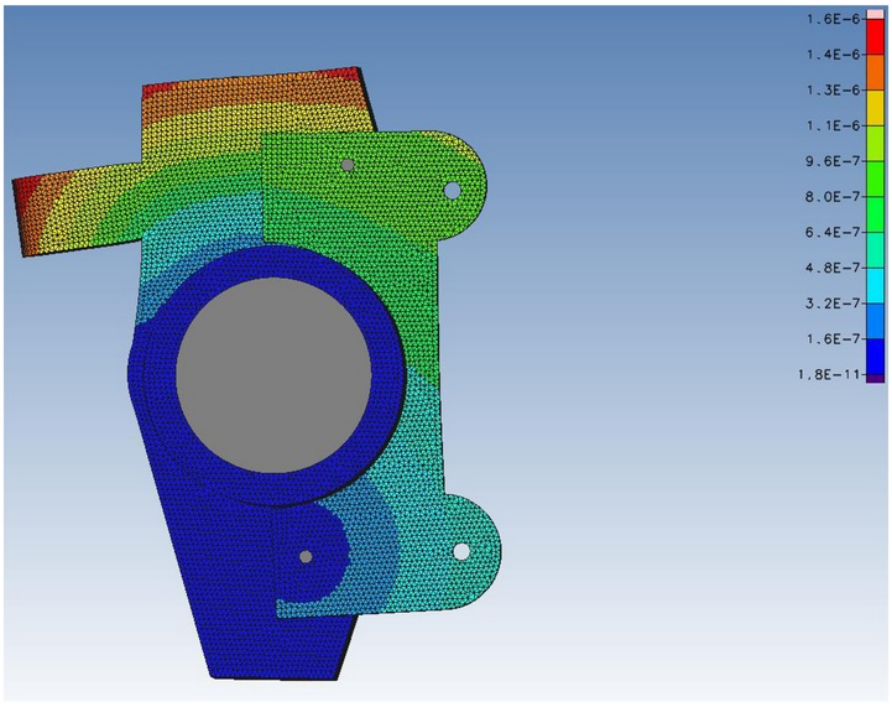
Top braking vertical



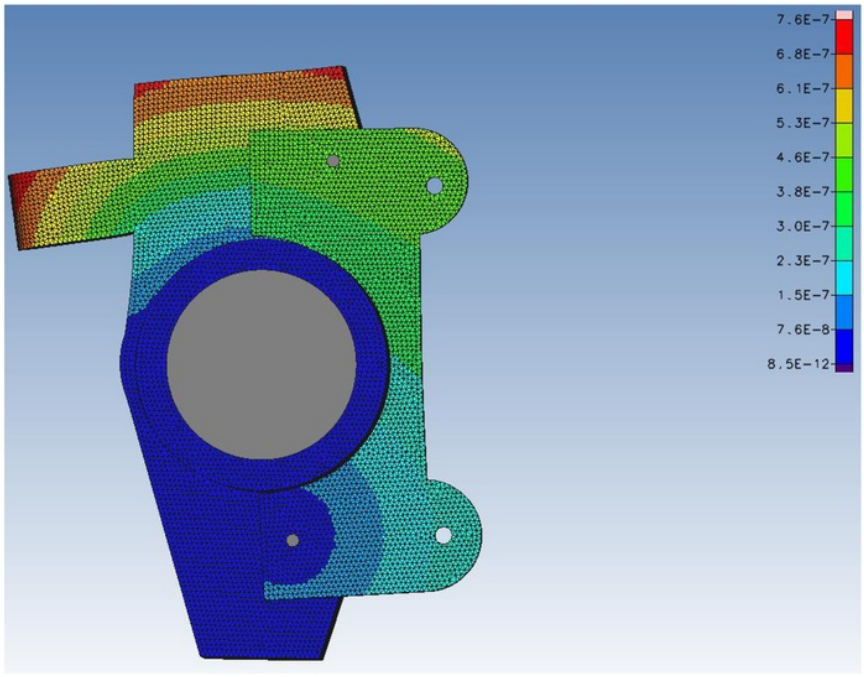
Top linear horizontal



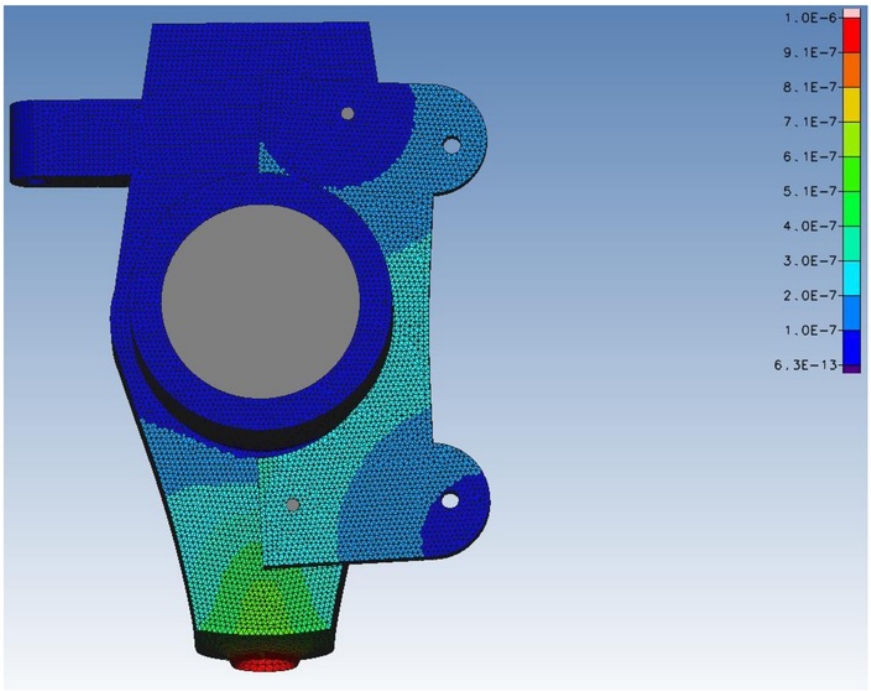
Top cornering horizontal



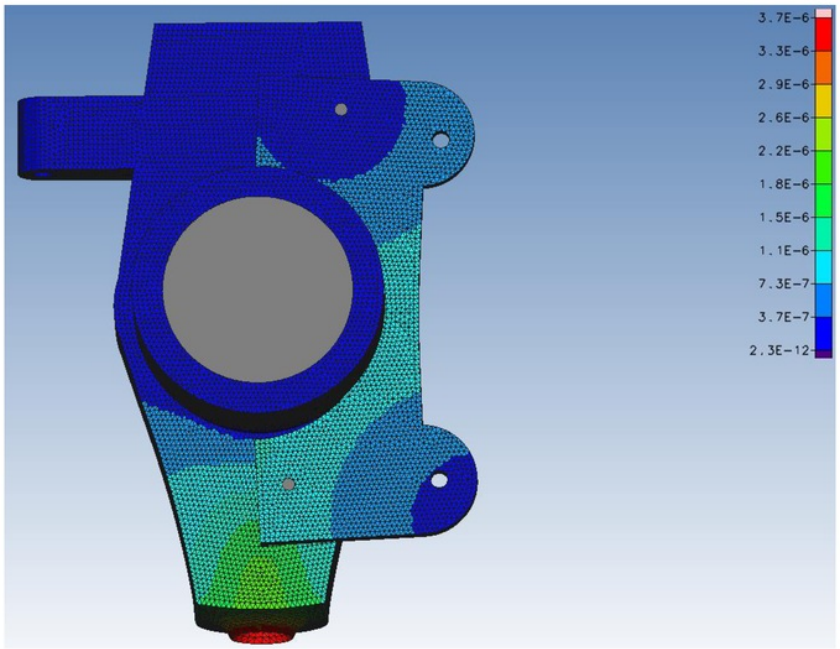
Top braking horizontal



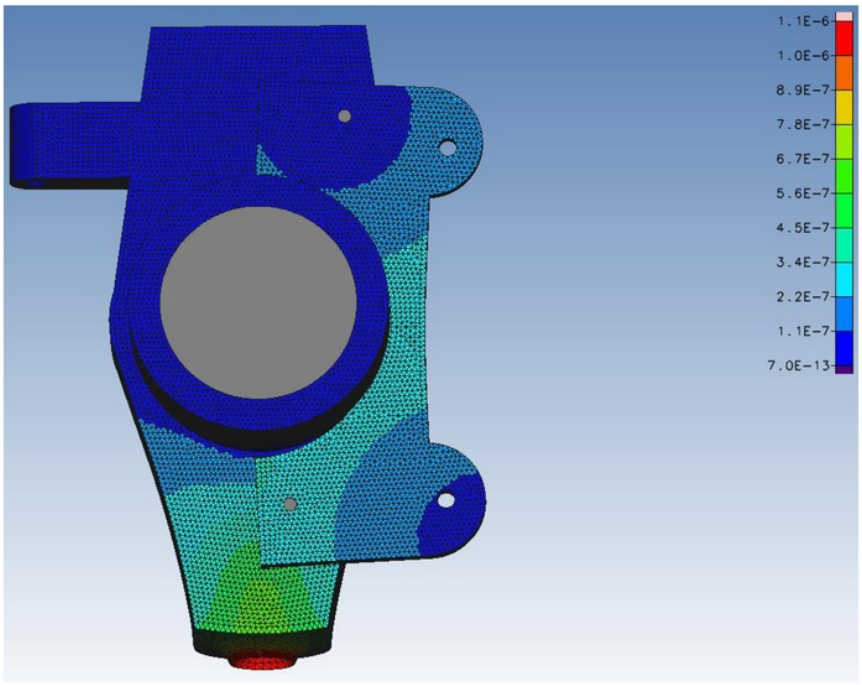
Bottom vertical linear



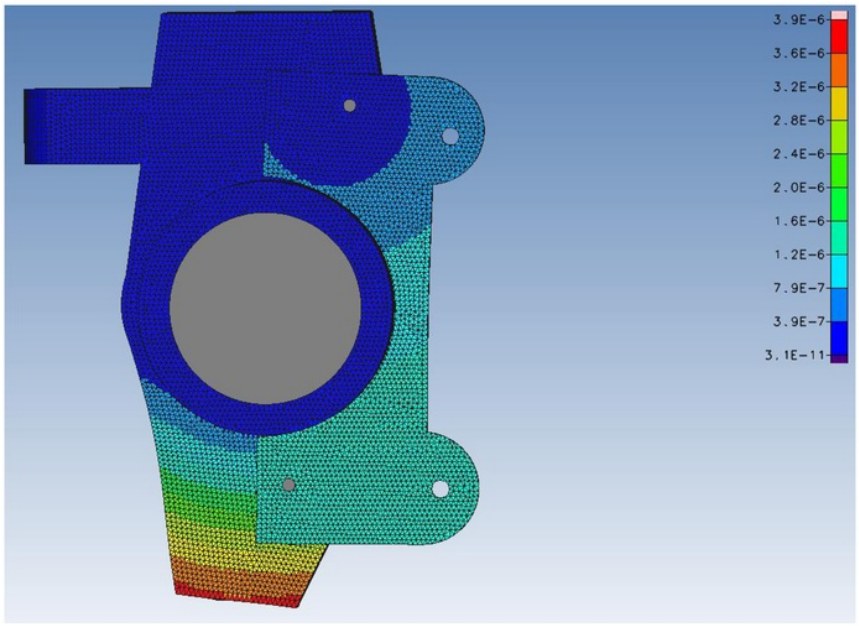
Bottom vertical cornering



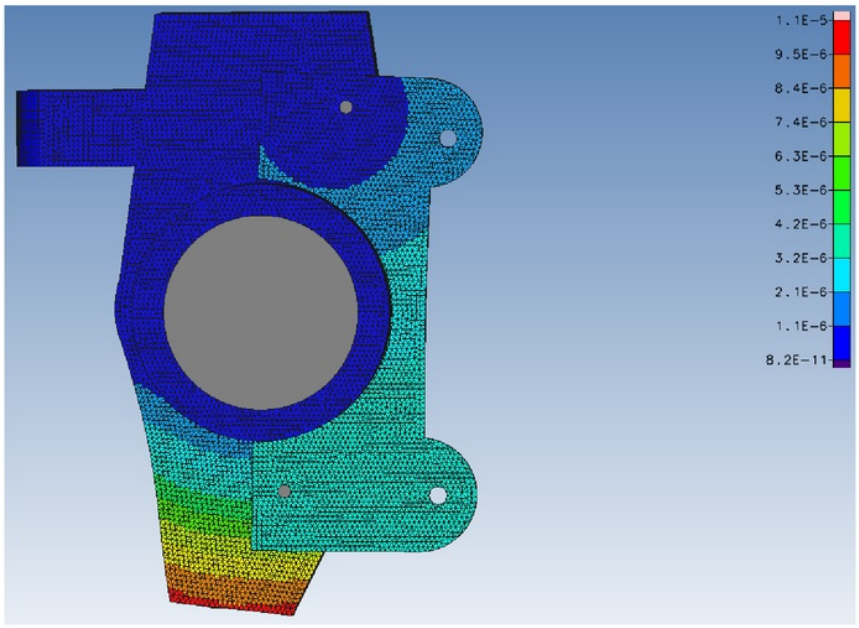
Bottom vertical braking



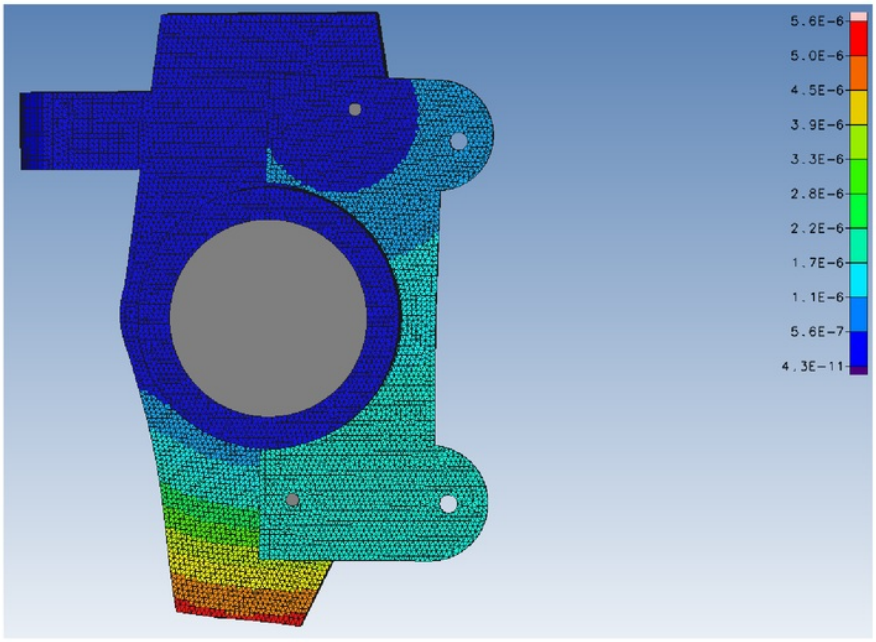
Bottom horizontal linear



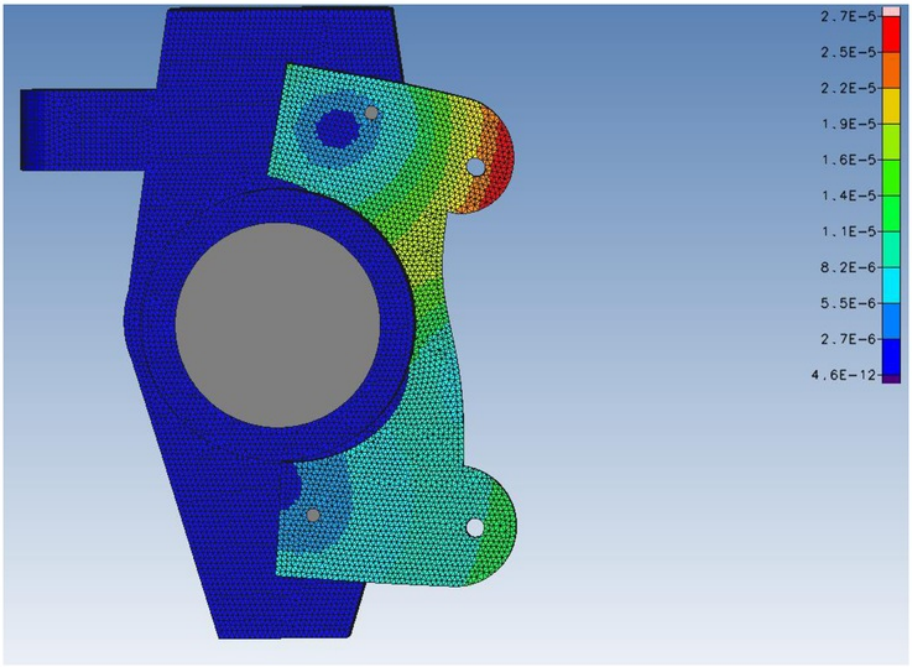
Bottom horizontal cornering



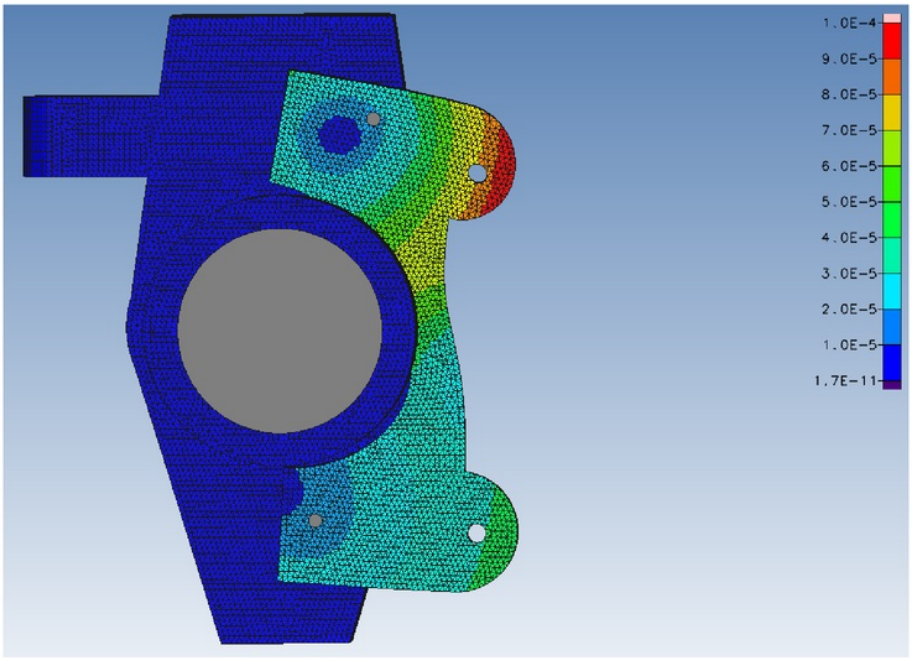
Bottom horizontal braking



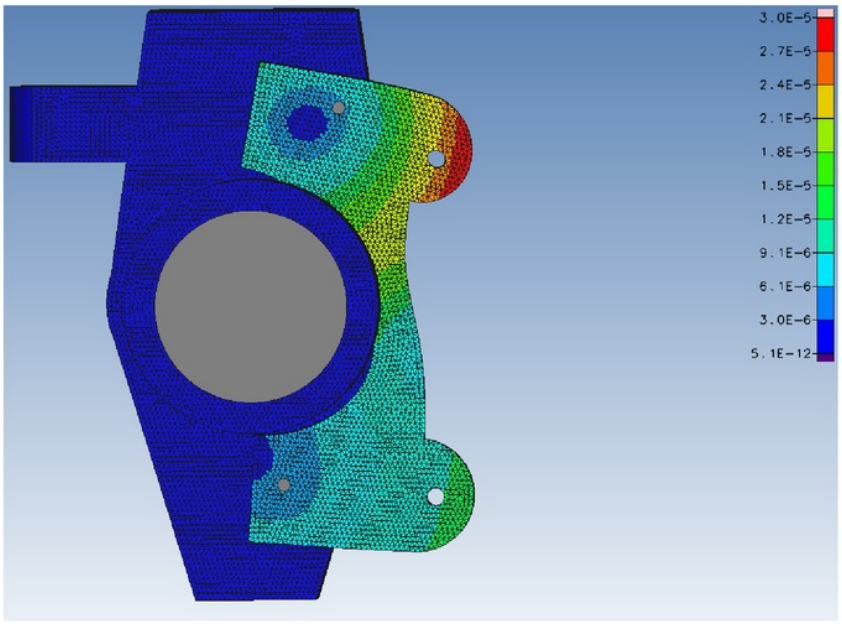
Brake top vertical liner



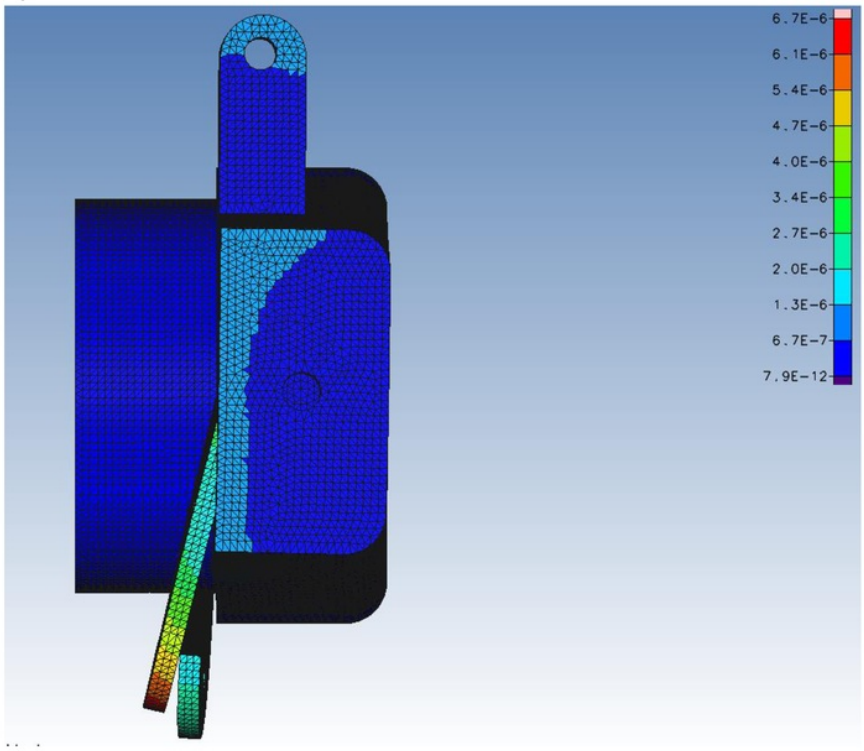
Brake top vertical cornering



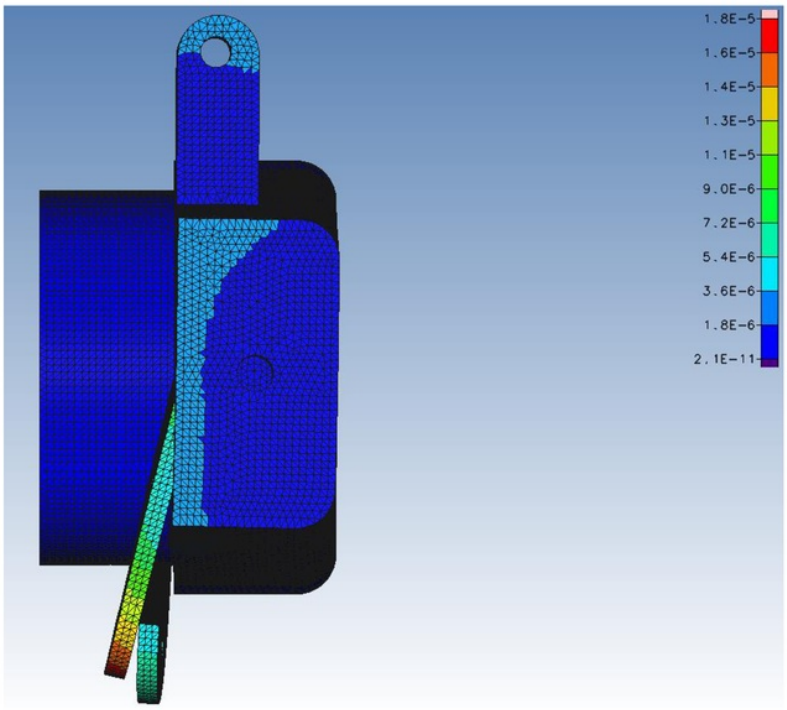
Brake top vertical braking



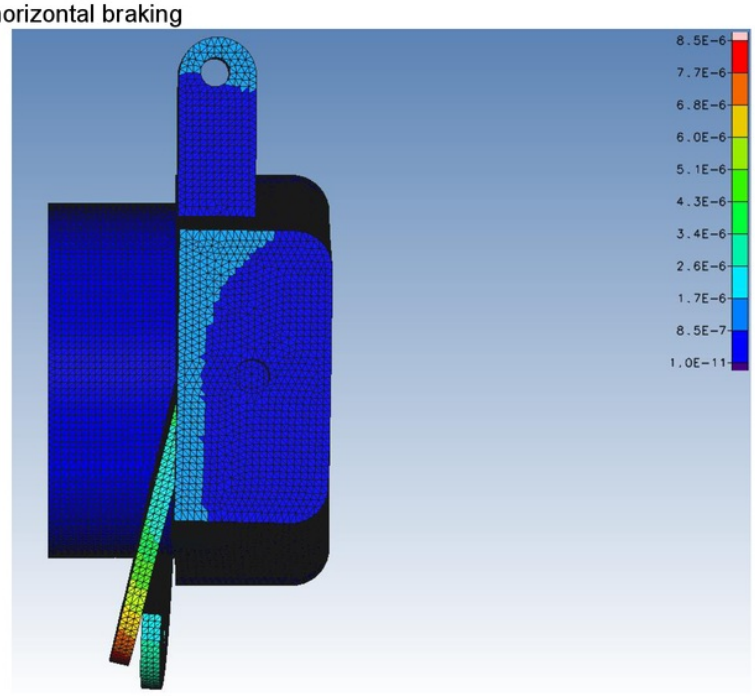
Brake top horizontal linear



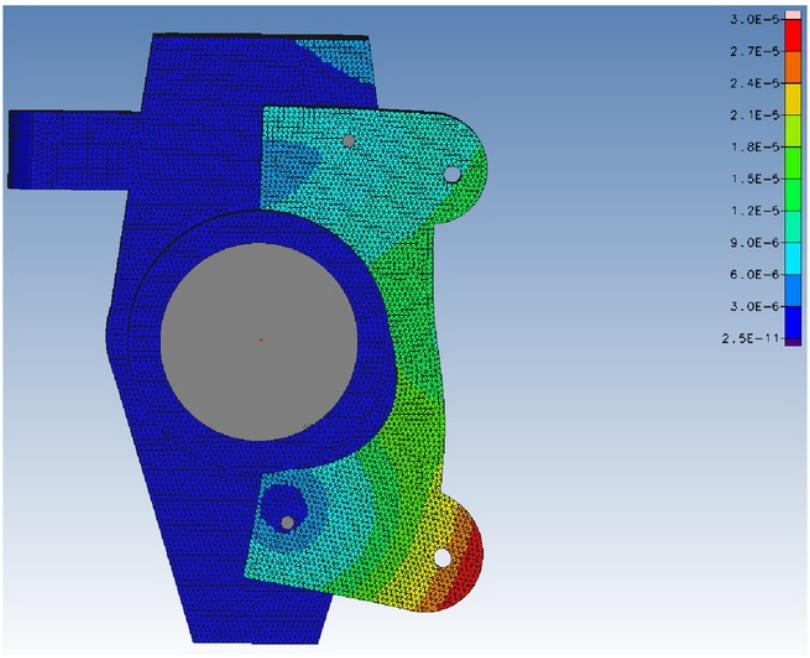
Brake top horizontal cornering



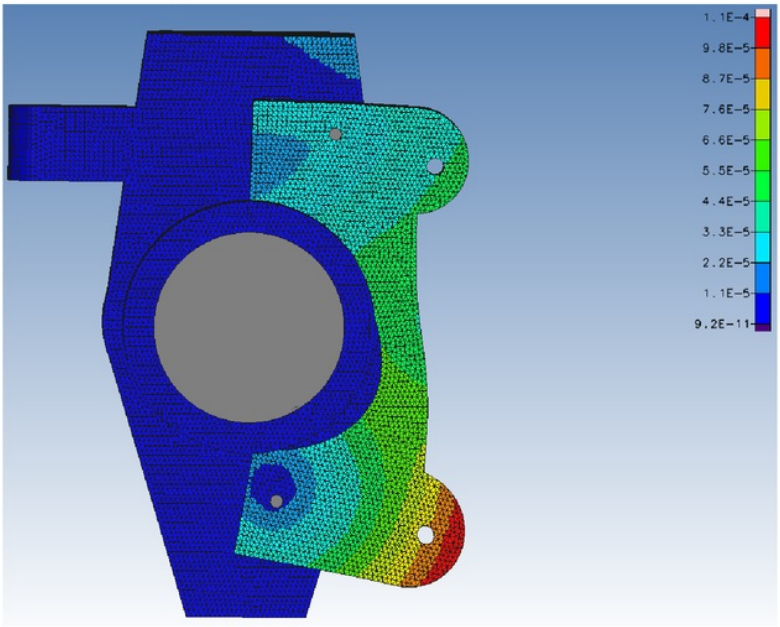
Brake top horizontal braking



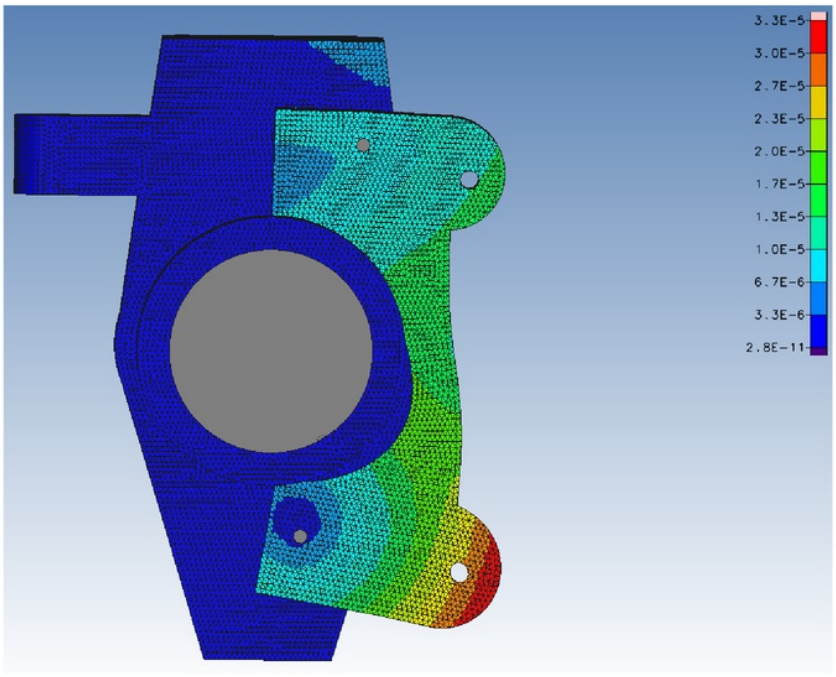
Brake low vertical linear



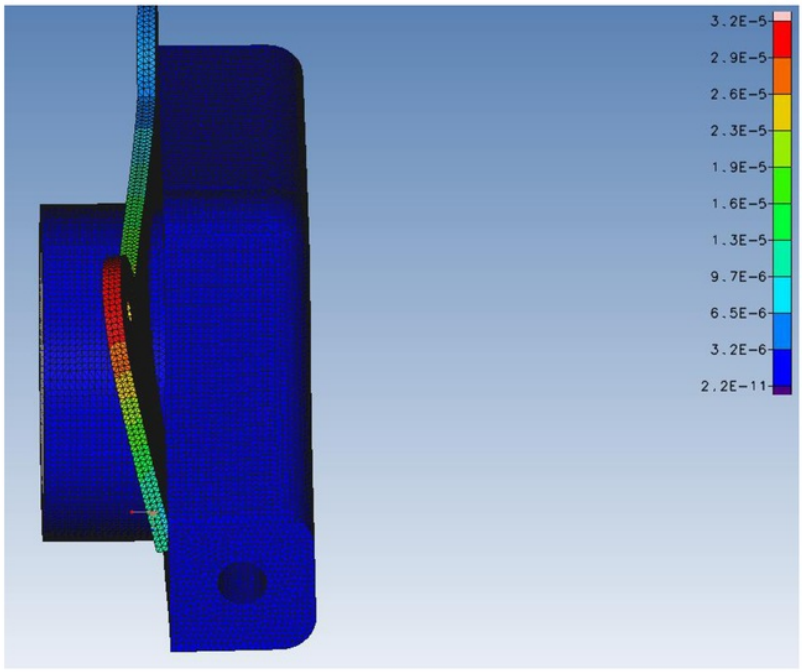
Brake low vertical cornering



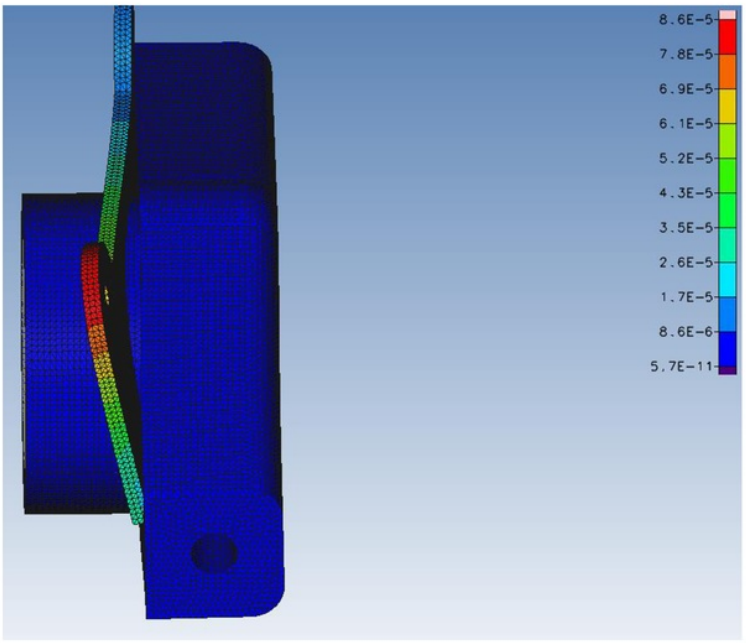
Brake low vertical braking



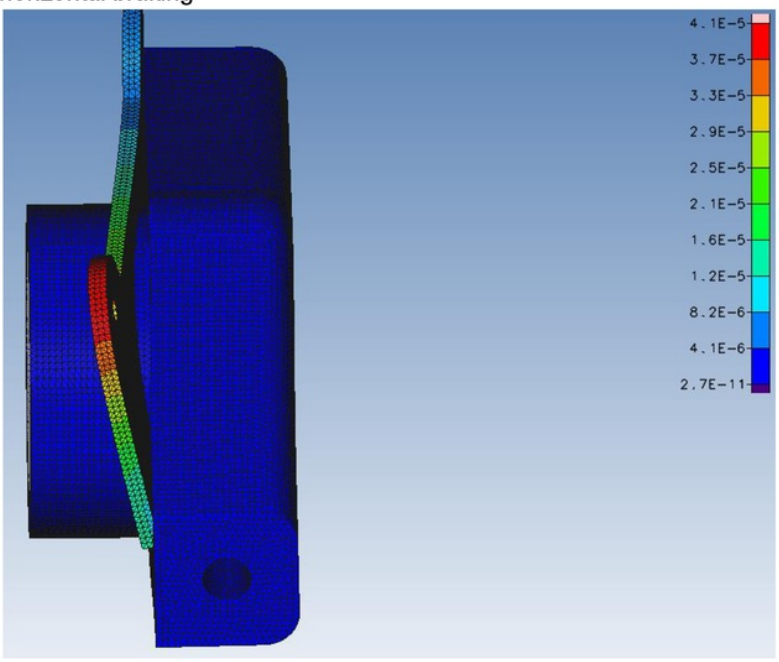
Brake low horizontal linear



Brake low horizontal cornering

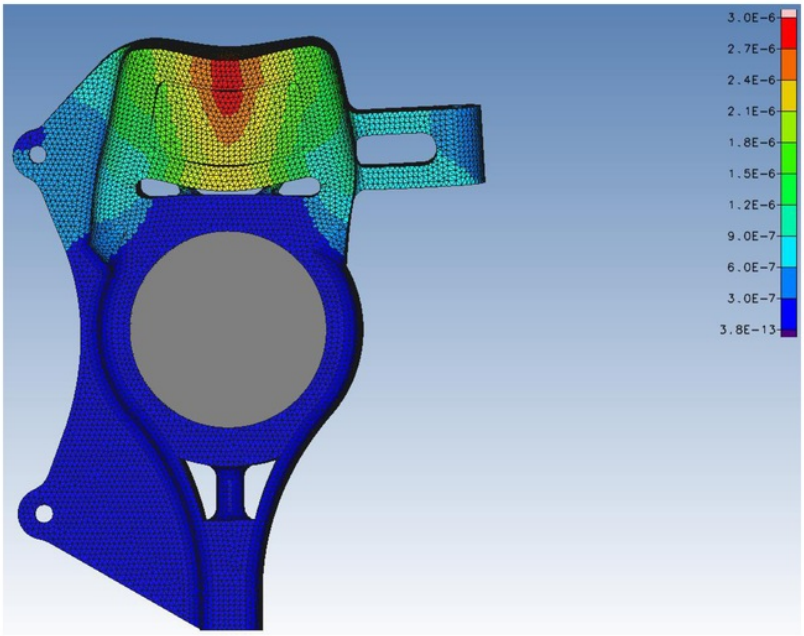


Brake low horizontal braking

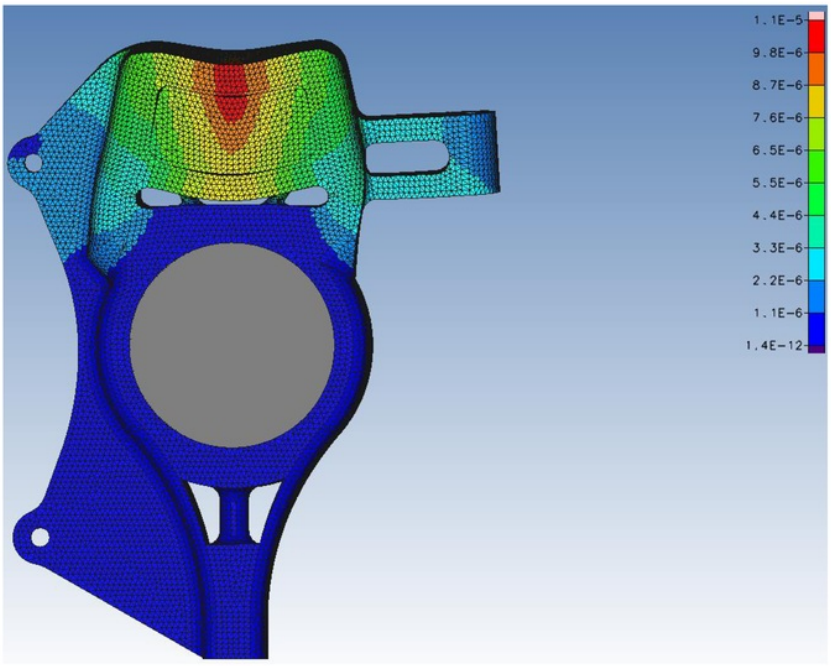


New Upright

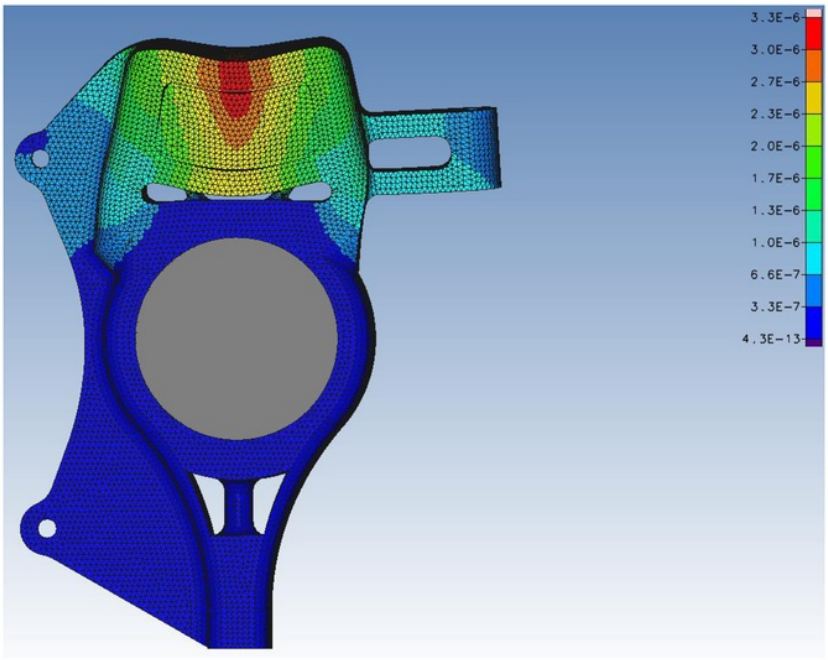
Top vertical linear



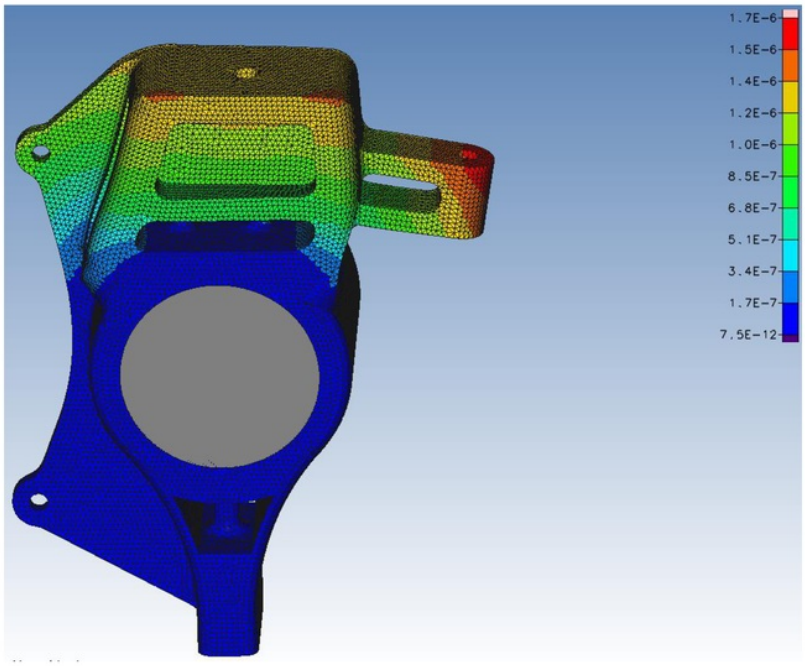
Top vertical cornering



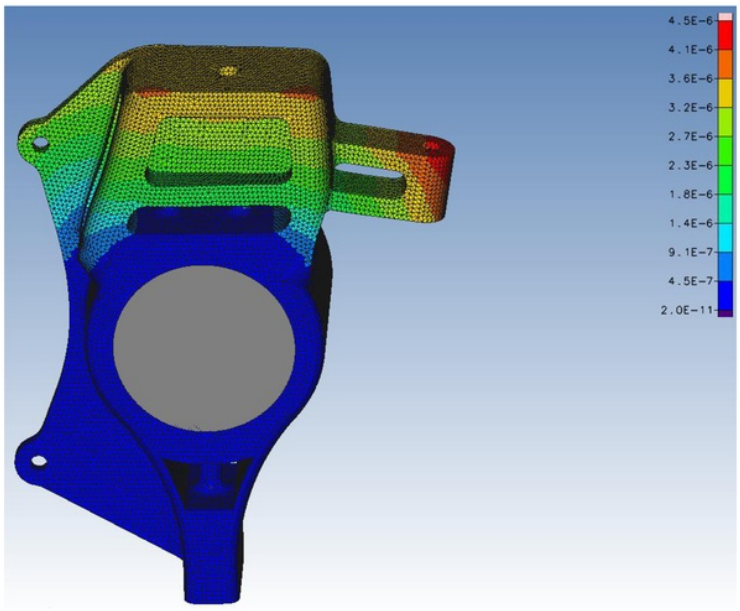
Top vertical braking



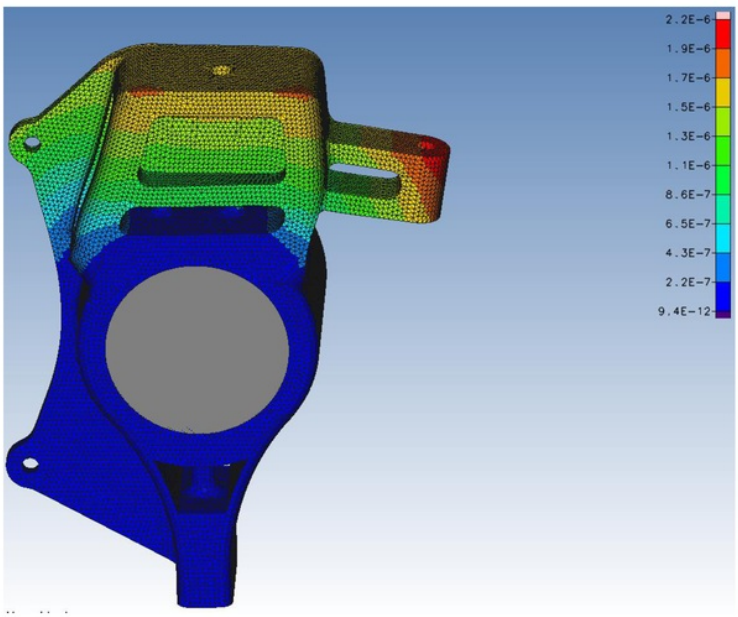
Top horizontal linear



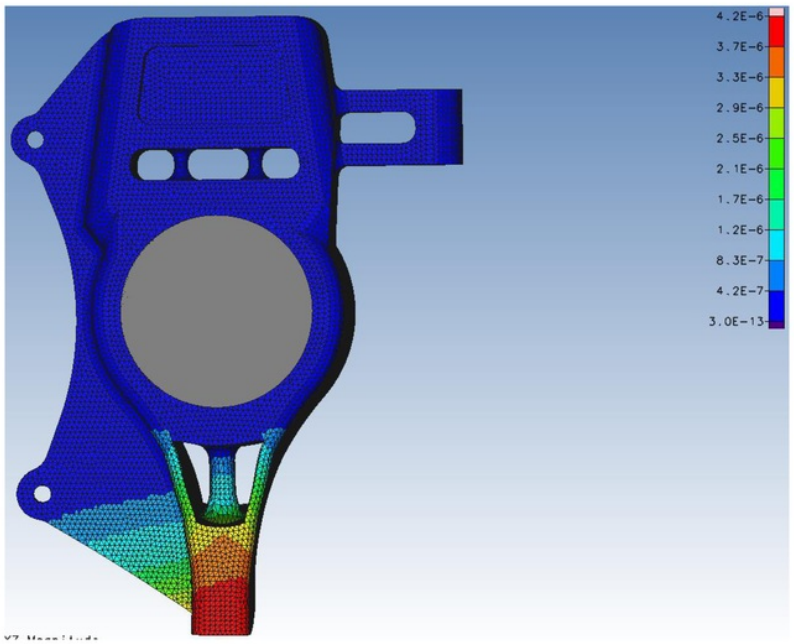
Top horizontal cornering



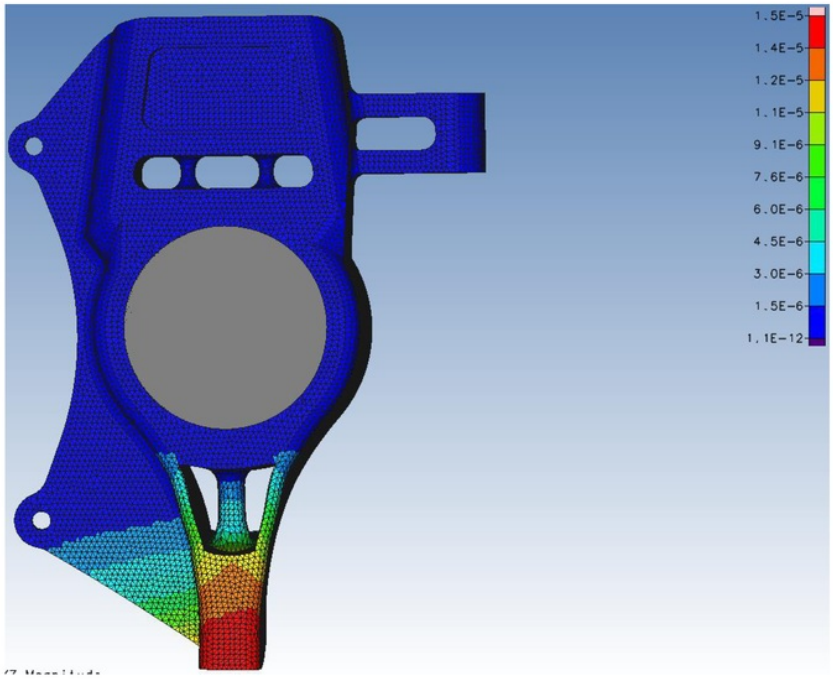
Top horizontal braking



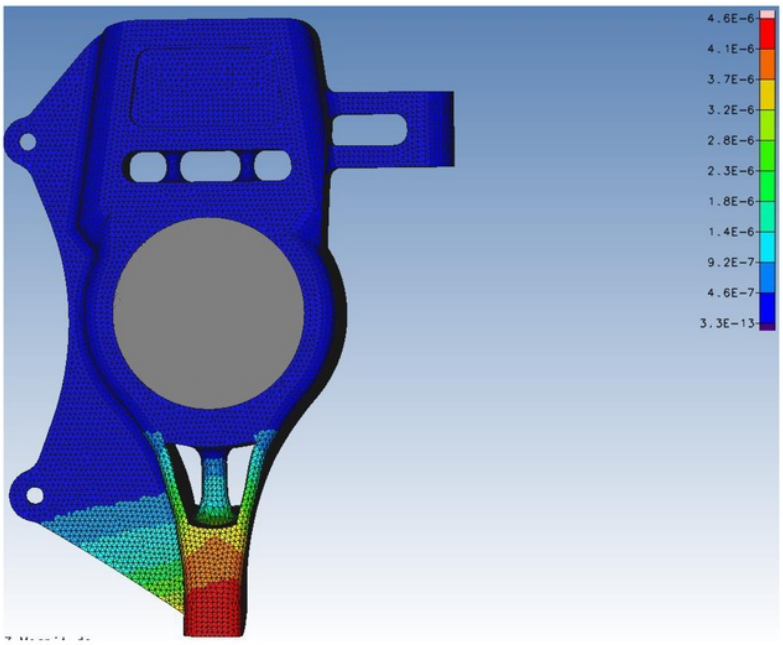
Bottom vertical linear



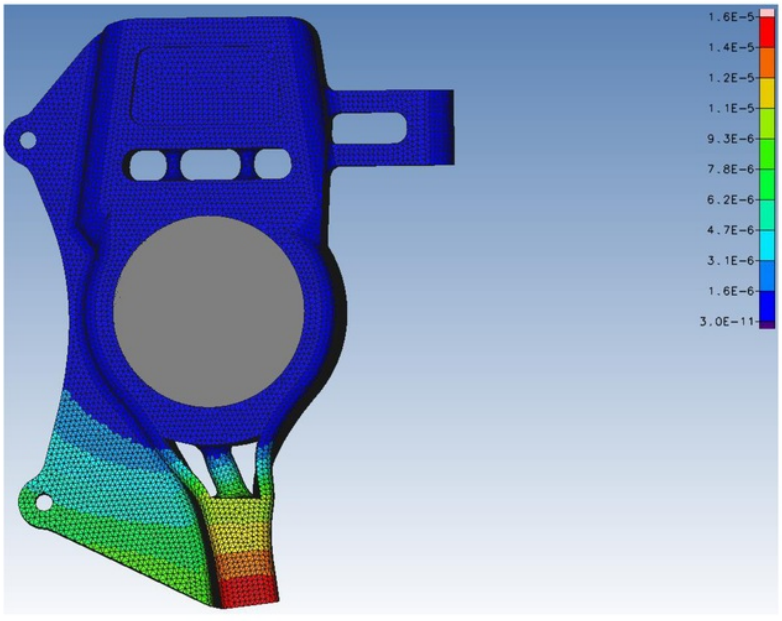
Bottom vertical cornering



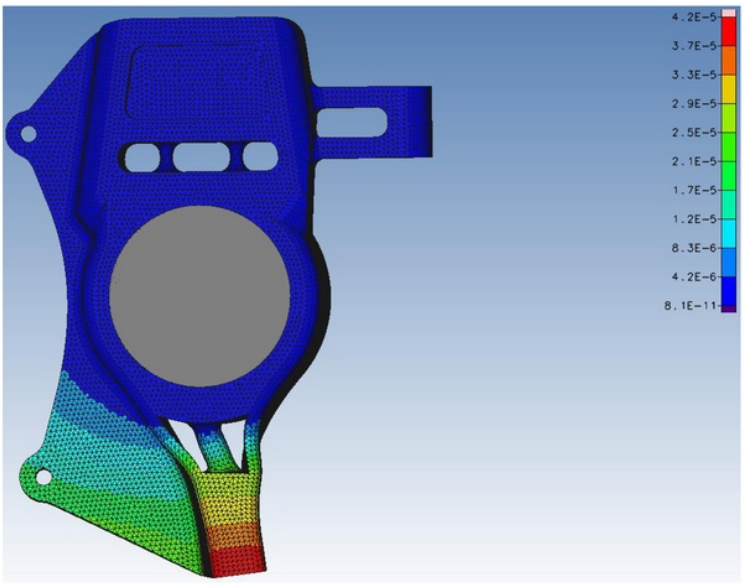
Bottom vertical braking



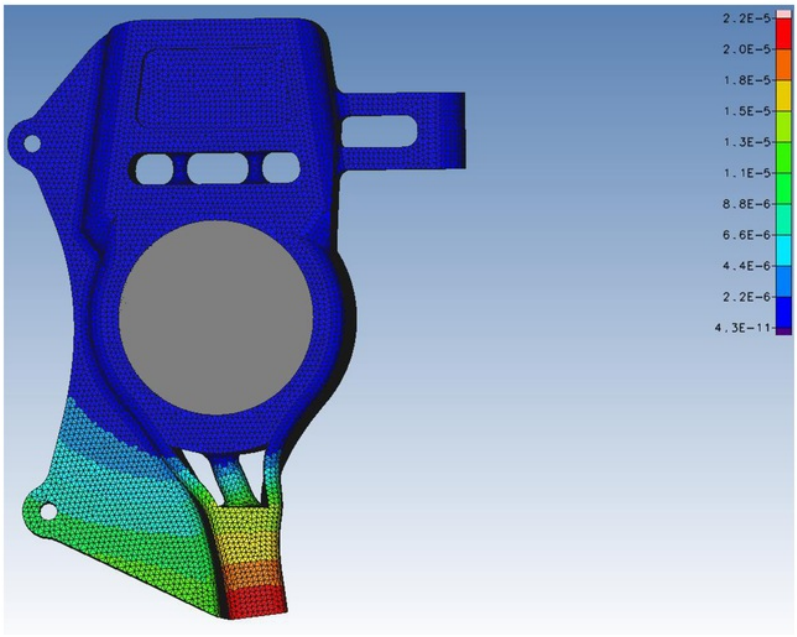
Bottom horizontal linear



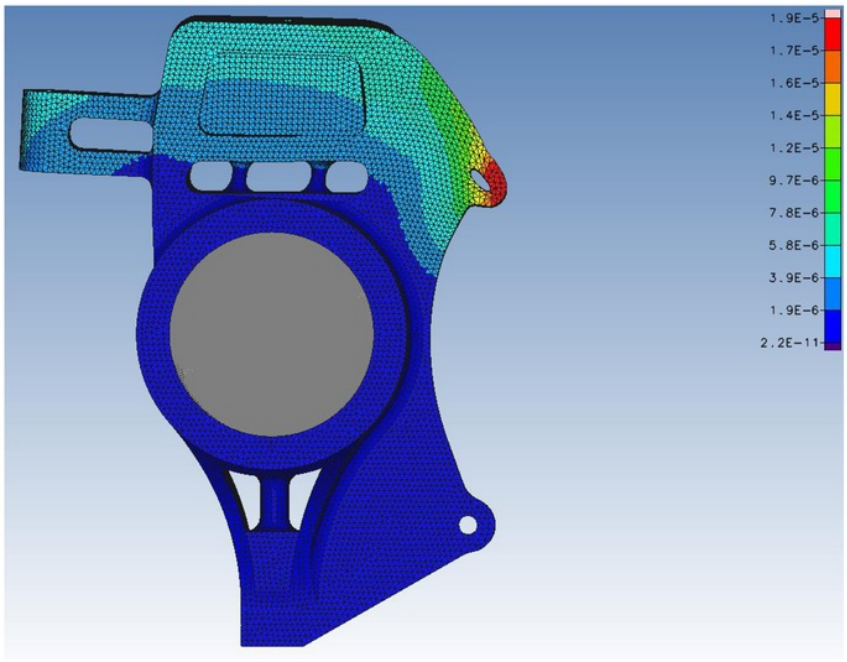
Bottom horizontal cornering



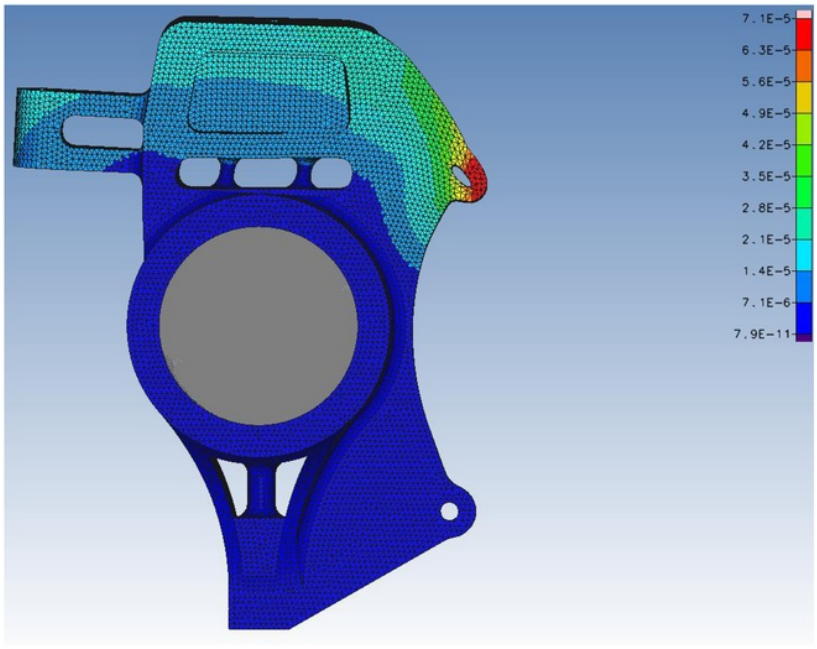
Bottom horizontal braking



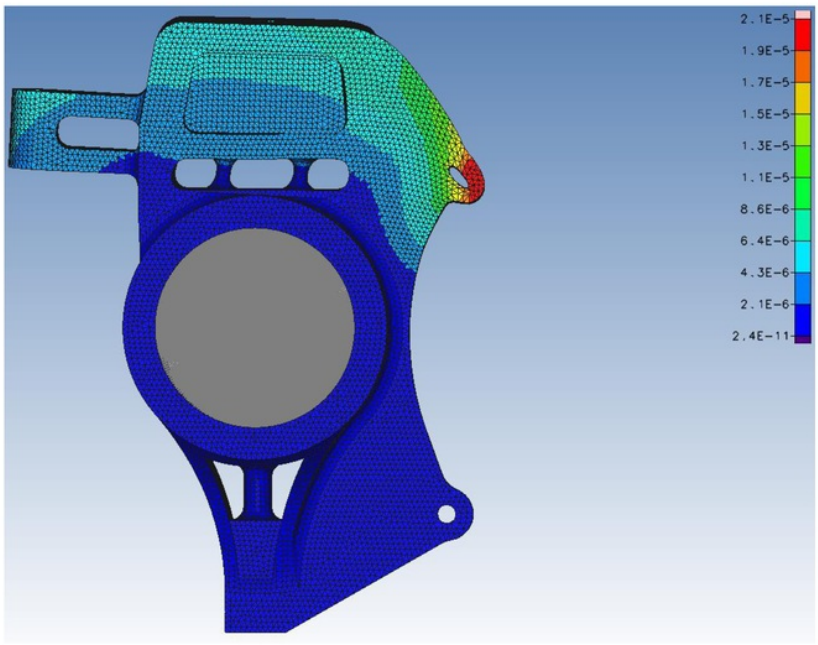
Brake top vertical linear



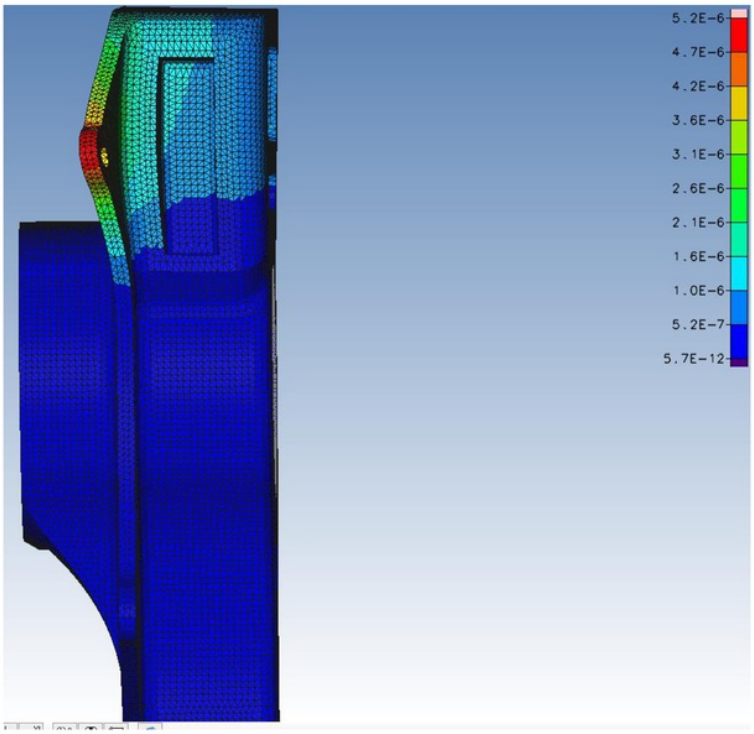
Brake top vertical cornering



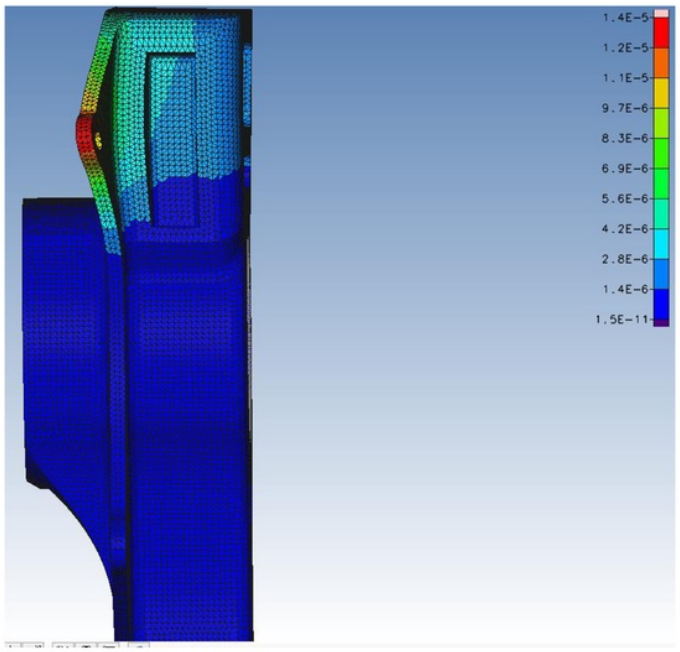
Brake top vertical braking



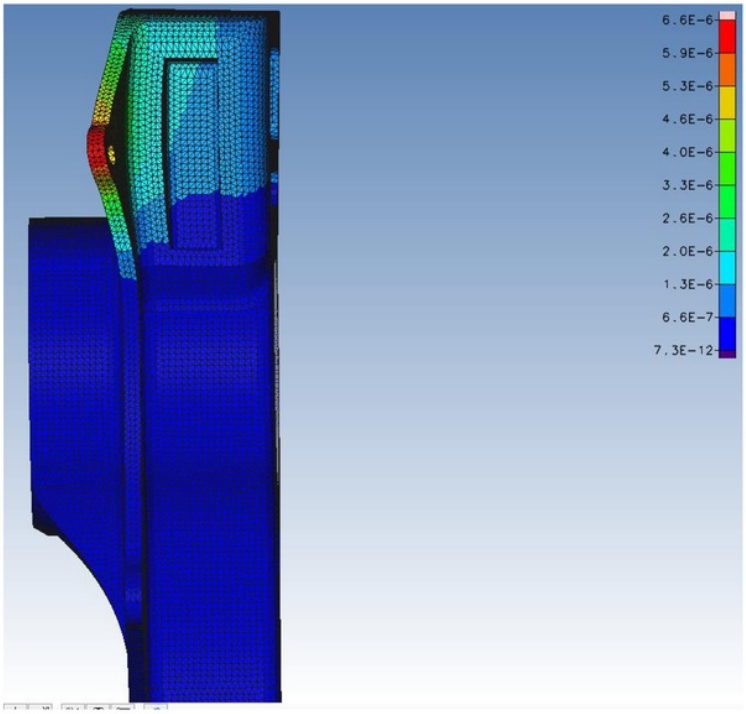
Brake top horizontal linear



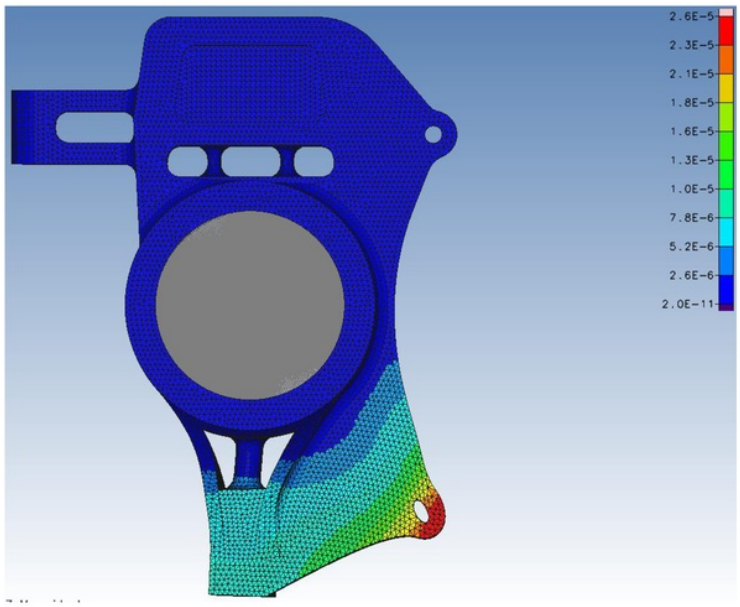
Brake top horizontal cornering



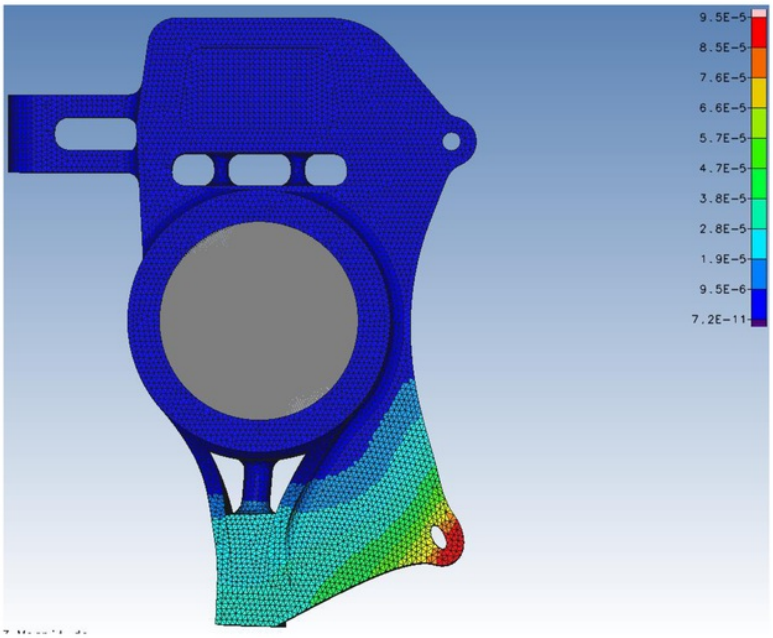
Brake top horizontal braking



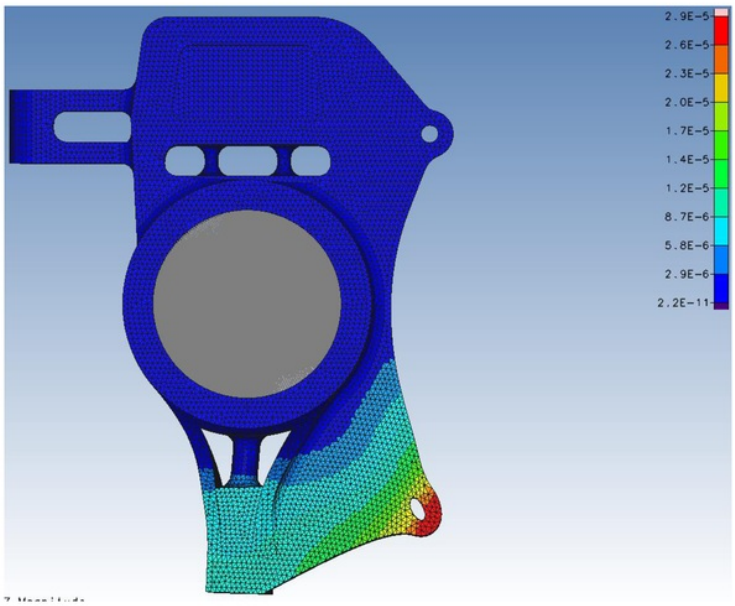
Brake low vertical linear



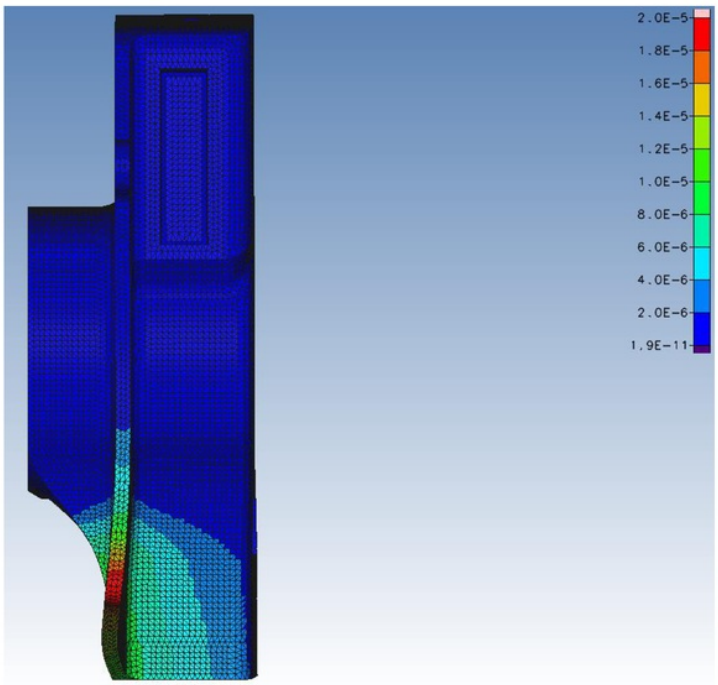
Brake low vertical cornering



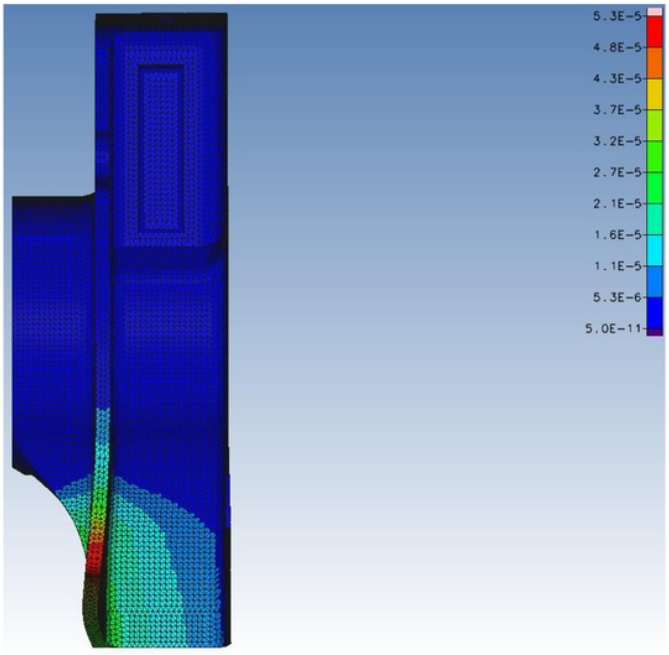
Brake low vertical braking



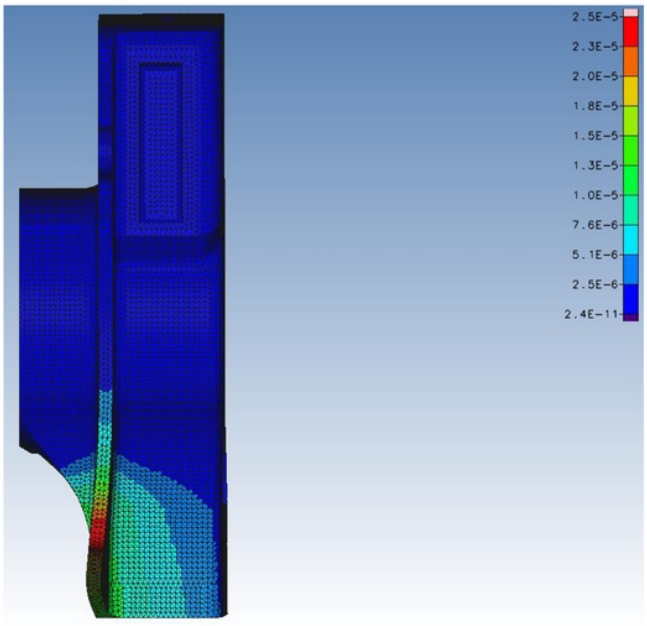
Brake low horizontal linear



Brake low horizontal cornering



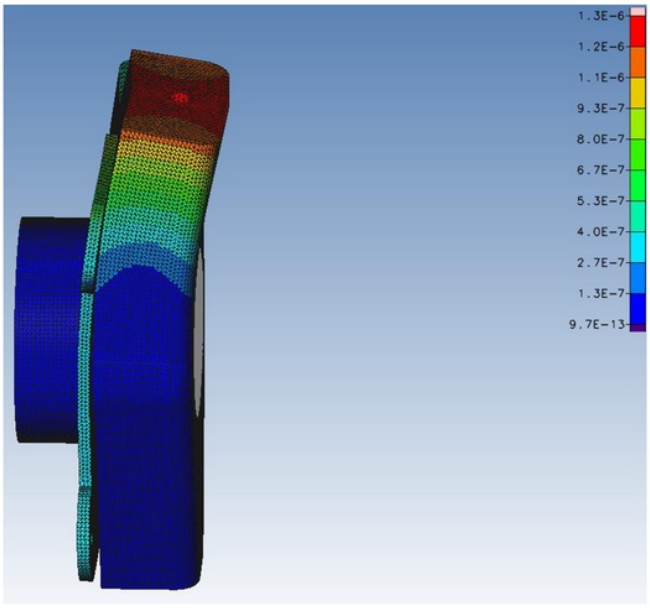
Brake low horizontal braking



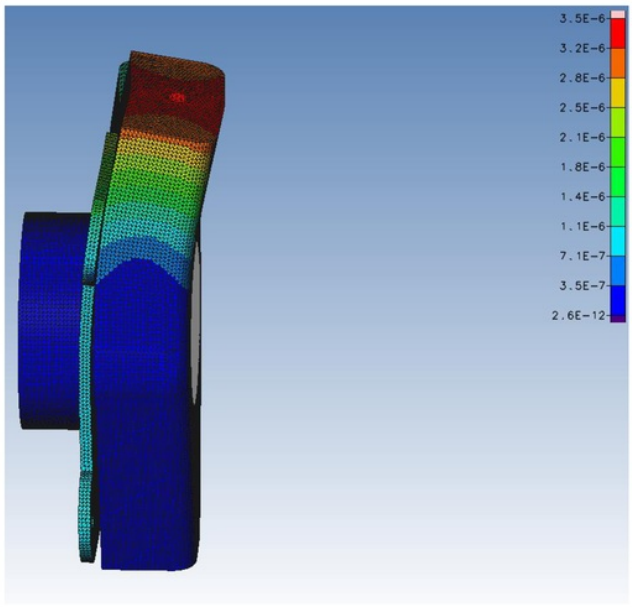
The following FEA screenshots are the results of the horizontal load being applied in the Y direction on both the current and new upright design.

Current

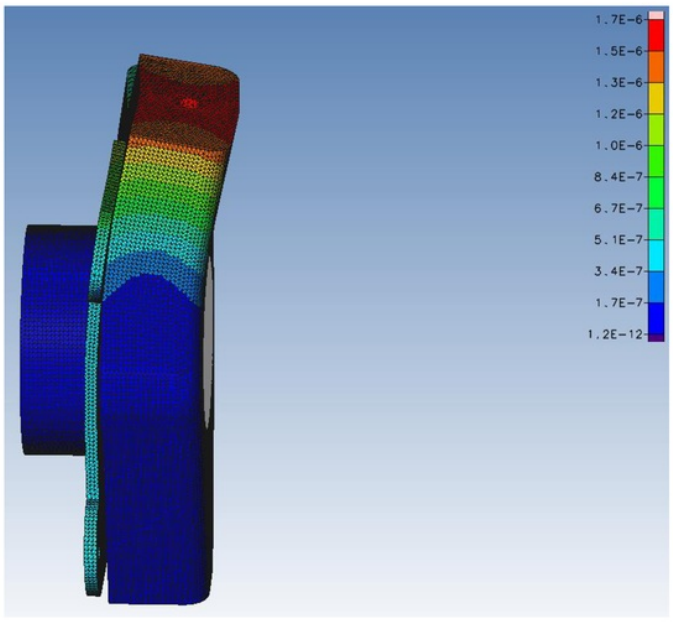
Top horizontal linear



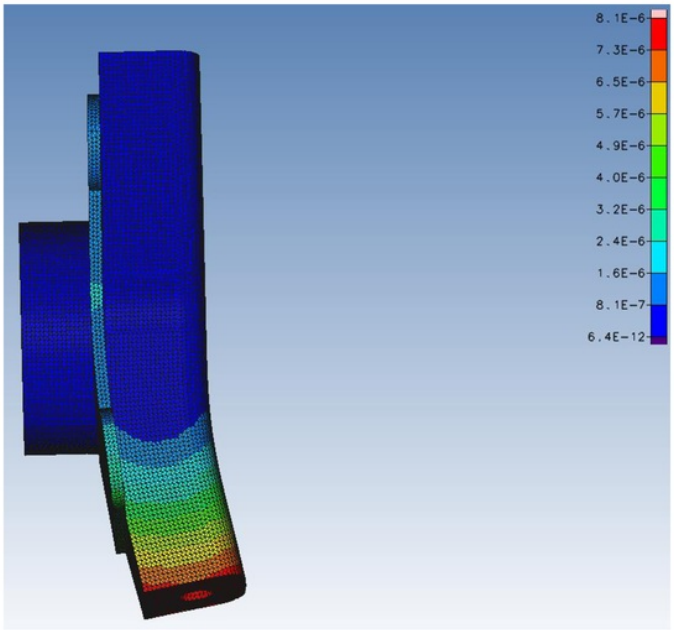
Top horizontal cornering



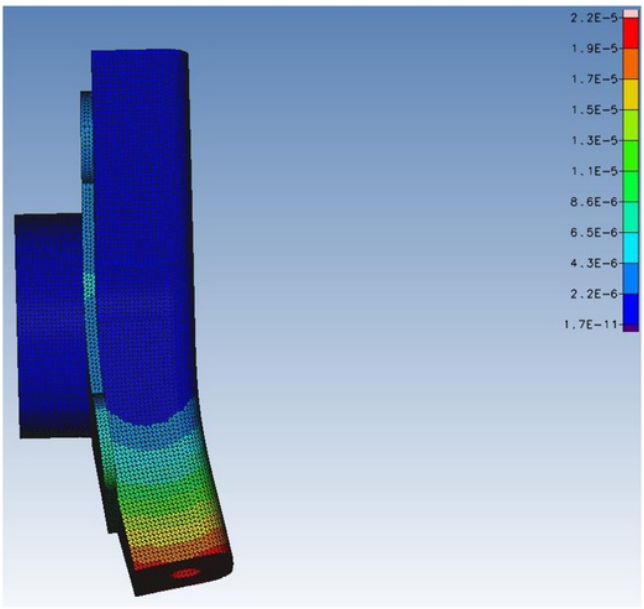
Top horizontal braking



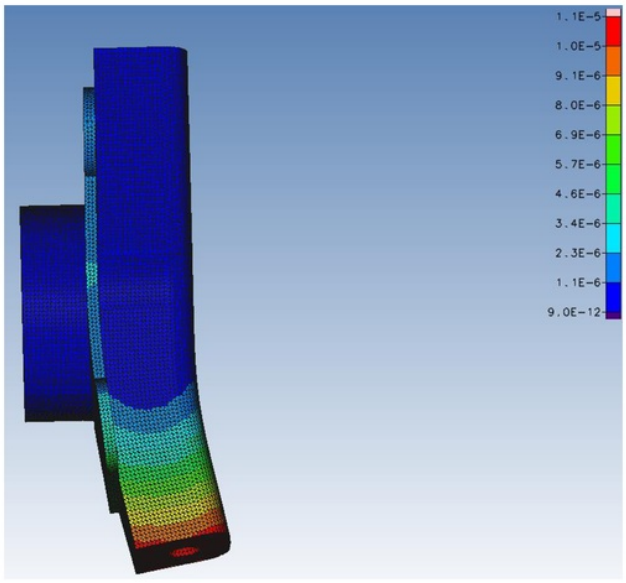
Bottom horizontal linear



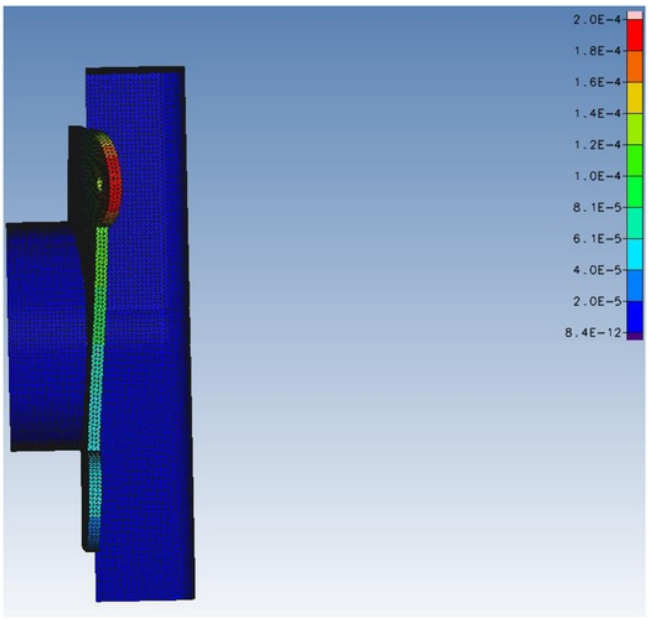
Bottom horizontal cornering



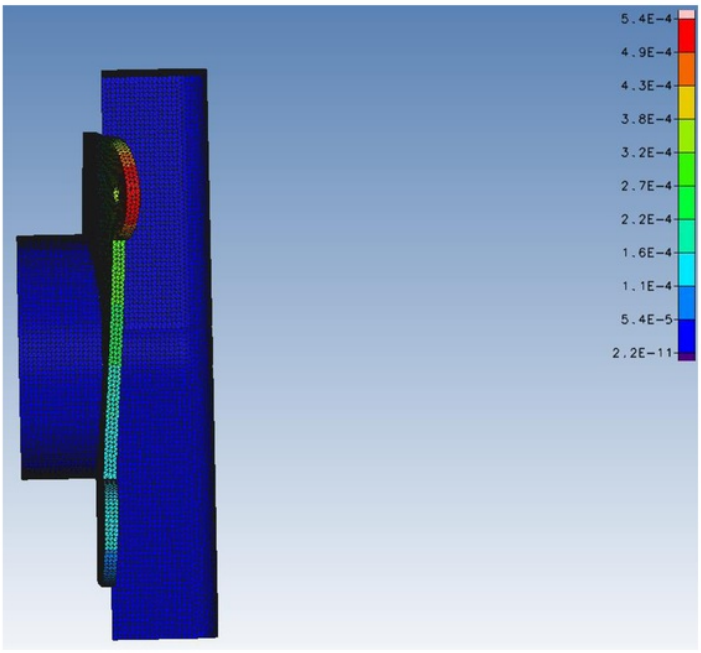
Bottom horizontal braking



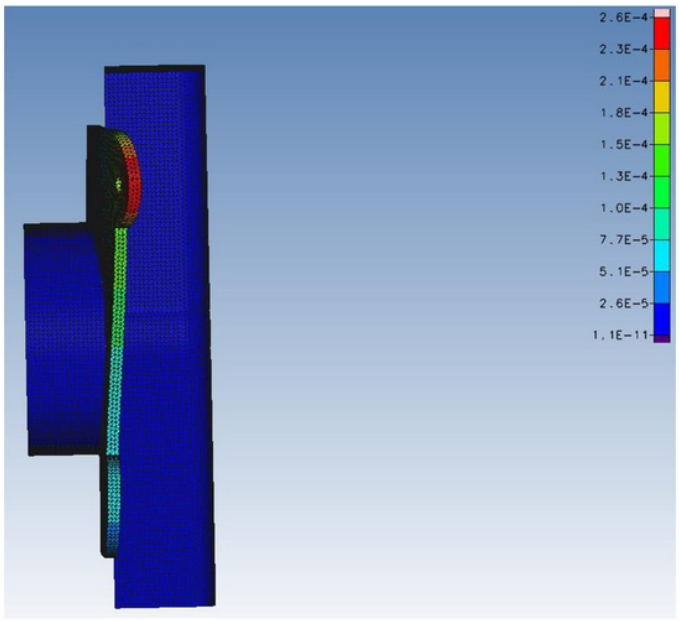
Brake top horizontal linear



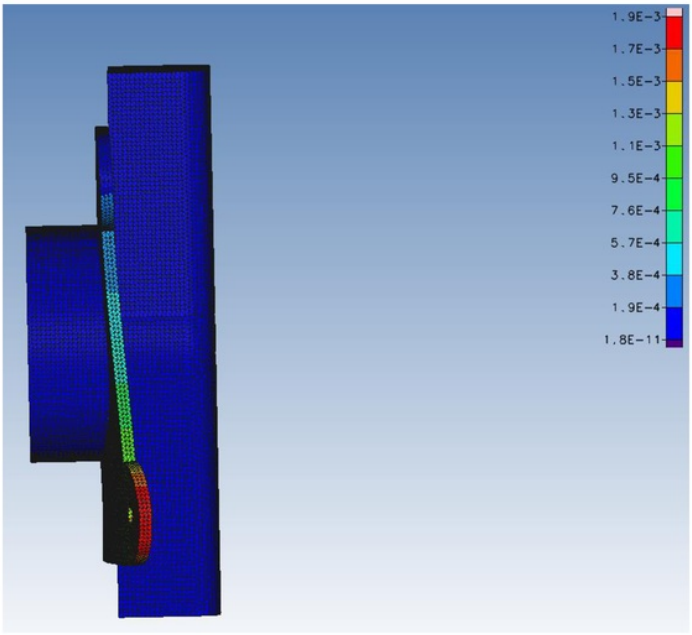
Brake top horizontal cornering



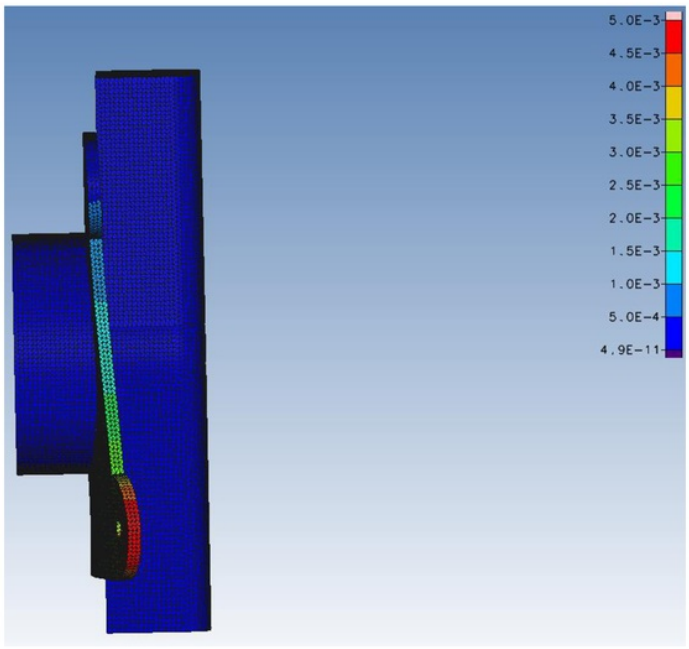
Brake top horizontal braking



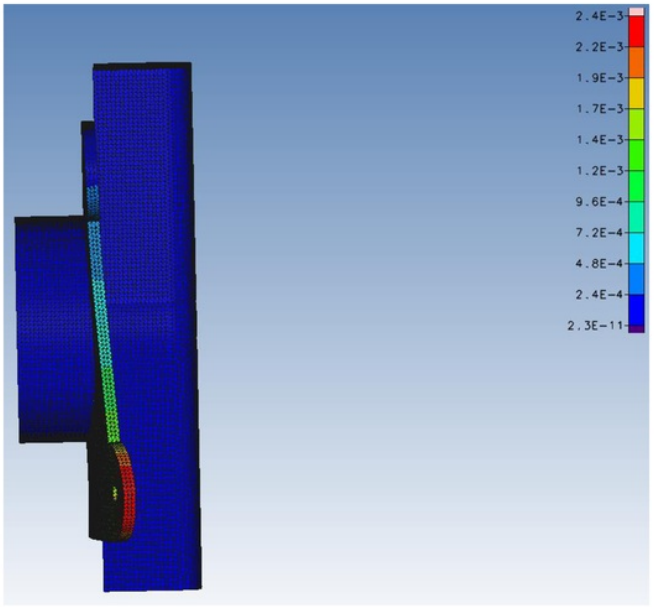
Brake low horizontal linear



Brake low horizontal cornering

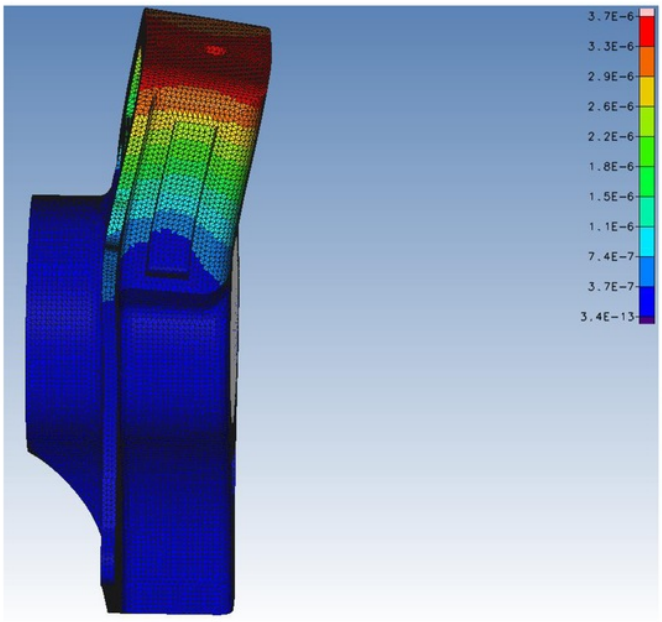


Brake low horizontal braking

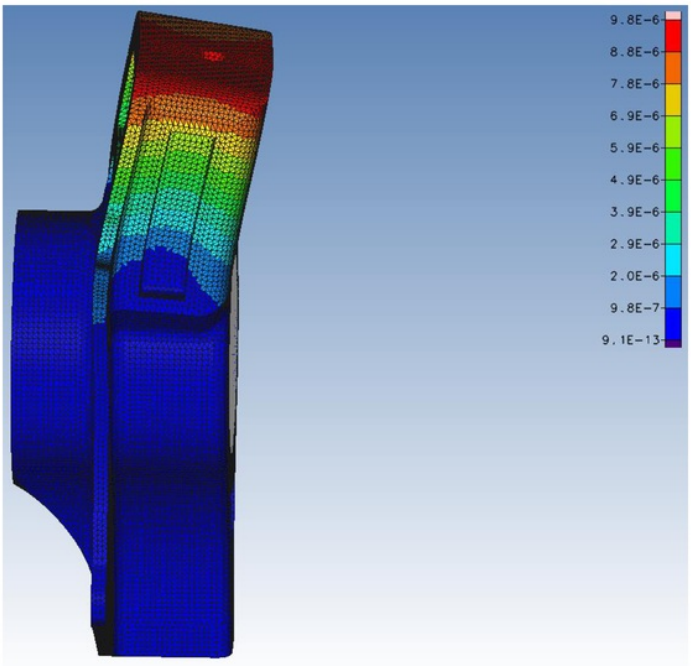


New

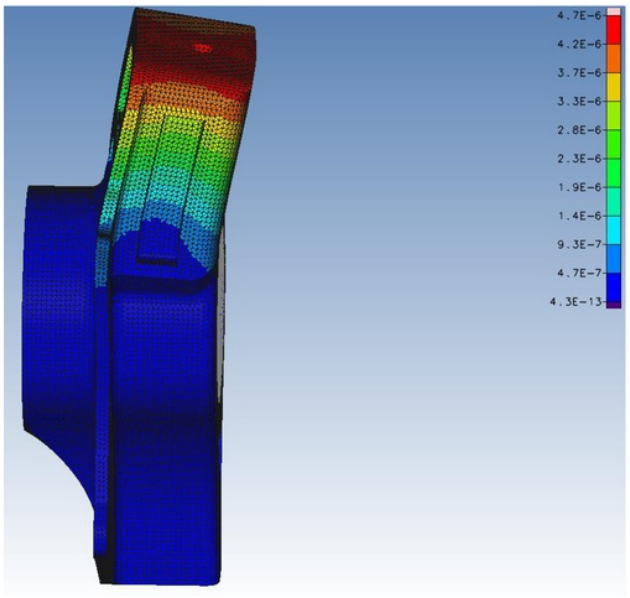
Top horizontal linear



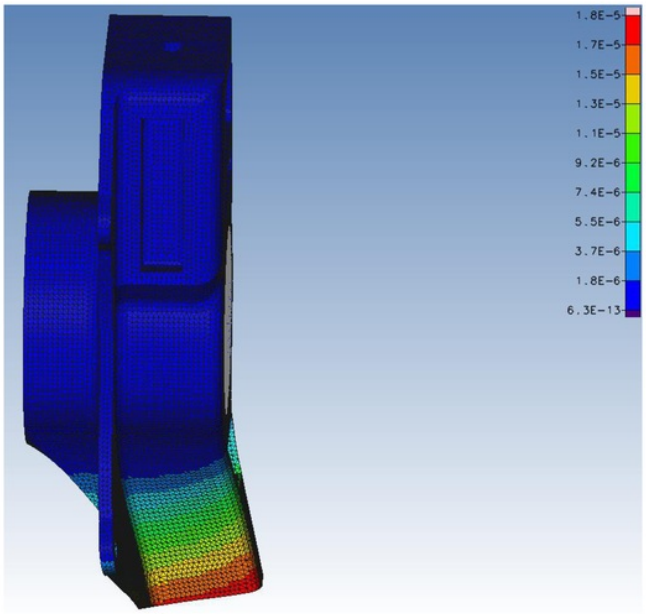
Top horizontal cornering



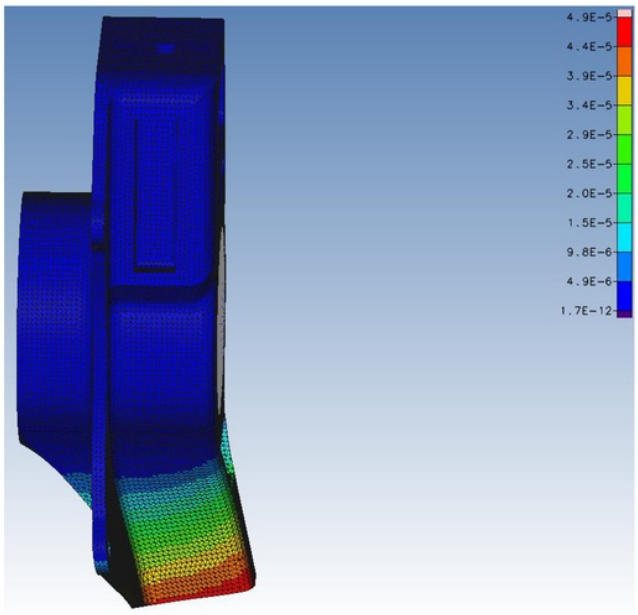
Top horizontal braking



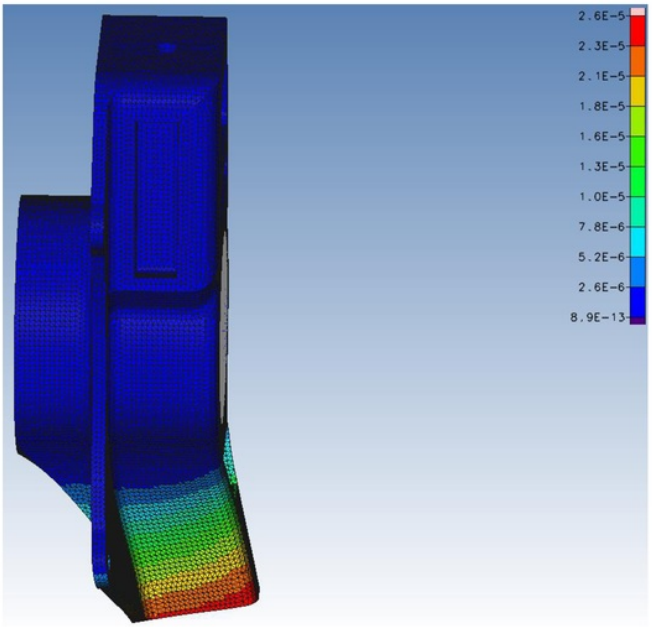
Bottom horizontal linear



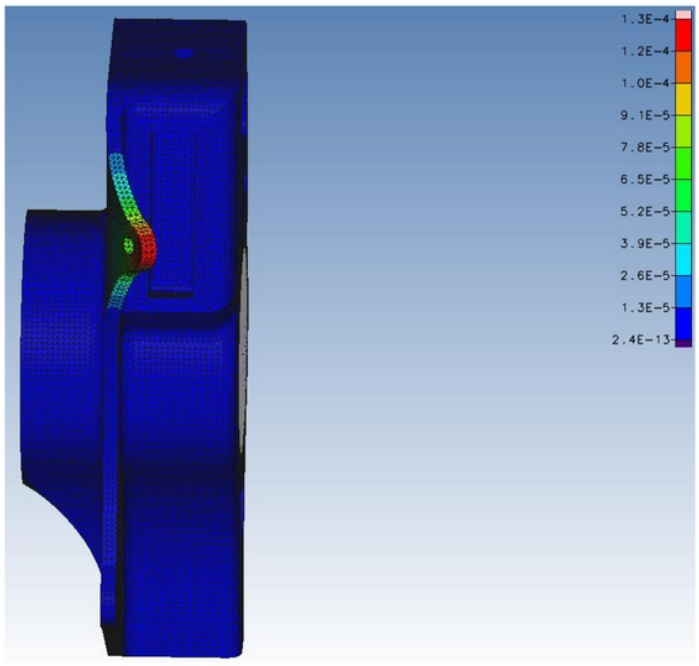
Bottom horizontal cornering



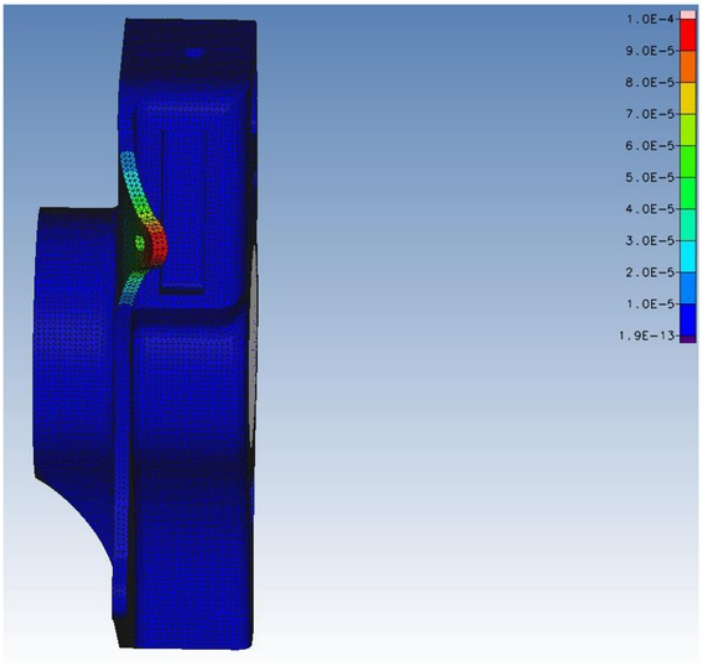
Bottom horizontal braking



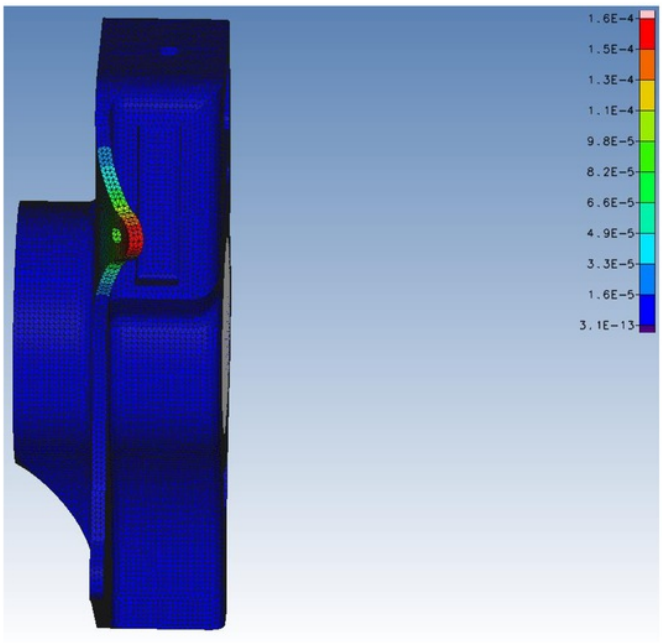
Brake top horizontal linear



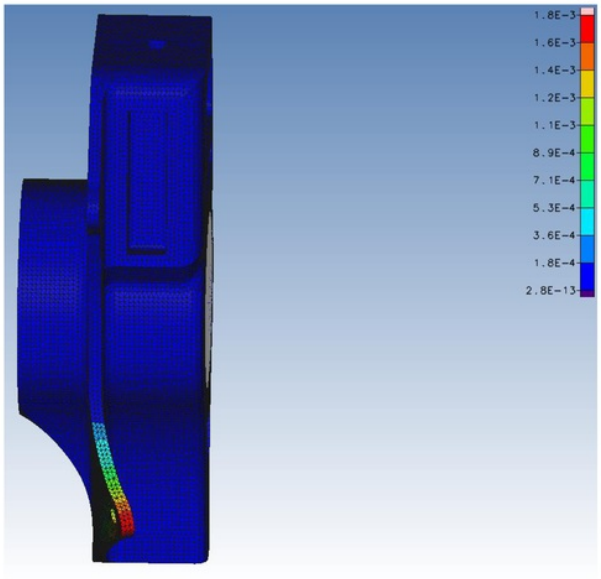
Brake top horizontal cornering



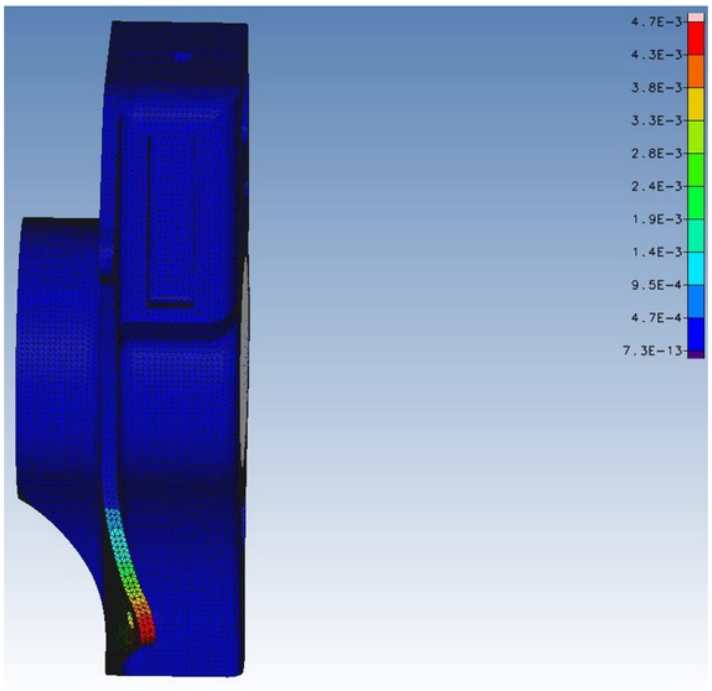
Brake top horizontal braking



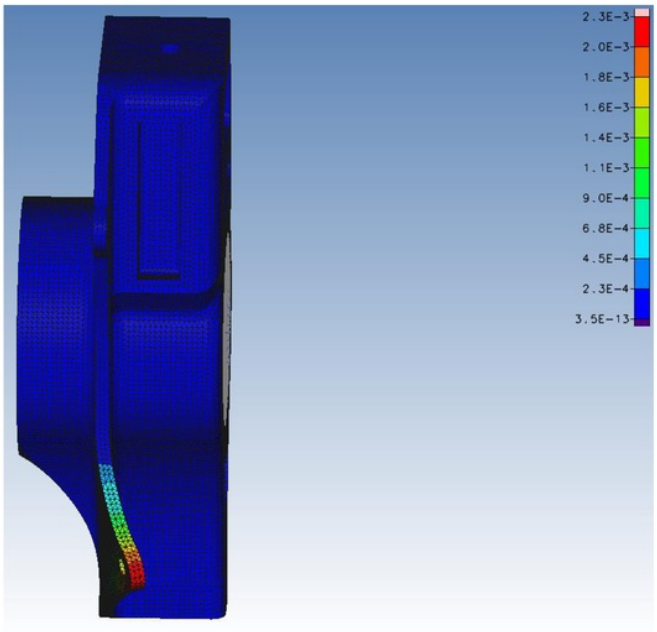
Brake low horizontal linear



Brake low horizontal cornering



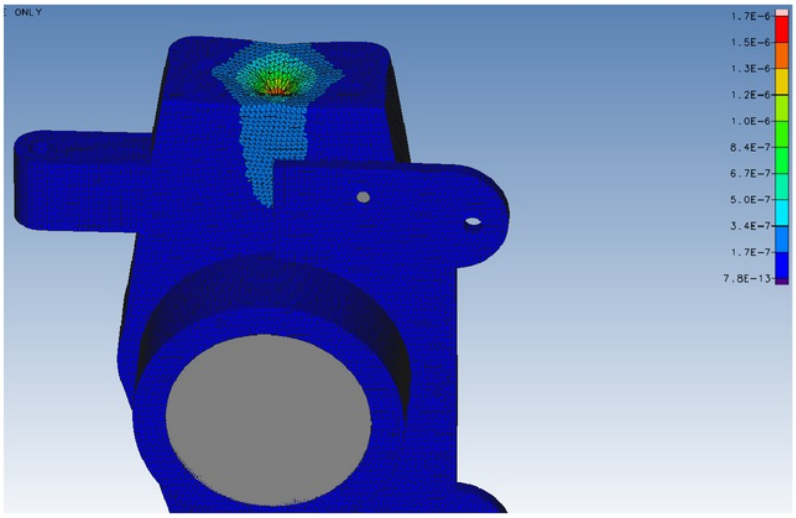
Brake low horizontal braking



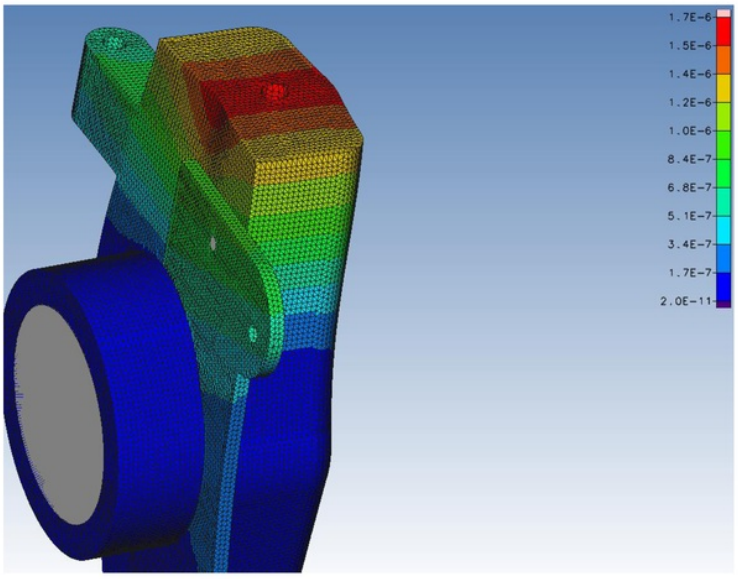
Lastly, all the results of the worst case testing can be found.

Current

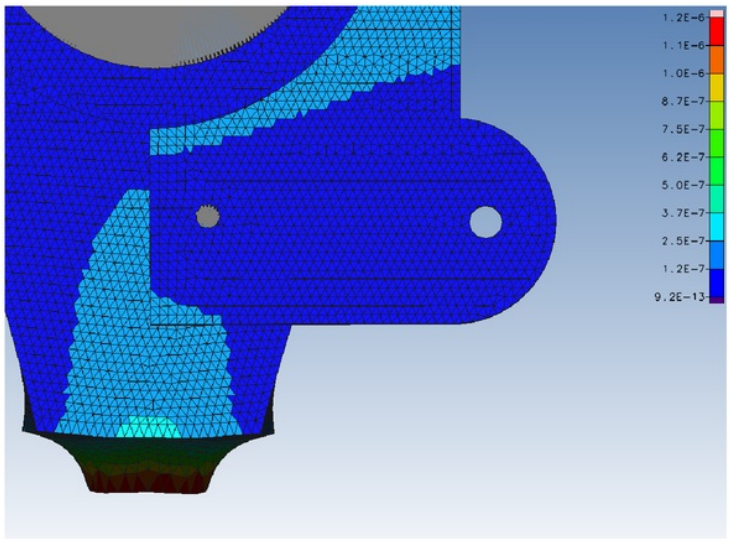
Top vertical



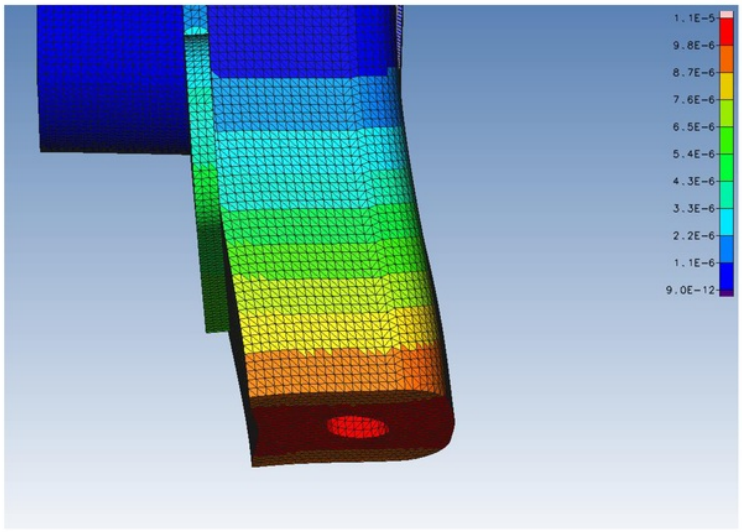
Top horizontal



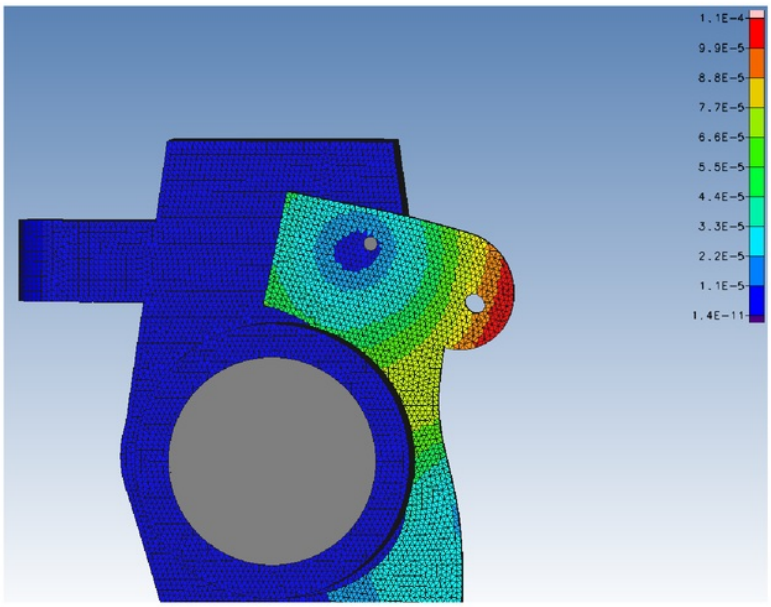
Bottom vertical



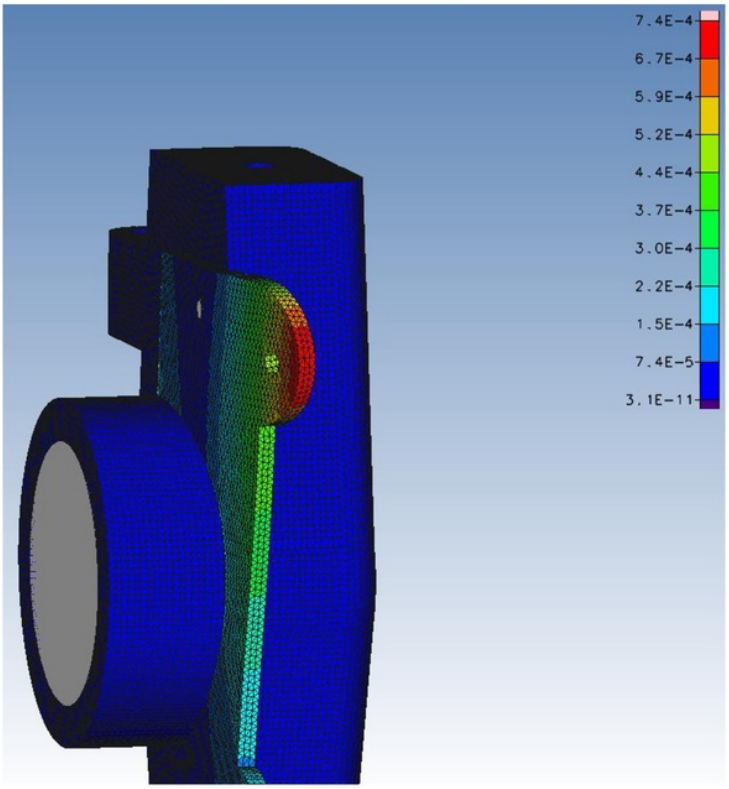
Bottom horizontal



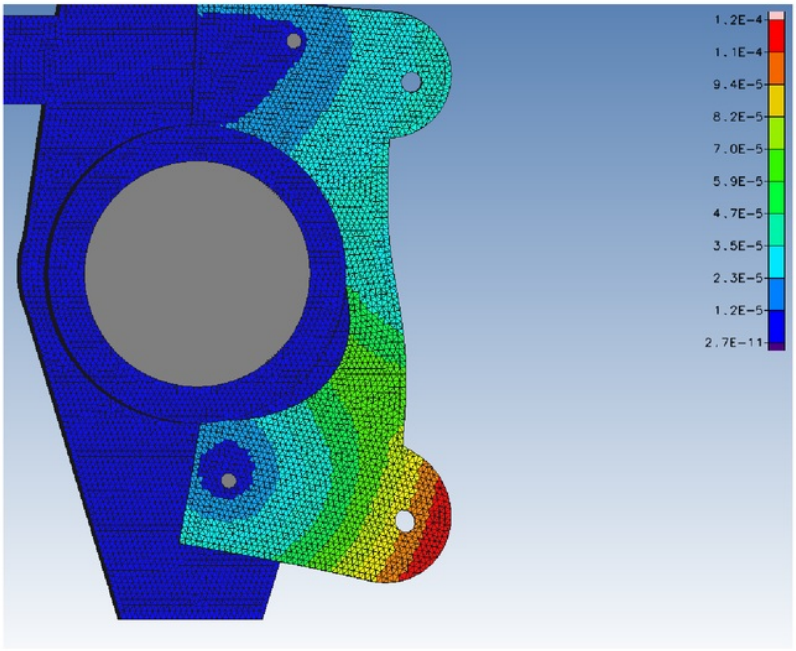
Brake top vertical



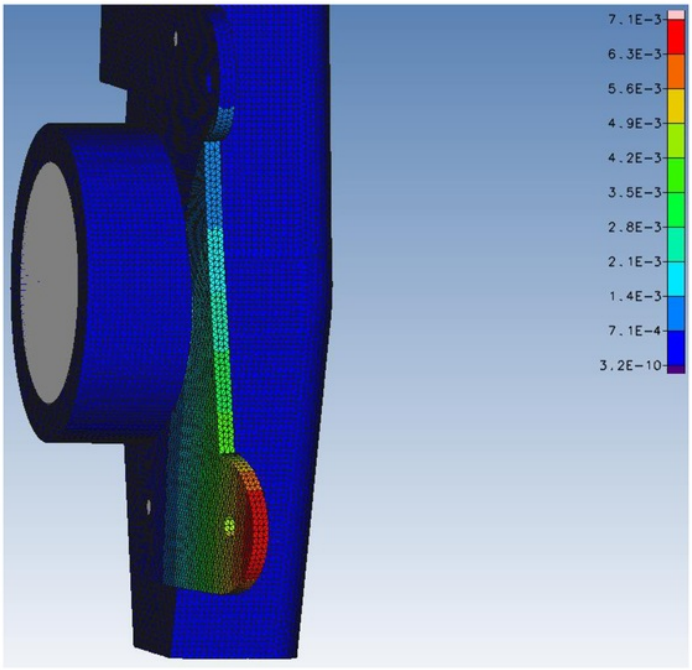
Brake top horizontal



Brake bottom vertical

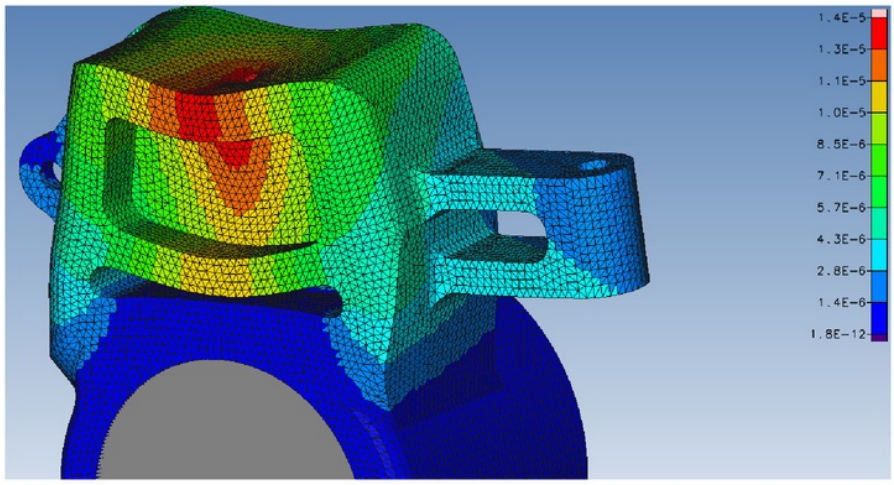


Brake bottom horizontal

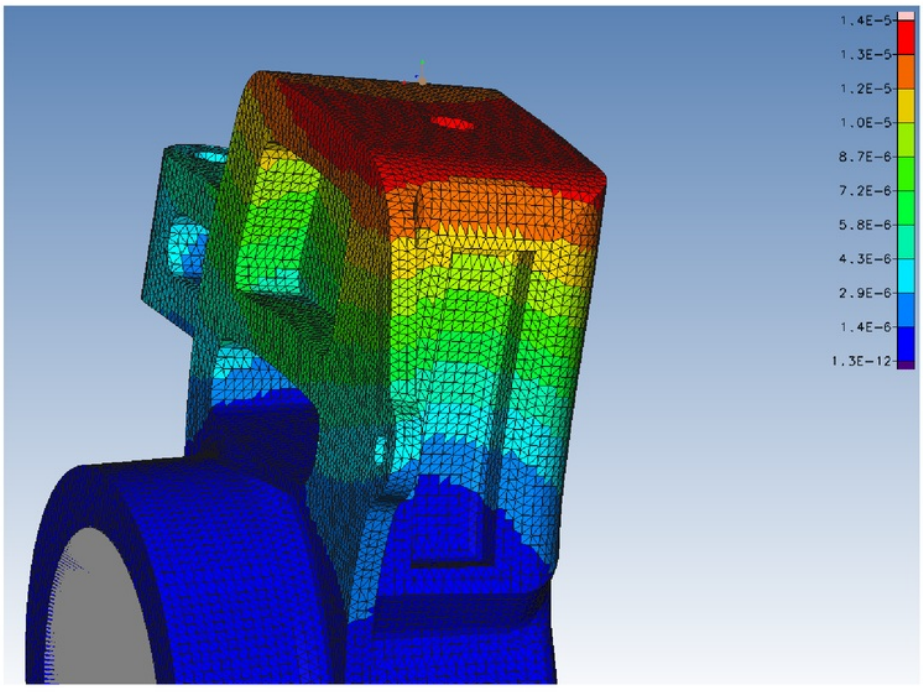


New

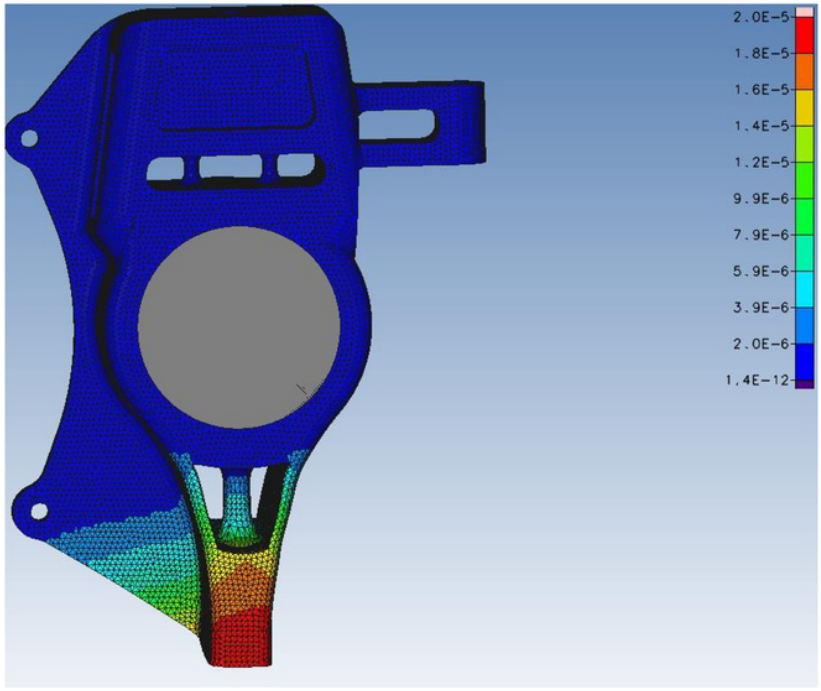
Top vertical



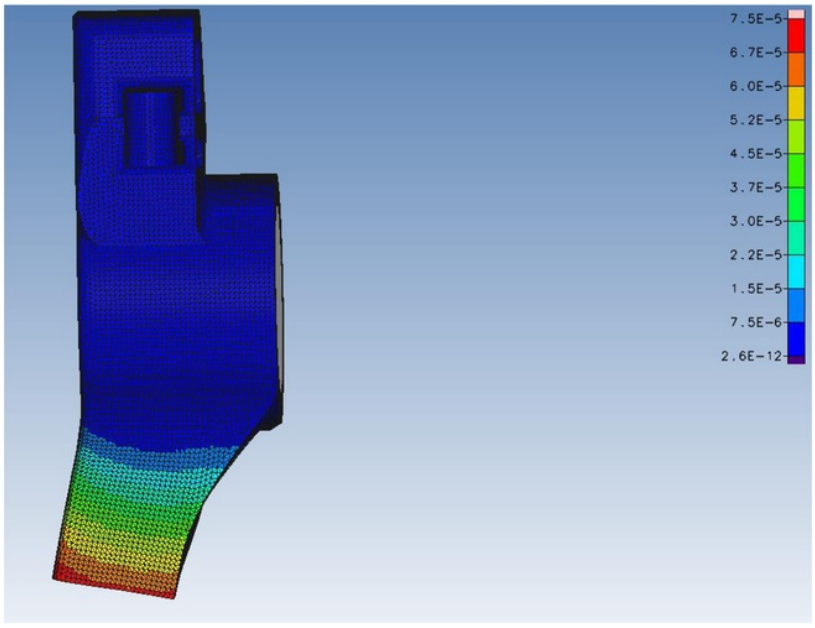
Top horizontal



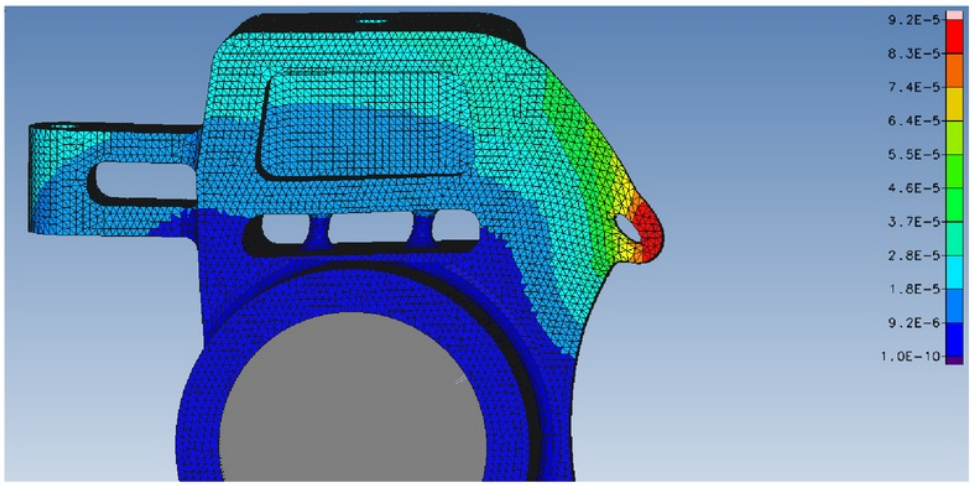
Bottom vertical



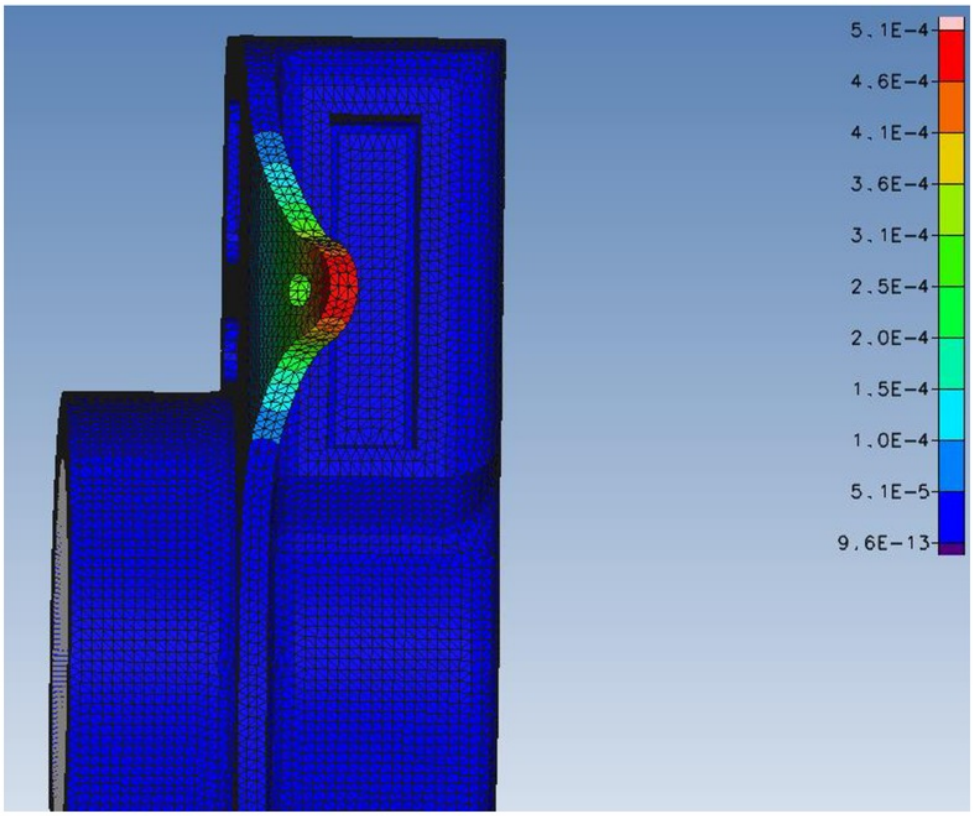
Bottom horizontal



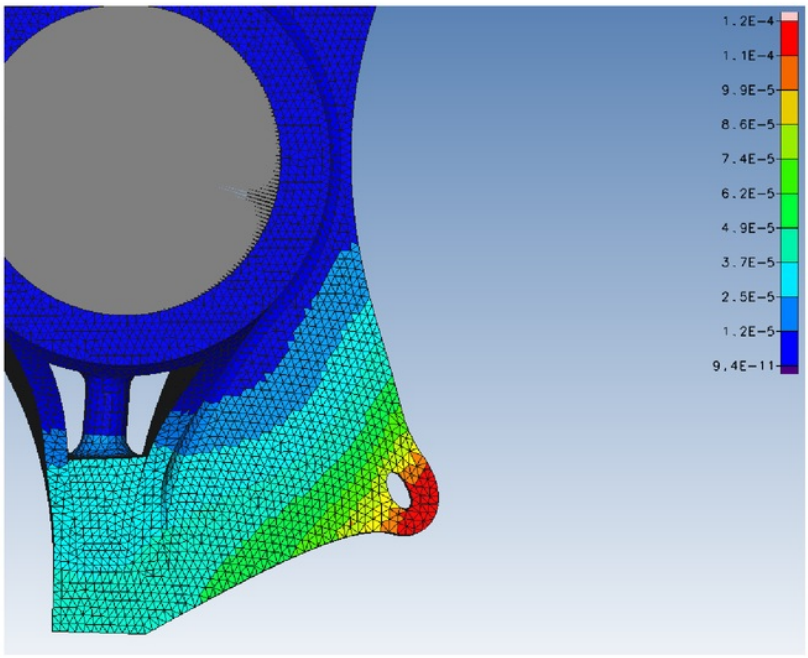
Brake top vertical



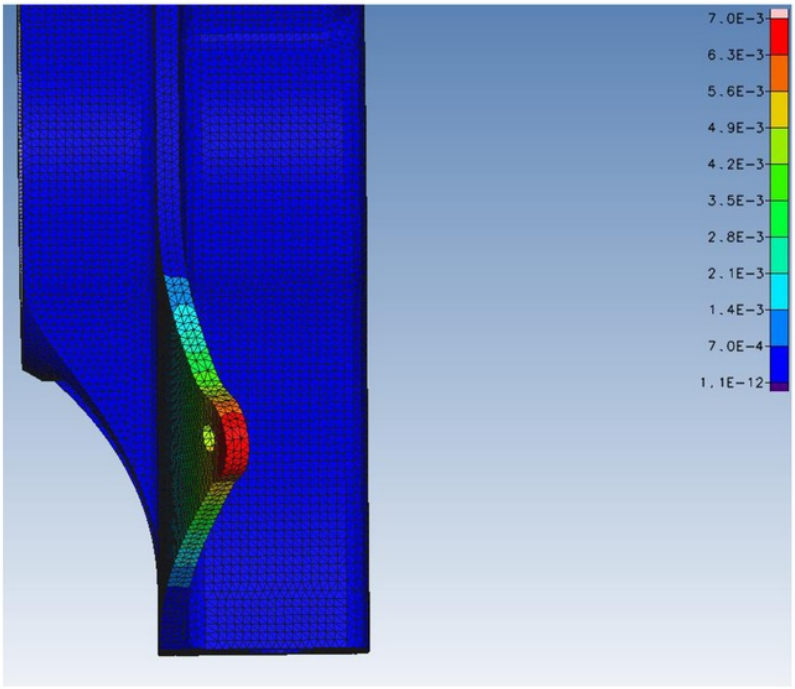
Brake top horizontal



Brake low vertical



Brake low horizontal

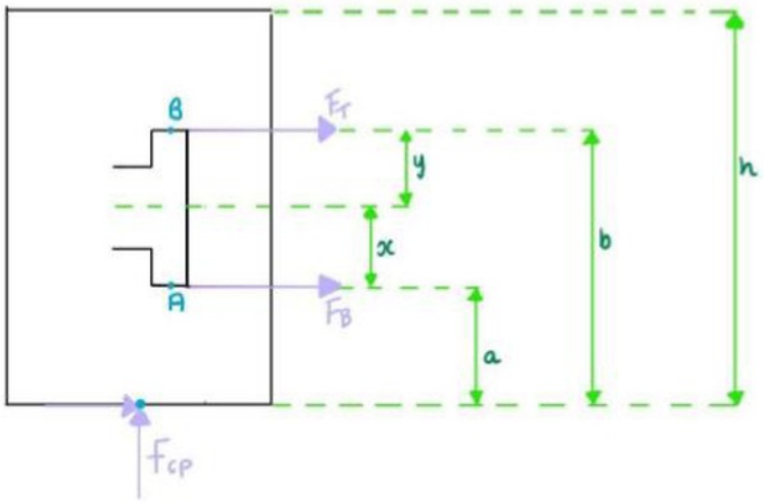


8.5 Appendix 5… Horizontal Track Load Calculation

To allow the upright to be tested fully peak loads that occur when on track needed to be found. The following appendix will document how the horizontal forces were calculated.

In order to find the horizontal forces acting at the corresponding attachment point, moments were taken about that attachment point.

The following diagram was used and taken from a report by an ex-student. (Meredith, 2018)



Where:

A= bottom attachment point

B= upper attachment point

F_{cp}= Contact patch force

F_T= laterally acting top force

F_B= laterally acting bottom force

x = distance from centreline of axle to bottom attachment point

Y= distance form centreline of axle to top of attachment point

a= distance from floor to bottom attachment point

b= distance from floor to top attachment point

h= overall height of wheel

Distance		mm	m
Middle to upper brake	yb	65.4	0.0654
Middle to lower brake	xb	67	0.067
Overall height	h	330	0.33
Top brake and floor	bb	175	0.175
Bottom brake and floor	aa	43	0.043
Suspension top	b	271.6	0.2716
Suspension low	a	48.1	0.0481
Middle to top suspension	x	117	0.117
Middle to suspension low	y	106.5	0.1065

The table above shows the corresponding measurements that were taken from the cad model of the current upright.

The initial forces taken from the track data are as follows.

	Vertical (N)	Horizontal (N)
Fcp force linear	1720	1580
Fcp force cornering	6205	4210
Fcp Breaking	1904	2005

The equations used to calculate the moment can be seen below.

Moments about A:

Clockwise motion = anti clockwise motion

$$FB * (b-a) = F_{Cp} * a$$

$$FB = F_{Cp} * a / (b - a)$$

FB = force at point B

F_{Cp} = Contact patch force

Moments about B:

Clockwise motion = anti clockwise motion

$$FA * (b-a) = F_{Cp} * b$$

$$FA = F_{Cp} * b / (b - a)$$

FA = force at point A

F_{Cp} = Contact patch force

The forces were calculated in an excel worksheet, an example of one of the calculations can be seen below.

Cornering force on brake attachment

$$Top = 4250 * 0.043 / (0.175 - 0.043) = 1371.44N$$

$$Low = 4250 * 0.175 / (0.175 - 0.043) = 5581.439N$$

The calculated forces can be seen below.

	Horizontal Force (N)		
	Linear	Cornering	Braking
Top	340	905	430
Bottom	1920	5115	2705
Brake Top	514.7	1371.44	653.14
Brake Bottom	2094.7	5581.44	2658.14